2018

Developmental variation in the amygdala: Normative pathways across puberty and stress-linked deviations

Justin D. Russell
Iowa State University

Developmental variation in the amygdala: Normative pathways across puberty and stress-linked deviations

by

Justin D. Russell

A dissertation submitted to the graduate faculty

in partial fulfillment of the requirements for the degree of

DOCTOR OF PHILOSOPHY

Major: Psychology

Program of Study Committee:
Monica A. Marsee, Co-major Professor
Carl F. Weems., Co-major Professor
Craig A. Anderson
Douglas A. Gentile
Elizabeth A. Shirtcliff

The student author, whose presentation of the scholarship herein was approved by the program of study committee, is solely responsible for the content of this dissertation. The Graduate College will ensure this dissertation is globally accessible and will not permit alterations after a degree is conferred.

Iowa State University

Ames, Iowa

2018

TABLE OF CONTENTS

ABSTRACT

Psychologists and neuroscientists have long accepted that the brain changes in size and shape throughout the course of child development . These changes are by no means uniform – the underlying processes of myelination and pruning vary in pace across brain regions (Lenroot & Giedd, 2006). Conversely, trends in regional development are likely uniform across our species (Stiles & Jernigan, 2010). In fact, deviations from normative trends in neurodevelopment are thought to be a core factor underlying psychopathology across the lifespan (Giedd et al., 2008; Giedd & Rapoport, 2010). This assertion, however, presumes a well-defined reference for "normal" brain development – common trends in the growth of individual brain regions across the time course of child development. Yet, despite a decades-old call to inform the study of what is abnormal in psychology with knowledge of what is normal (Cicchetti, 1984), our collective knowledge of the typical course of neural development is strikingly limited. The proposed study aims to enhance knowledge about normative brain maturation by examining longitudinal trends in the development of the amygdala, a region with important implications for a wide range of developmental processes.

CHAPTER 1. INTRODUCTION

Psychologists and neuroscientists have long accepted that the brain changes in size and shape throughout the course of child development (Giedd et al., 1999; Reiss, Abrams, Singer, Ross, & Denckla, 1996). These changes are by no means uniform – the underlying processes of myelination and pruning vary in pace across brain regions (Lenroot & Giedd, 2006). Conversely, trends in regional development are likely uniform across our species (Stiles & Jernigan, 2010). In fact, deviations from normative trends in neurodevelopment are thought to be a core factor underlying psychopathology across the lifespan (Giedd et al., 2008; Giedd & Rapoport, 2010). This assertion, however, presumes a well-defined reference for "normal" brain development – common trends in the growth of individual brain regions across the time course of child development. Yet, despite a decades-old call to inform the study of what is abnormal in psychology with knowledge of what is normal (Cicchetti, 1984), our collective knowledge of the typical course of neural development is strikingly limited. The proposed study aims to enhance knowledge about normative brain maturation by examining longitudinal trends in the development of the amygdala, a region with important implications for a wide range of developmental processes.

Though there is a need for continued investigation into normative trends in neurological development using improved methods and advanced computational techniques, it is necessary to acknowledge that a legacy of research exists in this area (Brain Development Cooperative Group, 2012; Brain Development Cooperative Group & Evans, 2006; Casey, Giedd, & Thomas, 2000; Giedd, 2004; Giedd et al., 1999; Giedd, Vaituzis, et al., 1996; Goddings et al., 2014b, 2014a; Gogtay et al., 2004; Lenroot & Giedd, 2006; Reiss et al., 1996). Much of this work has focused on broader brain regions, such as lobar volumes, or gray\white matter concentrations,

whose size and visibility makes them easier to measure. Yet, with ever faster computation times, higher-resolution imaging techniques, and novel conceptualizations of brain structure (Bassett & Sporns, 2017; Hage, Alaraj, & Charbel, 2016), there is a new impetus to provide a more detailed look at smaller, subcortical structures long theorized to play important roles in the socio-affective development of children.

The proposed study will investigate normative and stress-induced variation in amygdala development. Below, I provide a comprehensive overview of several background areas describing the amygdala, its research history, contemporary investigations into its functional and structural properties, and the burgeoning research examining its interplay with psychosocial stress. The advance of neuroimaging methodology is providing extraordinary insights about the amygdala's role in human behavior. However, contemporary theoretical and empirical work with the amygdala continues to rely on formative research with animal subjects, and humans with unusual neurological damage. Therefore, *Chapter 2 – The Structure and Function of the Amygdala: A Historical Perspective*, begins with an overview of its anatomical properties (*A Brief Neuroanatomical Description of the Amygdala*), and continues into a review of research identifying the structural and functional properties of the amygdala, and pre-neuroimaging investigations with humans (*Investigation through Lesioning and Stimulation*).

As late as the 1990's, assumptions about the amygdala's role in human behavior came from observations of animals with disrupted or removed amygdalae. Major advances came with the widespread use of functional magnetic resonance imaging (fMRI; *Functional Investigations of the Human Amygdala*), which provides a window into the human amygdala's activation response to various stimuli, and its role in emotion-driven acquisition of behavior. Studies using fMRI illuminated the amygdala's role in foundational psychological concepts, such as response

to unconditioned stimuli (*Unconditioned Amygdala Stimulation*) and conditioned stimuli (*Conditioned Amygdala Stimulation*). Moreover, this work suggested the amygdala's role in broader socioemotional functioning, and led researchers to consider its role in children's emotional development.

Relatedly, a co-occurring body of work began to examine morphological changes in the amygdala from birth to adulthood. *Chapter 3 – Amygdala Development* reviews the body of research investigating normative trends in amygdala development, specifically the original work of Jay Giedd and colleagues (*Giedd and Colleagues Examine Large Samples of Healthy Youth*), and the many studies following on their work (*Contemporary Studies of Neurodevelopment*). I close this section by reviewing research testing amygdala development in the context of pubertal maturation, and describe the need for continuing investigation (*Puberty as an Index of Development*). Continuing, in *Chapter 4 – Stress and Amygdala Development* I consider the theoretical effects of psychosocial stress on the brain and the amygdala specifically. Stress systems in the brain (i.e., the HPA axis) are reviewed first, and their interplay with the amygdala is described (*Stress and the Brain*). Continuing, I review the limited work examining psychosocial stress and amygdala development (*Stress and the Developing Amygdala*). I close by considering a novel frontier in research linking stress and the growing amygdala, the impact of socioeconomic status (*Socioeconomic Disadvantage*). I next provide a summation, introduction to my methods, and statement of my hypotheses in *Chapter 5 – Summation*. The methodology and analytical plan are described in *Chapter 7 – Methods*. Results from the present study are provided in *Chapter 7 – Results,* and thereafter described in *Chapter 8 – Discussion*.

CHAPTER 2. THE STRUCTURE AND FUNCTION OF THE AMYGDALA: A HISTORICAL PERSPECTIVE

Overview

The bulk of knowledge about the amygdala comes from decades of animal studies linking amygdala activity to stimuli and behaviors (LeDoux & Schiller, 2009). Increasing and decreasing amygdala activity in animals (via electrochemical stimulation, or lesioning) can produce major changes in responses to frightening stimuli, emotion-based learning, and inter-animal interactions (Whalen & Phelps, 2009). Although research with animals provided major breakthroughs related to the amygdala, it is difficult to translate these findings to humans. Common approaches in animal neuroscience, such as lesioning or *in vivo* stimulation, are infeasible with human subjects (Glenn, Lieberman, & Hajcak, 2012). Today, the neuroimaging revolution is providing major gains in knowledge of the human brain. Still, many of our assertions about findings from neuroimaging rely on assertions developed from animal models (LeDoux & Schiller, 2009). Therefore, an informed understanding of current conceptualizations requires review of the origins of the amygdala itself, and the broader field of affective neuroscience.

A Brief Neuroanatomical Description of the Amygdala

Anatomical Structure

Burdach (1819) first identified small bits of gray matter deep within the middle of each temporal lobe in the human brain. He named it "amygdala," using the Latin root describing its almond form (LeDoux & Schiller, 2009). The amygdala is found in a wide variety of human and animal species. In humans, the amygdala is located in the dorsomedial area of the rostral portion of the temporal lobe. It is immediately anterior to the hippocampus, separated by the anterior recess of the lateral ventricle's temporal horn (Di Marino, Etienne, & Niddam, 2016). Though

the amygdala is commonly described as a unitary structure it is actually a composite of several subgroups of nuclei with different forms, but similar functions (LeDoux, 2007). These "clusters" are categorized into two groups. The basolateral amygdala consists of the basal, lateral, and accessory-basal nuclei, whereas the amygdaloid (or cortico-medial) complex includes the central, medial, and cortical nuclei (Johnston, 1923). There is a consensus that these clusters should be grouped together as the "amygdala", based on their structural proximity and functional similarity. However, debate about the appropriate boundaries, subdivisions, and even the existence of the amygdala as an independent structure continues (Swanson & Petrovich, 1998).

Neural and Somatic Connections

Decades of research suggest that the amygdala plays a major role in emotional learning (for an exhaustive review, see Aggleton, 2000; Whalen & Phelps, 2009). It is not surprising, therefore, that the amygdala possesses numerous connections to other regions of the brain (Janak & Tye, 2015; LeDoux, 2000). Technological barriers (e.g., image resolution) limit precise knowledge of the connections to and from the human amygdala (Saygin et al., 2017). Most knowledge stems from studies of the rat and primate brain, and reveals a complex web of reciprocal connections linking the amygdala to other regions of the brain (Janak & Tye, 2015). The amygdala communicates with many different structures as it interprets stimuli, moderates arousal in response, and informs behavior. The pathways arrive or depart from various nuclei groups in the amygdala (e.g., the cortico-medial) and can take complicated routes as they carry information throughout the brain. Moreover, there is burgeoning evidence that these pathways are progressively reorganized across development (Saygin et al., 2015). This is an extraordinarily complex, and continually evolving area of research. For simplicity, therefore, I will provide only a brief overview of *some* amygdala connections (a more comprehensive review can be found in Di Marino et al., 2016).

Afferent signals into the amygdala generally converge on the lateral nuclei of the amygdala. These can be divided into four groups according to their source or general function. The first group of afferents specifically transmits *olfactory information*, and arrives directly to the amygdala from the olfactory cortex. This pathway is more critical in non-human species who rely more on scents to experience the world. Information gathered from non-olfactory sensory sources is transmitted along a second group of afferent connections, though these fibers arrive from two different locations. One set of sensory inputs originates in the thalamus, which serves as a convergence point for information from each of the sensory cortices. LeDoux (1998) originally described this as the 'low road' of sensory processing, in that information traveling along this pathway arrives quickly, but tends to be imprecise. A second set of sensory inputs, the 'high road' originates from the individual association cortices that process information from each sensory modality. The extra processing (and connections) along this pathway slows the arrival of information, but provides more elaborate detail about sensory information (Phelps & LeDoux, 2005). A third group of afferents communicates visceral information – sensation produced by the organs, such as "butterflies in the stomach" or "heart fluttering". These fibers originate in the hypothalamus, which regulates the body's autonomic arousal, and receives sensory feedback from the affected organs. A final group of afferent connections provides the amygdala with more general, affect-relevant information about bodily states, such as arousal (from the locus coeruleus; Di Marino et al., 2016; LeDoux & Schiller, 2009).

Efferent fibers from the amygdala largely originate in the central nucleus, though they connect to a great many regions of the brain (Di Marino et al., 2016). Many of these connections mirror those of afferent fibers, and proceed along similar tracts to provide the same structures with response information. These links allow the amygdala to effect emotional and physiological

responses to stimuli (Di Marino et al., 2016). Many of these connections are responsible for some of the classic emotional responses in psychology. In response to danger, a signal sent along the pathway connecting the amygdala to the periaqueductal gray can induce a "freeze" response (Janak & Tye, 2015). It may also induce an anti-nociceptive effect in the raphe nuclei that diminishes pain in advance of a "fight or flight" response (Nakamura et al., 2013). Efferent connections to the hypothalamus provide the amygdala with control over the stress response system. The amygdala may initiate a downstream effect on the hypothalamus that alters autonomic arousal, or activates the HPA axis (hypothalamic-pituitary-adrenal), thus preparing the body for a stressful encounter (Di Marino et al., 2016). Outgoing connections to sensory cortices allow the amygdala to modulate awareness of sensory stimuli, theoretically serving as a gateway for information accessing the conscious mind (Di Marino et al., 2016; LeDoux & Schiller, 2009).

Investigation through Lesioning and Stimulation

Animal Subjects Research

Contemporary knowledge of the amygdala's structure and function is critically informed by the use of modern neuroimaging techniques, such as MRI and PET. However, these techniques are relatively recent additions to the neuroscientist's toolbox. In the formative decades of neuroscience (and still today) researchers relied on invasive surgical methods to study components of the brain (Dalgleish, Dunn, & Mobbs, 2009). The ethical issues inherent to performing major brain surgery on healthy human participants required researchers to make inferences animal based on findings from animal subjects. As a result, much of the foundational knowledge derived from work with non-human primates.

Though the German anatomist Burdach distinguished the amygdala as early as 1819, the surgical methods used by early neuroscientists lacked the precision to investigate its function.

Rather, researchers tested the effects of ablating or stimulating the encompassing temporal lobe (Brown & Schäfer, 1888). Landmark work by Klüver and Bucy (Bucy & Klüver, 1940; Klüver & Bucy, 1937, 1938, 1939a, 1939b; Bucy, 1985) identified a constellation of emotional, behavioral, and memory symptoms following removal of the temporal lobe. Animals experiencing what would become known as Klüver-Bucy Syndrome failed to demonstrate emotive responses to stimuli, such as aggression in response to provocation, or fear in response to threat.

Lawrence Weiskrantz (1956) was among the first to hypothesize that these affective symptoms might be attributable to the amygdala. In accordance with the behaviorist tradition dominant at the time, Weiskrantz tested his hypothesis using a fear-based learning task. Subjects were assigned to groups who received either a bilateral amygdalectomy (*AM*) or a sham surgical procedure (*S*). These animals were then tested in a conditioned avoidance and a conditioned depression task (Weiskrantz, 1956). *AM* subjects learned the conditioning tasks more slowly, requiring 100-150 more trials (versus *S*) to acquire the behaviors. Once acquired, the behaviors became extinct more rapidly in the *AM* group. Both results provide support for Weiskrantz hypothesis, and suggest that the ablated-amygdala animal may be experiencing a, "decreased response to 'anxiety-producing' situations" (Weiskrantz, 1956, p. 389) that may cause it difficulty in discriminating between rewarding and punishing stimuli.

While Weiskrantz and others identified effects of lesioning the amygdala, a similar line of research tested electrochemical stimulation. Goddard (1964) tested the effect of amygdala stimulation on avoidance. Goddard's research team implanted electrodes carrying a low-voltage 60 Hz current into the amygdala of rats, and observed their behavior (versus groups of normal and sham procedure controls) in a series of fear-motivated conditioning tasks. Subjects were

observed in separate tasks promoting fear-induced avoidance behavior and a conditioned fear response (i.e., operant and classical conditioning, respectively), as well as a comparison task involving hunger-motivated approach behavior. Subtle variations in task parameters over the course of several experiments demonstrated that amygdala stimulation diminished subjects' ability to learn when motivated by fear, though not hunger. Critically, it appeared that the stimulated subjects did continue to experience fear, but did not use that aversive memory to inform future behaviors. Goddard (1964) and subsequent researchers interpreted these results as evidence that the amygdala may not necessarily be the source of fear, but instead may function to consolidate memories pairing an unconditioned stimulus with an aversive stimulus. Goddard's study is included here primarily for contributing to affective neuroscience (specifically, the amygdala's links to fear). However, it is worth noting that Goddard's findings relating the amygdala to memory formation, though initially ignored by the field, are now considered groundbreaking in cognitive neuroscience (McGaugh, 2000, 2002).

Human Subjects Research

Investigation of the amygdala's role in the human experience proceeded along a similar, though more temperate path. Consistent with a broader trend in neuroscience, knowledge of the amygdala in humans advanced at a more gradual pace, often informed by animal studies (LeDoux & Schiller, 2009). Similar to animal-based research, investigators started from an initial focus on the larger, temporal lobe, though progressively migrated to study of subcortical structures (Dalgleish, 2004). As described, early knowledge of the amygdala benefited enormously from neurosurgery and electrical stimulation techniques used with animal subjects. Although these methods had enormous utility in animal research and general medicine, the risk they imposed on the subject made them unreasonable for most human subjects (Glenn et al., 2012). Their application in humans was limited to clinical cases where most other treatment

avenues had been exhausted. The bulk of early research on the temporal lobe and amygdala in humans, therefore, comes from case-reports and small-sample studies describing the impact of these procedures, and drawing corollaries to findings in animal studies.

Early investigations in epilepsy

Penfield and colleagues tested whether electro-cortical stimulation could trigger seizure in epileptic patients. Observations of patients experiencing stimulated and endogenous seizures suggested amygdala involvement powerful emotional experiences, as well as vivid memory recall, visual hallucinations, and prodromal aura (Feindel & Penfield, 1954; Penfield, 1958; LaBar & Warren, 2009). Chapman and colleagues (1954) described reports from five patients undergoing stimulation as part of evaluation for treatment of medial temporal epilepsy. Four of five reported rapid-onset sensations of anxiety and fear during cortical stimulation, and showed elevated heart rate and blood pressure. Though limited in their methodology and sample size, these early studies provide the first inclination of the amygdala's role in the production of human emotion.

Cases of selective amygdala damage in humans.

By the 1990's, though progress in MRI had begun to advance brain research, the vast majority of knowledge about the human amygdala continued to be derived from investigations of patients with temporal lobe epilepsy, or non-specific damage to the medial temporal lobe. In-depth investigations of damaged or disordered temporal lobes had been critical in advancing knowledge about structures proximal to the amygdala, for example, the hippocampus in the case of Henry Molaison ("H.M."). However, in the case of the amygdala, its small size, location, numerous connections, and close proximity to other structures, make selective damage to the amygdala exceedingly rare.

Several major breakthroughs came through the discovery of several unique cases in the 1990's. S.M., a 30-year-old female with an otherwise normative neurological profile, exhibited highly specific bilateral calcification of the amygdala (Feinstein, Adolphs, Damasio, & Tranel, 2011). In a series of studies, S.M. struggled to identify fearful emotion in others, or experience fear in response to stimuli such as handling snakes, spiders, or watching scary movies.[1] In a case referred to as N.M., doctors detected bilateral gliosis in the amygdala secondary to regional infarction (Sprengelmeyer et al., 1999). Neuropsychological testing again revealed no notable abnormalities in functioning outside the damaged area. However, in the aftermath of the infarction, N.M. was also unable to detect fear from facial expressions, body postures, or sounds, and described experiencing a lack of strong emotion (positive or negative) in his life. Notably, N.M. regularly sought out extreme experiences such as "hunting deer in Siberia while hanging on a rope from a helicopter" (Sprengelmeyer et al., 1999, p. 2455) and noted that he had completed police training while living in the United States only to "'pep up' an otherwise boring stay in that country" (p. 2455).

While the early work of Penfield and colleagues coupled with case studies of S.M., N.M. and others to illuminate amygdala function in the human brain, these findings seem trivial when stacked against results from work with animal subjects. Critically, research with animal subjects fell under fewer ethical constraints than comparable work with humans. In particular, animal researchers were able to violate the cranium and outer cerebrum in testing the surgical, electrical, or chemical influences on the amygdala. The medical dangers to humans prohibited similar

[1] Years after the first case report on S.M., Feinstein et al. (2011) discovered that S.M. was susceptible to fear resulting from *internal* sensation – such as the feeling of suffocation resulting from oxygen deprivation.

studies in health cases. Not until the advent of magnetic resonance imaging in the 1980's were researchers afforded with a viable method of exploring the inner workings of the human brain.

Functional Magnetic Resonance Imaging Investigations of the Human Amygdala

Perhaps due to the initial description of S.M.'s lack of fear (as well as supporting research in similar cases), amygdala research has been dominated by investigations exploring activation in response to information that communicates fear or danger (e.g., faces, voices). Initial studies examining fear impairments in individuals with amygdala damage coincided with a methodological shift towards use of MRI to examine *in vivo* functioning of neurological structures. The advent of blood-oxygen-level dependent (BOLD) contrast imaging sparked a methodology known today as functional magnetic resonance imaging (fMRI), that allows researchers to track regional activity in the brain, or brain "function", by monitoring changes in the flow of oxygenated blood (for a historical review of functional neuroimaging, see Raichle, 1998). From the mid-1990's onward, researchers began using fMRI (as well as positron emission tomography; PET) to examine amygdala activity in response to stimuli.

These studies tend to use a similar approach, known as event-related fMRI (Josephs, Turner, & Friston, 1997), that allows researchers to detect the brain's hemodynamic response to individual stimulus presentations (versus "groups" or "blocks" of stimuli). During an active session, participants will be presented with a series of stimuli (e.g., facial expressions) as the scanner captures time-locked changes in regional blood flow. The flow of oxygenated blood (i.e., BOLD signal) changes in response to metabolic need from brain regions activated in response to the stimulus. Typically, these studies will calculate a composite level of regional activation (e.g., in the amygdala) across trials, and compare this value to a baseline estimate of activation (reflecting the "resting state" of neural activation). The difference between the two is attributed to regional activation in response to the stimulus.

Hundreds, if not thousands of studies have since used fMRI to assess amygdala activation. These studies examine differences across stimulus types (e.g., visual, auditory), emotional valence, specific emotion type, and participant characteristics such as psychopathology. Among adults, research shows substantial variability in amygdala response between individuals, though relative temporal stability time within individuals. Indeed, this makes conceptual sense, given the relative lack of change in amygdala connections or morphometry during this period. Longitudinal changes in responsivity to stimuli would more likely be found across childhood and adolescence, when the amygdala is still developing. Despite a conceptual basis for such investigations, there is a paucity of research examining amygdala activation in children, at least in comparison to the enormous corpus of work with adults.

Researchers are coalescing around an idea that the amygdala may be involved in linking perceptual stimuli to certain emotions (e.g., fear, happiness) depending on that stimuli's cognitive association with positive or negative outcomes for the individual. Some of these links may be inborn or *unconditioned*, as evident when an animal naturally changes behavior in response to signals that a predator may be close. At other times, links between stimuli and emotion may be learned or *conditioned*, such as when a stimulus is repeatedly paired with a consequence. Indeed, investigations into amygdala functionality can be roughly divided according to their focus on unconditioned or conditioned stimuli.

Unconditioned Amygdala Stimulation

Generally Aversive Stimuli

Adults

For the purposes of this discussion, an unconditioned stimulus is one that elicits amygdala activation in most humans without any in-lab conditioning procedure. An example of

such a stimulus is described by Irwin and colleagues (1996), who presented participants with violent, gruesome images such as mutilated bodies, and observed the resulting change in amygdala activation (in comparison to neutral images). The violent images theoretically evoked a sense of imminent risk to life and limb (fear), and indeed, results demonstrated they produced a greater amygdala response than the neutral controls. Reiman et al. (1997) later replicated this effect using aversive film clips (though via positron emission tomography; PET), and Cahill et al. (1996) demonstrated that that amount of amygdala activity during the clips predicted participant recall three weeks later.

Children

Direct replication of this work with children is uncommon, perhaps due to ethical concerns about psychological harm stemming from exposing children to gruesome imagery. However, highly similar research, albeit with different aims, can be found in media effects literature. Public interest in the effects of violent media content on children has spawned studies examining the neural implications. For example, Gentile, Swing, Anderson, Rinker, and Thomas (2016), assessed regional activation as adolescents alternately played violent or non-violent variations of a popular first-person shooter video game. The authors report an interactive effect of content (violent vs. non-violent) and exposure history (greater vs. less history of violent video game play) on amygdala activation. Playing a violent video game elucidated *less* amygdala activation among participants who reported that they regularly played these types of games, compared to those who did not. This study, as well as other fMRI work examining effects of media exposure, suggests the amygdala may be inured to repeated emotion-relevant stimuli, such as violent imagery (Breiter, Etcoff, et al., 1996; Irwin et al., 1996). This finding closely aligns with results from animal subjects showing reduced amygdala activation over the course of repeated presentations of an emotionally salient stimulus.

Emotional Faces

In addition to stimuli such as graphic images that provide a direct signal of danger, a second line of research has assessed amygdala responses to secondary signals, such as observing the fear of another individual. Darwin (1872/1964) posited that human emotions share a common evolutionary origin, and likely represent complex variations on a discrete set of behaviors adapted for their communicative benefits. Indeed, humans are thought to use emotional expressions in communication with greater frequency and complexity than any other species. It makes conceptual sense, therefore, that the human amygdala would be highly responsive to emotionally-relevant information contained in social signals, such as vocal tone or facial expressions. Ekman and colleagues identified six primary affect states that appear universally across cultures, though found the strongest similarities in expression of fear, anger, and happiness (Ekman, 1992; Ekman & Friesen, 1971). Perhaps following from animal subjects' research, or the case studies of patients with selective amygdala damage, the vast majority of work examining amygdala responsivity to human communications has focused on fear.

Adults

In one of the first studies using fMRI to examine amygdala function in humans, Breiter et al. (1996) examined differences in responsivity to fearful and happy, versus neutral facial expressions drawn from a standardized image set (Ekman & Friesen, 1971). Both types of emotional expressions evoked a greater response from the amygdala activity than did neutral faces, though the finding was more robust for fear. The amygdala appeared to habituate to the emotional stimuli, as indicated by a decreased response across trial blocks. In a similar study using PET, Morris et al. (1996) directly compared amygdala activation in response to happy or fearful faces. Substantially higher levels of amygdala activation were observed in response to fear. Moreover, the difference between activation response to fearful and happy faces varied

depending on the "intensity" of the faces. Whalen et al. (1998) used a backwards visual masking procedure to test whether amygdala response depended on conscious interpretation of the stimuli. Though subjects only reported seeing the visual masks (neutral faces), they continued to demonstrate greater amygdala responses to fearful (versus happy) faces. In combination, these findings characterize the amygdala as a module responsible for rapid, unconscious responses to emotionally relevant stimuli. Notably, this is consistent with Zajonc's (1980) landmark model of affective processing that suggests responses to emotionally relevant information are largely automatic, and occur outside of awareness.

Children

These early studies set the groundwork for research testing for developmental differences in the amygdala's response to socioaffective information. Baird et al. (1999) reported significant bilateral amygdala activation in response to fearful faces (versus images comprised of random grayscale pixels) but did not detect any age or gender effects. Kilgore, Oki, and Yurgelun-Todd (2001) examined amygdala responses to fearful faces in a youth sample, and found that activation in the left amygdala (but not the right) declined with age, though only in girls (see also Killgore & Yurgelun-Todd, 2004b, 2004a). However, in a subsequent study, this group failed to detect any age or gender effects in response to fearful faces (Yurgelun-Todd & Killgore, 2006). Thomas et al. (2001) compared amygdala response to fearful and neutral faces across adult and youth participants. Whereas adults exhibited greater bilateral activation in response to fearful faces relative to neutral faces, the reverse was true of children, who showed greater activation with *neutral* faces than with fearful faces. Monk et al. (2003) reported the opposite - that adolescents, but not adults, showed greater activity in response to fearful faces relative to neutral. Guyer et al. (2008) compared amygdala responses to fearful faces in larger groups of adolescents and adults (n ~30 for each). Teens showed greater bilateral activation than did adults, though

within-group effects of age were non-significant. Hare et al. (2008) examined age-related differences in amygdala activation in the context of an emotional faces Go-NoGo task. Consistent with Monk et al. (but not Thomas et al.) this study found greater activity in response to fearful faces among adolescents than adults. The authors, however, posit a curvilinear trend in across age, noting that *pre*-adolescents in their sample did not differ from adults in amygdala response to fearful faces.

Conditioned Amygdala Stimulation

Although much of this early research focused on biologically based conditioning, such as fear resulting from images of mutilated bodies, many other studies have examined amygdala activation in the context of an acquired response to stimuli. LaBar et al. (1998) monitored amygdala activation during a fear-conditioning paradigm that paired an electric shock (unconditioned stimulus) with an image stimulus (conditioned stimulus) presented in a pseudorandom series with a control image. Amygdala activation was elevated early in the acquisition and extinction of the fear response, mimicking a corresponding trend in autonomic arousal. Büchel, Morris, Dolan, and Friston (1998) conducted a similar experiment pairing an aversive noise-blast with select images in a series of neutral facial expressions. Participants again showed elevated amygdala activity during acquisition, though this faded rapidly as the amygdala appeared to habituate. Morris et al. (1998) observed amygdala activity in response to a fear conditioning paradigm that paired aversive noise to masked (i.e., not consciously perceived) angry facial expressions, and further confirmed elevated amygdala activity during acquisition. The amygdala's involvement in subconscious responses to information indicates that it may be part of an adaptively developed automatic or "default" response.

A similar line of research examined amygdala responses to stimuli whose "aversiveness" stemmed from psychopathology. Breiter et al. (Breiter & Rauch, 1996; 1996) used fMRI to

assess amygdala activity in a sample diagnosed with obsessive-compulsive disorder (OCD). During initial acquisition of baseline levels of brain activity, the OCD participants (and individually matched normative controls) were asked to hold an innocuous stimulus (e.g., a "clean" towel). This stimulus was then replaced with a similar "provocative" stimulus (e.g., a "dirty" towel). As anticipated, OCD patients showed much stronger limbic (i.e., amygdala) activation during provocation than did controls. The findings suggest that elevated amygdala activation in response to threatening stimuli may be an important cause or correlate of psychopathology. Similar research implicates abnormal amygdala responsivity in depression, anxiety, social phobia, and post-traumatic stress disorder (Birbaumer et al., 1998; Drevets et al., 1992; Rauch et al., 1996; Shin et al., 1997).

In comparison to adults, considerably fewer studies have examined amygdala activity during aversive conditioning among youth or explored how this changes across development. Whereas most aversive conditioning research with adult or animal subjects relies on electroshock, this approach presents ethical and practical issues in research with child participants. Alternative stimuli, such as noise blasts, air puffs, or discordant tones are more commonly used with children, however, these methods may lack the potency necessary to condition a response (Glenn et al., 2012). Currently, the bulk of research into aversive conditioning or 'fear learning' appears to occur with youth presenting with disrupted affective processing, such as cases with anxiety or callous-unemotional traits. Research examining fear learning processes in normative youth is uncommon. Few studies (if any) have explored developmental differences in the neurological processes underlying the acquisition of fear-conditioned behavior, particularly among typically developing youth. Given the accumulating evidence that the amygdala plays a role in affective responses to innately conditioned stimuli,

exploration of its influence in responding to externally conditioned stimuli, particularly across development, is a logical continuation of current efforts.

In the 200 years since Burdach's discovery of a small grayish mass in the deep medial temporal lobe, appreciation of the amygdala's role in the human experience grew by leaps and bounds. Today, the amygdala appears to be a critical component of a system involved in how we process and respond to affective stimuli. Developmental psychologists recognize childhood as a period of remarkable change in socioemotional functioning. Theoretically, the maturation of the amygdala may underlie changes in children's ability to acknowledge, regulate, and learn from emotional experiences. Yet, in the early 1990's, neuroscientists possessed a limited understanding of *any* neurological changes across childhood. Knowledge stemmed almost exclusively from reports on small samples of post-mortem pediatric brains (Lenroot & Giedd, 2006). The following section describes advances stemming from the widespread use of anatomical MRI, and ongoing work linking brain changes in childhood to broader physical development.

CHAPTER 3. AMYGDALA DEVELOPMENT

Early Small Sample Studies

Initial studies using both MRI and CT first appeared in the late 1970's, and provided qualitative reports of age-related differences in scan images (Arimitsu, Di Chiro, Brooks, & Smith, 1977; Barkovich & Kjos, 1988; Barkovich, Kjos, Jackson Jr, & Norman, 1988; Holland, Hnaas, Norman, Brant-Zawadzki, & Newton, 1986; M. A. Johnson et al., 1983; Kleinman, Zito, Davidson, & Raptopoulos, 1983; Levene et al., 1982; McArdle et al., 1987a, 1987b). This early research provided notable breakthroughs, particularly in regards to myelination changes across development. In images acquired using conventional MRI, the higher water content of myelinated axons in white matter causes it to appear brighter than surrounding tissue. Qualitative reports of scan changes across early development illuminated the rostral-to-caudal progression of myelination beginning in the first year of life. Prior to the onset of myelination, the contrast between grey and white matter in the brain is *reversed* (due to the lack of myelin), and white matter tracts appear comparably darker than other regions (Barkovich et al., 1988).

New insights came about in the early 1990's, as researchers overcame the initial barrier of extracting reliable numeric information scan images (Lenroot & Giedd, 2006). Whereas early studies relied on qualitative descriptions of visual differences across scans, new methodologies allowed researchers to quantify those differences, and enter them into statistical models. Jernigan and Tallal (1990) performed one of the first quantitative neuroimaging studies to include children, reporting on scans acquired from a normative sample of nine children (ages 8-10) and 15 adults, and finding that cortical grey matter appeared to decline with age. In a follow-up study, Jernigan, Trauner, Hesselink, and Tallal (1991) examined scans from 39 individuals (ages 9 to 35), and identified age-related decreases in frontal and parietal lobe volumes, largely driven

by loss of grey matter. This decline extended to subcortical gray matter structures that showed similar reductions in volume with age. Pfefferbaum et al. (1994) reported age-related differences from a larger sample of 88 individuals aged 3 months to 30 years of age, though predominantly in adolescence (mean age 14 years). Results similarly showed an age-related decrease in grey matter, though also a significant increase in white matter.

Reiss, Lee, and Freund (1994) conducted one of the earliest studies examining age-related variation in amygdala volumes among typically developing youth. These 26 children (6 females; mean age 10.3 years) were included as normative controls in a project examining neuroanatomic variations associated with fragile X syndrome. Temporal lobe structures were quantified and evaluated for both between and within-group effects. Although numerous age-related differences were identified among youth with fragile X, no effect of age was observed for typically-developing youth (a positive correlation between right hippocampal volume and age was marginally significant). Reiss et al.'s description of image processing methods, as well as a clear delineation of operational boundaries for their regions of interest provided a major contribution to pediatric neuroimaging. However, their null findings in regards to normative youth contradict the aforementioned research suggesting that grey matter decreases with age. This suggests the possibility that temporal lobe structures exhibit a unique developmental trajectory. Alternatively, the study may have lacked the power necessary to detect effects in small-volume structures, such as the amygdala. Subsequent research would suggest both to be true.

Giedd and Colleagues Examine Large Samples of Healthy Youth

Due to either conceptual or methodological limitations, research in this era generally focused on gross deviations in neuroanatomical development. Severe and easily discernible abnormalities in the brain are a logical starting point for researchers seeking to link

neuropsychiatric disorders to neural structure. Still, brain development is fractal in nature, incorporating change at very large and very small scales. By the mid 1990's, evidence had accumulated suggesting that disorders might also stem from more subtle differences in neural development. However, interpretation of these studies suffered due to limited power to detect effects of smaller volumetric differences on behavior (Lenroot & Giedd, 2006). Investigators further lacked a well-defined reference for how the "normative" brain developed. Though researchers had long acknowledged the brain increased in size from birth through adulthood (Dekaban & Sadowsky, 1978), the developmental trajectories of individual brain regions remained unclear.

Some of this information could be pieced together from the many cross-sectional (and handful of longitudinal studies) reporting data from typically developing controls. However, there continued to be a need for research examining normative trends in brain development using a sample large enough to power detection of small anatomical variations across age. Giedd et al. (1996) further justified the need for such an investigation by describing an ongoing methodological problem in current work. Neuroimaging research comparing subject and control groups regularly relied on a radiologist to review scans collected for clinical purposes and designate them "abnormal" or "normal," respectively. This approach has two issues. First, individuals with diagnostic status are more likely to be referred for clinical scans, and are therefore overrepresented in the pre-sorted subject pool. Second, and relatedly, smaller anatomical differences may not be apparent to the naked eye (even that of a trained radiologist), but influence behavior in ways only apparent when these differences are aggregated across a larger group of individuals. In effect, this means that radiologists' may have been inadvertently

designating some children with “abnormal” brain structures as “normal”, and vice versa (Giedd, Snell, et al., 1996; Lenroot & Giedd, 2006).

In a series of publications, Jay Giedd and colleagues reported on analyses from an initial collection of scans from approximately 100 youth (sample size varies across reports) collected as part of a massive, ongoing, neuroimaging project conducted at the National Institute of Mental Health Giedd, Rumsey, et al., 1996; Giedd, Snell, et al., 1996, 1996; Lange, Giedd, Xavier Castellanos, Vaituzis, & Rapoport, 1997). Rather than rely on scans acquired for clinical purposes, Giedd et al. (1996) used local advertising to recruit normative youth from the community. Children not excluded through a preliminary phone screening were asked to complete a more detailed in-person assessment to identify and exclude any participants who did not meet specified criteria characterizing “typical development” (see Giedd, Snell, et al., 1996). A final sample of approximately 100 children was included in the study, with a roughly equal split of male and females. Intelligence, academic achievement, height, weight, and pubertal development (Tanner stage) were assessed in each participant. Multiaxial anatomic scan images were obtained via spoiled-gradient recalled-echo on a 1.5T GE scanner, using slice thickness of either 1.5mm (axial and sagittal planes) or 2.0mm (coronal). Several cross-sectional studies were published from these data, variously describing age-related differences in the cortical and subcortical structures (Giedd, Rumsey, et al., 1996; Giedd, Snell, et al., 1996; Giedd, Vaituzis, et al., 1996; Lange et al., 1997).

Giedd, Vaituzis, et al. (1996) specifically examined age-based variation in structures of the temporal lobe. The emotive and cognitive functions served by subregions of the temporal lobe, such as the amygdala, are well known to change dramatically from early childhood through adulthood. Though researchers had yet to examine age-related differences *in vivo*, a

corresponding pattern of morphometric change in supporting structures seemed likely. Further, evidence suggested that these changes might be triggered by the hormonal fluctuations accompanying child development. Murphy et al. (1993) found smaller temporal gray matter volume in women with Turner syndrome, a genetic condition involving gonadal dysgenesis, disrupting production of steroid hormones (Sybert & McCauley, 2004). Several studies with murine models suggested that cells of the amygdala might be sensitive to sex steroids, particularly estrogen (Hines, Allen, & Gorski, 1992; McEwen, 1981; Mizukami, Nishizuka, & Arai, 1983). Drawing on these findings, Giedd et al. (1996) anticipated sex-specific differences in temporal lobe structures, including the amygdala, across age. Accordingly, the most rapid changes and most exaggerated sex-specific effects were anticipated to occur during adrenarche, when the endocrine system is highly active.

Although boys showed slightly (but significantly) larger temporal lobes than girls, this result was largely attributable to difference in cortical tissue, rather than subcortical structures. Though main effects of gender or age on volumes of the temporal lobe or its component structures were non-significant, the authors report an interaction between the two. Specifically, the hippocampus increased in size with age, but only for females. Conversely, left amygdala volumes were positively correlated with age, though only in males. However, no effect of age on temporal lobe volume was observed, nor an effect of gender on substructure (e.g., hippocampus, amygdala) volume across development. Inspection of the scatterplots failed to reveal any exaggerated change around average ages of onset for adrenarche in girls or boys, contrary to hypotheses.

Notably, though Giedd et al. describe assessing Tanner stage (pubertal status) in their methodology, they chose to use age in years in their analyses. Whereas age is a temporal

measure of time since birth, pubertal status is a continually changing marker of biological development. The timing and tempo of these changes can vary by several years (Dorn & Biro, 2011; Parent et al., 2003), making age a somewhat imprecise index of developmental progress. Giedd et al.'s decision to use age in their analyses may have contributed to their failure to detect the hypothesized changes in temporal lobe structures near the onset of puberty. This issue of pubertal status versus age as a temporal index continues to re-appear in developmental neuroscience (Goddings et al., 2014a, 2014b), as will be shown below.

Contemporary Studies of Neurodevelopment

Since Giedd et al. (1996), numerous smaller studies have reported age-related differences in amygdala volumes among typically-developing youth. The bulk of data comes from work including normative youth as control participants, though some studies have specifically focused on normative processes of neurological development. Weems et al. (2013; 2015) summarized findings linking age with amygdala volumes, and found the collective results to be strikingly inconsistent. As described above, Giedd et al. (1996) initially reported a positive correlation between age and amygdala volume in a sample of youth ages 4 - 18, but only for boys, and only on the left side. In the two decades since, work with similar age ranges has variously found the same association, reverse effects of age as well as gender or laterality, or no link with age at all (Chen et al., 2004; Karchemskiy et al., 2011; Schumann et al., 2004; van der Plas, Boes, Wemmie, Tranel, & Nopoulos, 2010).

Chen et al. (2004) compared the size of temporal lobe structures in patients with bipolar disorder (BD) and normative controls ranging in age from 10 1996 21 years. Among healthy controls, age was linked to smaller left amygdala volumes (r = -.48, p = .03), yet right amygdala volumes did not tend to vary. Schuman et al. (2004) contrasted amygdala and hippocampal volumes in a sample of boys with autism diagnoses with same-gender typically developing

controls (ages 10 – 16). Though results again indicated a significant effect of age on amygdala volumes in control youth, the effect was reversed. Age was now associated with *larger* amygdala volumes. Moreover, in contrast to Chen et al. (as well as Giedd et al., 1996), the effect of age now appeared in both the left and right amygdala ($r = .77$; $p < .05$, and, $r = .67$; $p < .05$, respectively). Van der Plas et al.(2010) reported amygdala volumes in a normative sample of 116 boys and girls. Results were similar to those found by Giedd and colleagues, in that age was associated with greater amygdala volume in boys ($r = .36$, $p < .05$), though in the right amygdala instead of the left. Karchemskiy et al. (2011) compared amygdala volumes in youth ages 9 – 19 deemed at-risk for BD (i.e., offspring of parent(s) with BD, yet, no history of manic episode), controls approximately matched on gender, age, and IQ. These studies illustrate the state of research examining age-related differences in the amygdala, and are representative of a broader trend in developmental neuroscience over this period. Despite numerous publications culminating from major investments by researchers and participants, a comprehensive understanding of the amygdala's changes across development remained elusive.

Uematsu et al. (2012) provide one of the most comprehensive cross-sectional investigations of the association between amygdala (as well as hippocampal) volumes and age (though see also (Østby et al., 2009), who report a slight increase in bilateral amygdala volumes with age). The authors included scans from participants ranging in age from 1 month to 25 years. Scatter plots of volume by age reveal similar, but not uniform, curvilinear trends in left and right amygdala growth, with subtle differences across boys and girls. For both genders and literalities, amygdala volumes increase rapidly in infancy. The pace of growth decelerates in toddlerhood, and the curvilinear trend reaches an inflection point at approximately 5-6 years of age. Volume continued to increase until middle childhood (age 8-9), largely plateaus during adolescence, and

may then decline in early adulthood. Growth rates of each amygdalae tapered off earlier in girls than boys. Relatedly, amygdala volumes peaked roughly 18 months earlier in girls (11.4 and 9.6 years, respectively) than in boys (12.6, 11.1). Both findings are consistent with a larger body of work suggesting that overall, girls brains reach peak volume more rapidly, though remain smaller in volume compared to boys (Giedd et al., 2008; Giedd, Snell, et al., 1996; Lenroot et al., 2007).

One of the most recent attempts to identify age-related changes in the amygdala comes from Albaugh et al. (2017), who examined data gathered from a large, normative youth sample gathered as part of the National Institutes of Health MRI Study of Normative Brain Development (described below in Methods). Scans were initially acquired from a Census-representative sample of typically-developing youth ages 4-18, and repeated on up to three separate visits at two-year intervals (n =371, scans = 723). Collection occurred at a geographically distributed network of study sites across the US. Of the many criteria used to define typical development, the investigators chose to exclude youth with mental health problems (i.e., any subscale score on the Child Behavior Checklist > 70), effectively limiting the range of symptom severity in the sample.

Albaugh et al. (2017) used mixed-methods modeling to test for differences in amygdala volumes as an effect of age, as well as any moderating effect of sex or CBCL subscale score (specifically Aggression, Anxiety/Depression, and Attention Problems). Total brain volume and scan site were entered into the model as covariates, to adjust for individual differences in brain size and site-wise effects, respectively. A linear model of amygdala development across age showed superior fit over competing quadratic and cubic models, with volumes increasing across age. Amygdala volume appears to increase with age, though the authors do not provide statistics

to quantify the effect.[2] Similarly, the authors report a significant effect of sex on volume trajectories, though do not provide a value. Interestingly, despite the restricted range in mental health symptom severity, scores on the Anxiety/Depression subscale of the CBCL were positively associated with total amygdala volume.

Puberty as an Index of Development

The research reviewed above shares a common goal: identification of the normative changes in the amygdala across development. Each of these studies attempts to identify a trend line from data points corresponding to amygdala volumes at different ages. Collectively, these studies suggest there is *some* change in the amygdala across development. However, results variously suggest the change is positive or negative, linear or curvilinear, and specific to the left or right amygdala, in either boys or girls. The findings presented by Albaugh et al. (2017) provide one of the most authoritative perspectives on amygdala development, given the comprehensive methodology and large sample size. As in previous studies, the amygdala volumes are considered with respect to age in years, and the results depict a linear increase from early childhood through adulthood.

However, the use of age as an index of brain development may be contributing to the chronic inconsistency in results. Morphometric changes in brain structures are strongly influenced by the biological mechanisms acting in concert to effect human development. The growth trend in the amygdala is likely a proximate effect of these processes, specifically, the neuroendocrine influence on the developing brain (Goddings et al., 2014b). Critically, these mechanisms do not abide by chronometric time, but instead progress at a pace that varies both between and within individuals. Although age is a more reliable index of biological development

[2] The significance of model parameters is reported, though the parameter values are not.

in the first years of life, the association is increasingly attenuated beyond early childhood. The cumulative effects of environmental, genetic, and epigenetic influences cause substantial variation in the timing and tempo of human growth. As a result, children of the same age are likely to show significant variance in their developmental status. However, by considering brain growth in relation to age, researchers implicitly assume that all youth of a given age will be at the same point in development. Variance resulting from developmental differences across youth of the same age is discounted, resulting in a loss of precision.

Gonadarche and the amygdala

Puberty refers to a process of major physiological and psychological development occurring between early childhood and young adulthood, guided in part by the independent processes of adrenarche and gonadarche (Blakemore, Burnett, & Dahl, 2010). Of the two mechanisms, gonadarche is the subject of considerably more brain-related research. Beginning around 9-10 in girls, and shortly thereafter in boys, gonadarche refers to maturation of the gonads, and the associated increase in production of sex steroids (Witchel & Plant, 2014). Gonadal release of testosterone stimulates genital growth in males, and estradiol initiates reproductive processes (menstruation, ovulation) and development of secondary sex characteristics in females (Shirtcliff, Dahl, & Pollak, 2009).

There is some evidence to suggest that increased released of sex steroids in the context of gonadarche may underlie changes in the amygdala. Neufang et al. (2009) detected sexual dimorphism in the amygdala volumes of a youth sample (n = 30), and found these differences were attributable to testosterone levels in the blood. Herting et al. (2015) subsequently examined longitudinal effects of sex steroids on subcortical brain volumes. A three-way time by sex by testosterone interaction predicted right amygdala volumes. In boys, higher levels of starting testosterone were associated with decreasing amygdala volumes across adolescence.

Comparatively, lower testosterone levels in both boys and girls, predicted an *increase* in amygdala volumes across adolescence. Estradiol exhibited the reverse effect in girls. High levels of estradiol were linked to increases in amygdala volume, though low levels predicted decreases. Both studies illuminate the potential effects of sex steroids on the growing amygdala, and make the case for broader, longitudinal research examining neuroanatomical change in the context of pubertal development.

Adrenarche and the amygdala

Adrenarche refers to the maturation of the zona reticularis of the adrenal gland, and is thought to occur between ages six and nine in girls, and a year later in boys (Byrne et al., 2017). Maturation of the adrenal gland is triggered by upstream components of the hypothalamic-pituitary-adrenal (HPA) axis (Barendse et al., 2018), and is associated with gradually increasing release of adrenal androgens dehydroepiandrosterone (DHEA), its sulfate (DHEA-S), and testosterone (Styne & Grumbach, 2016). Increasing concentrations of DHEA contribute to the first appearance of secondary sex characteristics, such as the transition from fine, light vellus hair to thicker, darker terminal hair in the axillary and pubic regions (Randall et al., 2000). Indeed, the appearance of such hair is a commonly used indicator of adrenarche.

The neuroanatomical effects of adrenarche are less well understood than those of gonadarche. Much of the current knowledge surrounding the effects of adrenarcheal hormones on neurodevelopment stems from animal subjects research. Results from murine models suggest that DHEA, DHEA-S, and testosterone may encourage the growth and survival of neurons (Fargo, Galbiati, Foecking, Poletti, & Jones, 2008; Maninger, Wolkowitz, Reus, Epel, & Mellon, 2009). These hormones have been implicated in theoretical models positing their role in lasting change in the activation and organization of brain regions (Schulz, Molenda-Figueira, & Sisk, 2009; Phoenix, Goy, Gerall, & Young, 1959). Yet, though adrenarcheal hormones appear to

influence neurological development in non-primates, the specific phase of adrenarche is thought to be specific to humans and great apes (Campbell, 2011). Few studies have attempted to elucidate the impact of these hormones in the context of adrenarche. Nguyen et al. (2013) reported a positive association between DHEA and gray matter (cortical thickness) in the right temporal lobe among 4 to 13-year-olds. Klauser et al. (2015) identified a negative correlation between DHEA and white matter. To my knowledge, these studies represent the bulk of investigations into the biological links between adrenarche and neurological development. I am unaware of any research examining the effects of adrenarcheal hormones on the amygdala in humans, specifically.

Neuroimaging research links puberty and neurodevelopment

Goddings et al. (2014b, 2014b) conducted a rare, longitudinal investigation of neurodevelopmental change across puberty, using data from the NIMH longitudinal brain imaging project (described above; see Giedd, 2008; Giedd, Snell, et al., 1996). The sample was derived from the larger project data bank, and included 275 typically developing youth (42% female), who, a) were scanned two or more times between the ages of 7 – 20, b) provided age and pubertal status at each scan, and c) were unrelated to other participants. MRI scans were acquired using a 1.5T GE scanner acquiring multiaxial sequences of T1-weighted images at contiguous 1.5mm slices (2.0mm coronal). Tanner stages were used as a proxy measurement of pubertal development. Tanner (1962) originally described five stages of puberty (1 – 5) reflecting progressively increased visibility of secondary sex characteristics (pubic hair growth, breast development; Shirtcliff et al., 2009). In Goddings et al. (2014b, 2014b), researchers used picture-based interviews using illustrations depicting physical changes at each stage (S. J. Taylor et al., 2001) and asked participants to identify the state that best described their own level of development. Although self-report methods of assessing pubertal status demonstrate only modest

concordance with gold-standard physical examination, they may be more feasible for youth research conducted outside a clinical setting (Shirtcliff et al., 2009).

Goddings et al. (Goddings et al., 2014a, 2014b) used mixed effects modeling to examine the growth process of several subcortical structures across pubertal development. Initial analyses examined Tanner stage as a predictor of growth trajectory in linear, curvilinear, and cubic models tested separately across males and females. Pubertal development and age are not equivalent, though they are highly correlated. Therefore, analyses tested whether addition of age, and an age by Tanner stage interaction term improved the model's fit to the data, suggesting those terms accounted for incremental variance. A general increase in amygdala volumes was observed, though the form of the change varied across males and females. A second-order (curvilinear) model best captured amygdala change in females, where a positive slope in early puberty reached an undulation point by stage 3, and appeared to plateau thereafter. A cubic effect of pubertal status on volume was seen in males, where a null slope became positive around stage 2, and appeared to plateau again at stage 4. For both sexes, age accounted for incremental variance beyond Tanner stage in predicting change in amygdala volume.

The findings provided by Goddings et al. (2014b, 2014b) provide two major advances to developmental neuroscience. First, the findings further illustrate the dynamic changes in the brain across development. The use of a longitudinal approach provides for a more authoritative examination of how subcortical structures increase or decrease in size as children progress from early childhood to adulthood. The enormous resources necessary to undertake a large-sample longitudinal investigation of brain changes across puberty has tended to prohibit similar research. Second, by focusing on change across pubertal development, Goddings et al. encourages researchers to move beyond questions of "what" in brain development, and towards explorations

of "why." Arguably, the two are mutually informative. By considering change across puberty, instead of chronological age, neuroscientists can tap into the knowledge of psychoendocrinology to identify corresponding fluctuations in hormone levels. Merging these two areas of knowledge may allow for more rapid advances in developmental neuroscience, particularly with regard to regions such as the amygdala, which are increasingly thought to play a major role in thought, feelings, and behavior across the lifespan.

There appears to be clear evidence that the amygdala undergoes extensive morphological change across childhood and into early adulthood. However, the nature of this change remains unclear. Despite seminal research in this area, and recent advances using large-sample datasets, reports on the trajectory of amygdala development continue to be inconsistent, with researchers describing linear, curvilinear, and null effects (Albaugh et al., 2017; Giedd, Vaituzis, et al., 1996; Goddings et al., 2014a, 2014b; Uematsu et al., 2012). Moreover, research examining change in the amygdala in relation to broader trends in physiological maturation remains limited. Emerging evidence suggests that morphometric changes in the amygdala may be driven in part by hormonal products of puberty. Examining change in relation to pubertal progress may provide further clarification. While this has been undertaken in cross-sectional work (Goddings et al., 2014a, 2014b), there is a need for longitudinal research that can more clearly elucidate patterns of change across time. Similar research examining durative changes in brain structures has suggested that neurodevelopment may be moderated by environmental influences, particularly exposure to psychosocial stress. Indeed, cross-sectional and short-term longitudinal research suggests a similar finding with regards to the amygdala (Tottenham et al., 2010; Weems et al., 2015, 2013). Yet, as in research with normative amygdala development, the specific effects of

stress remain unclear (Weems, 2017). In the following section, I discuss work linking stress and brain development generally, and focus on the amygdala specifically.

CHAPTER 4. STRESS AND AMYGDALA DEVELOPMENT

Our understanding of normative processes in cognitive, emotional, behavioral, and neurological development has been critically informed by research examining how these areas are affected by adversity (McLaughlin, 2016). Scientists are now using the insights offered by neuroimaging to identify links between extreme adverse childhood experiences and neurodevelopment (Teicher & Samson, 2016). This is a logical starting point for research, as extreme environments are likely to present the most extreme, and easily observed effects. However, investigation is now broadening to include the neurobiological effects of less disruptive, but considerably more commonly experienced influences such as parenting characteristics and socioeconomic disadvantage (Hackman & Farah, 2009; S. B. Johnson, Riis, & Noble, 2016; Whittle et al., 2017).

It is well accepted that chronic or severe exposure to intense psychosocial stress can have myriad influences on the developing brain (De Bellis, 2001; De Bellis et al., 1999, 2002). As a central component of the affective system, the amygdala may be uniquely influenced by life stress. The amygdala is closely intertwined with the hypothalamic-pituitary-adrenal (HPA) axis, which initiates a systemic stress response in the body. Products of the HPA axis may subsequently alter the function of the amygdala (Ulrich-Lai & Herman, 2009), a process which may underlie findings showing abnormal amygdala activity in the aftermath of traumatic stress (Hughes & Shin, 2011). Similar research is linking such exposure to durative morphological changes in limbic structures such as the amygdala (Teicher & Samson, 2016). However, this pattern of structural and functional effects is markedly more complicated in youth, where stress may further influence the amygdala's development (Weems, 2017). Although longitudinal research is limited, there is theoretical support for the notion that early childhood adversity may

fundamentally alter the curvilinear growth trajectory of the amygdala described by Uematsu et al. (2012) among others.

Certainly, the adverse effects of neglect and maltreatment on normative child development are undeniable. Broadly, developmental science has tended to dichotomize early childhood environments as "harsh", including maltreatment and neglect, or "normative". In actuality, adversity is a dimensional concept, and most, if not all, children will experience it in some form at some point in their lives. Neglect and maltreatment certainly constitute an extreme form of adversity, though they do not wholly encompass the concept. Developmental scientists are now calling for broader attention to more subtle forms of adversity, such as parenting quality and socioeconomic disadvantage (Belsky & de Haan, 2011; S. B. Johnson et al., 2016). However, at this point links between these constructs and neurodevelopment are largely theoretical, despite the firmly established links to cognitive and emotional processes (Whittle et al., 2017).

Moreover, there is a need to look at ecological influences outside of the microsystem, particularly the impact of socioeconomic status. In the United States, approximately 1 in 5 children live in poverty, and close to 40% live in near-poverty (DeNavas-Walt & Proctor, 2014; S. B. Johnson et al., 2016). There is a paucity of research examining the effects of socioeconomic disadvantage on the developing brain. Specifically, there is limited knowledge about how poverty impact the timing and tempo of brain development. This stems largely from a lack of longitudinal research considering socioeconomic status as a moderating factor.

Stress and the Brain

Exposure to a stressor provokes an adaptive change in bodily systems that begin to marshal resources in anticipation of a response. The concept of stress is variously defined, but here we will characterize it as the dynamic change resulting from exposure to a stressor – a

threatening event or stimulus (McEwen, 2000b). At rest, the body operates in a state of homeostasis. Various bodily systems operate in a "default" mode (homeostasis) that balances resource conservation and expenditure in a manner adaptively calibrated for the environment (McEwen, 1998, 2000a). A sufficiently strong stressor will cause the body to initiate a two-pronged "stress" response. Initially, the autonomic nervous systems will rapidly (on the order of milliseconds to seconds) moderate functioning of the pulmonary and circulatory systems, readying the body for reaction. If the stressor is sustained (minutes to hours), the body will augment resources by engaging the hypothalamic-pituitary-adrenal axis (HPA axis). This neuroendocrine triad employs a cascade of chemical signals which ultimately trigger the adrenal gland to produce glucocorticoid steroid hormones (Gunnar & Quevedo, 2007; Loman & Gunnar, 2010).

The amygdala is understood to be a primary catalyst for activation of the HPA axis. As described by LeDoux (2007), sensory information converges on the amygdala by way of multiple neural pathways that process the signals through varying levels of cognitive processing. If these stimuli are interpreted as a threat to safety and stability, the amygdala signals the hypothalamus, where cells begin production of corticotropin-releasing hormone (CRH). The presence of hypothalamic CRH stimulates the production of adrenocorticotropic hormone (ACTH) from the anterior pituitary (Loman & Gunnar, 2010). ACTH binds to receptors on the adrenal cortex (superior to the kidneys), initiating the secretion of glucocorticoids into the bloodstream. Cortisol is the main glucocorticoid in humans, and exerts a complex constellation of physiological effects on the human body that serve allostatic and homeostatic functions (Sapolsky, 2004). Excretion of cortisol into the blood stream allows it to return to the brain, where its small size and lipid solubility allows it to diffuse across the blood brain barrier (Banks,

2012). The presence of cortisol down-regulates activation of the anterior pituitary and hypothalamus, providing negative feedback that regulates the HPA axis (Loman & Gunnar, 2010).

Ultimately, the effects of the HPA axis return to the start. As cortisol levels in the brain rise, these molecules bind to glucocorticoid receptors located on CRH-expressing cells in the central amygdala (CeA). Stimulation of these cells triggers local release of CRH, and may modulate intracellular changes associated with fearful and anxious behaviors (Davis, 1992; Kolber et al., 2008; Makino, Gold, & Schulkin, 1994; van Bodegom, Homberg, & Henckens, 2017). CRH molecules attach to receptors in the basolateral amygdala complex (BLA), and activate cellular mechanisms that may underlie consolidation of emotional memories (Roozendaal, Brunson, Holloway, McGaugh, & Baram, 2002). Cells of the CeA release CRH locally in the region of the amygdala, but also remotely, through (indirect) projections to the hippocampus. The added concentration of CRH in the hippocampal region augments the output of the HPA axis (i.e., cortisol; Herman & Cullinan, 1997; Tottenham & Sheridan, 2009). Summarily stated, cortisol output by the HPA axis triggers changes in the amygdala related to its effects on memory and emotional behavior, and drives the amygdala to *further* enhance activity in the HPA axis. This circular effect of the amygdala on the HPA axis is consistent with theory conceptualizing this region's involvement in behavioral and emotional responses to fear and anxiety (Gray & McNaughton, 2000).

Particularly in the amygdala, chronic interaction with the HPA axis, and lasting high concentrations of CRH, are known to produce cellular changes. Though researchers regularly refer to the long-term effects of the HPA axis as "excitotoxic," this is arguably a misnomer as these effects may be excitatory, but not necessary toxic – which would imply an effect of

apoptosis (though see Ding, Han, & Shi, 2010). Rather, chronic exposure to the products of the HPA axis may cause cellular and structural changes that recalibrate the limbic system's response in manner that provides adaptive short-term benefits (though potential long-term difficulties) in a highly stressful environment (Del Giudice, Ellis, & Shirtcliff, 2011). These changes in excitability may stem from a more complex regional remodeling of amygdala neurons. Chronic stress has been linked to increased dendritic arborization of the basolateral amygdala (Vyas, Mitra, Rao, & Chattarji, 2002), a region critically involved in fear-based emotional learning (Fanselow & LeDoux, 1999). Regular exposure to CRH (produced locally by the amygdala) may sensitize neurons in the central amygdala, potentiating the downstream effect of the amygdala on the hypothalamus sensitization effect (Ulrich-Lai & Herman, 2009). These and other stress-linked changes in the amygdala are rooted in a fundamental cellular restructuring, which may drive broader morphological changes (Tottenham & Sheridan, 2009; Weems, 2017). Broadly, research examining the influence of adulthood stress on the brain generally supports the notion that HPA axis activation affects the amygdala. Despite some inconsistency in the results, there is a general consensus that adult stress is linked to a smaller, more reactive amygdala (Armony, Corbo, Clément, & Brunet, 2005; Liberzon et al., 1999; Rauch et al., 2000; Tottenham & Sheridan, 2009).

Stress and the Developing Amygdala

Although findings relating stress to the amygdala, specifically, have been ambivalent, there is stronger evidence for the impact of stress on the broader limbic system. Given these general findings, it would seem reasonable that similar effects of stress on limbic structures would be visible among stress-exposed youth. However, results in these studies have been as inconsistent, if not more, than those in research with adults, particularly with regard to the amygdala. Weems (2017) reported on six studies testing differences in amygdala volumes across

trauma-exposed and non-exposed youth. De Bellis et al. (1999) compared PTSD-afflicted youth with maltreatment histories, and a control sample, finding no differences in amygdala volumes. Subsequent studies conducted by De Bellis and colleagues similarly failed to detect amygdala volume differences among independent samples (De Bellis et al., 2000, 2002). In contrast, Mehta et al. (2009) reported larger right amygdala volumes (vs. controls) in a group of adolescent Romanian adoptees. Carrion et al. (2001) reported a trend towards smaller amygdala volumes in trauma-exposed youth.

Tottenham et al. (2010) examined whether the stress of poor caregiving in early life would be linked to morphological differences in the human amygdala. The authors acquired anatomical scans and behavioral assessments from 34 children who had experience prolonged institutional care in early life prior to being adopted (as well as non-institutionalized controls). These youths appeared to demonstrate a predilection towards mental illness (50% met diagnostic criteria for at least one psychiatric disorder), and anxiety disorders in particular (18%), findings supportive of early life amygdala dysfunction. Moreover, institutionally reared youth showed a predilection towards internalizing behaviors and anxious cognitions, as indicated by behavioral measures and results from a Go-NoGo Task. Amygdala volumes were extracted from 1.5T scan images and adjusted for cortical volume. Children who spent more time in institutional care tended to show larger amygdala volumes, $F\,(1,33) = 8.43$, $p < .007$. This remained significant even after children with diagnosable anxiety disorder were removed from the sample, suggesting it was not exclusively driven by this subgroup. Comparisons of early-adopted and late-adopted youth (before or after 15 mos.) with matched controls revealed that amygdala were significantly larger in late-adopted youth, who spent more time in institutional care.

The inconsistencies in the broader literature on the amygdala and pediatric trauma suggest the need to consider differential effects of stress across development. By early adulthood, the maturational course of the amygdala begun in infancy is thought to have reached its end (Uematsu et al., 2012). The differences in amygdala volumes among stress exposed adults can therefore be reasonably attributed to the effects of stress, specifically the products of the HPA axis. However, this is not the case in youth, where the amygdala appears to undergo morphological change throughout development (Uematsu et al., 2012; Wierenga et al., 2014). Research with youth must acknowledge that stress may have bipartite effects on the amygdala. Similar to adults, stress exposure could have an immediate, short-term impact on amygdala morphology (Weems, 2017). However, as depicted by Tottenham et al. (2010), exposure to stress might also exhibit a long-term effect by altering the biological programming dictating amygdala development.

If stress can shift the trajectory of amygdala development, then timing of exposure matters. Indeed, the amygdala appears particularly vulnerable to the effects of stress in the first few years of life, during its most rapid period of development (Payne, Machado, Bliwise, & Bachevalier, 2010). In animal models, poor caregiving during this period is associated with faster amygdala development (Kikusui & Mori, 2009). Tottenham et al.'s (2010) findings of enlarged amygdala volumes in the aftermath of early life stress suggest a similar effect in humans. Accelerated amygdala development secondary to early life stress may represent an initial shift in the larger developmental trajectory of amygdala growth. Following from Uematsu et al.'s (2012) depiction of curvilinear change in amygdala volumes, early life stress may cause the curve to 'peak' earlier in development. This notion aligns with Di Martino et al.'s (2014) theory of 'developmental mis-wiring', which suggests that emotional disorders may stem from accelerated

(or decelerated) neurological development. This research suggests that it may be imperative for researchers to move beyond cross-sectional investigations of the influence of stress on amygdala volumes, and towards broader longitudinal investigations that afford the ability to consider effects of stress on the timing and tempo of development.

Evidence is beginning to support a second sensitive period of amygdala development in the years surrounding pubertal development. Hormone fluctuation during adrenarche and gonadarche are theoretically linked to morphometric changes in the amygdala, perhaps underlying functional maturation into adolescence. Extreme stress during this period could have immediate and long-term implications for the amygdala by either 1) disrupting the endocrine processes mediating its development, or 2) instigating microstructural change in the amygdala or connected structures, perhaps via HPA byproducts (e.g., corticosterone; McEwen, Nasca, & Gray, 2016).

Weems (2017) presents a theoretical model describing the potential influences of stress on amygdala development. The immediate effects of stress on amygdala volume and the prolonged impact on amygdala development are considered in terms of variation on Uematsu et al.'s (2012) curvilinear trend. Recall that Uematsu et al. depict normative amygdala development as rapid volumetric growth in the first few years of life (birth to age five), followed by a deceleration (curve) that continues through adolescence and into adulthood where change terminates (null slope). Weems (2017) hypothesizes that stress may accelerate amygdala maturation (earlier peak), prolong maturation (later peak), or delay amygdala growth entirely (smaller peak). Theoretically, each profile of deviated amygdala growth is driven by its adaptive value to the individual. For example, the threat-detection capabilities of the developed amygdala may be more beneficial to children living in unpredictable, abusive environments.

This model is derived from empirical results, though much of the supporting evidence comes from small-sample, cross-sectional studies (Weems et al., 2015, 2013). Weems (2017) describes the need for additional, longitudinal work that can better clarify the links between stress, development, and amygdala volumes. Specifically, there is a need to move away from age as an index of development. Though age and developmental status are indeed correlated, age itself is not directly related to developmental progress (Dorn & Biro, 2011). Pubertal status, represented in Tanner stages, is a more precise, and accurate (though by no means imperfect) reflection of the progress of biological processes underlying development.

Socioeconomic Disadvantage

While I argue the need for greater precision in defining development, I also contend that there is a need to broaden consideration of the types of "stress" that can impact neurological development. The bulk of research testing effects of stress exposure on the brain focus on extreme forms of adversity, such as maltreatment, natural disasters, war, military training, assault, etc. Stress itself, however, exists along a continuum of severity. It is certainly reasonable to begin testing for neurodevelopmental effects among populations with the "worst" stress exposure. Such a focus allows researchers to elucidate effects despite limited sample sizes and thus, statistical power. However, it also limits our knowledge of the broader effects of stress on our species' development and limits the benefits of our research to a small, though critically vulnerable, swath of society. Most children will not experience stress in the form of war or maltreatment, but rather in the form of socioeconomic disadvantage or poor parenting practices. The latter may have the same or similar effects on the developing brain, albeit at a smaller scale.

Indeed, the adverse effects of socioeconomic disadvantage on phenotypic outcomes are clear and pronounced, particularly in the context of child development. Youth's socioeconomic status is linked to lifelong outcomes such as educational achievement, physical health,

psychological well-being, and even neuropsychological functioning (Al Hazzouri, Haan, Galea, & Aiello, 2011; Evans & Schamberg, 2009; Guralnik, Butterworth, Wadsworth, & Kuh, 2006; S. B. Johnson et al., 2016; Miller & Chen, 2013; Noble, McCandliss, & Farah, 2007). A growing body of neuroscience research is attempting to identify ways that brain development may mediate or moderate links between childhood poverty and life outcomes (Farah, 2017). These studies build on a well-developed line of research linking environmental deprivation to functional and anatomical abnormalities in the brains of animals as well as humans (Hirase & Shinohara, 2014; Hubel & Wiesel, 1962; McLaughlin et al., 2010; Sheridan, Fox, Zeanah, McLaughlin, & Nelson, 2012). Neuroscience research on poverty and brain development in humans is novel by comparison, and somewhat limited in regard to the amygdala, specifically. A review by Johnson and Riis (2016) finds only a handful of studies report on the function and structure of the amygdala in relation to childhood poverty.

Noble, Houston, Kan, and Sowell (2012) acquired scans from a socioeconomically diverse sample of 60 children. SES, specifically fewer years of parent education, correlated with larger amygdala volumes in youth. Educational achievement in parents is positively associated with levels of parental nurturing (Brooks-Gunn & Markman, 2005), which might buffer against the neurological impact of stress in low SES contexts. Children whose parents have fewer years of formal education may therefore be less insulated from the effects of their socioeconomic disadvantage. This finding of larger amygdalae in stress-exposed youth is consistent with similar research with similar findings among more severely exposed children (e.g., Tottenham et al., 2010). Still, several other studies have reported the reverse – smaller amygdala volumes in low SES youth (Hanson et al., 2015; Luby et al., 2013). While this might be a reflection of methodological limitations (e.g., limited power), it may also be the case that stress is altering a

non-linear pattern of amygdala development (Weems, 2017). For now, this assertion remains theoretical. The majority of work in this area is cross-sectional, precluding interpretation of maturational differences in the amygdala (though see Albaugh et al., 2017; Goddings et al., 2014).

From a broader perspective, the investigation into the neurological correlates of poverty has important implications for societal welfare. Impoverished children are at greater risk for a variety of social and cognitive deficits that adversely impact the likelihood that they will escape poverty in their lifetime. In the case of the amygdala, the stress of poverty may cause structural changes that provide short-term benefit in socioemotional functioning, but long-term disadvantage. Affective dysfunctions stemming from amygdala abnormalities, such as anxiety or callous-unemotional traits might limit academic achievement or earning potential. Critically, this consideration of neuroanatomical consequences of low SES allows us to move beyond the notion that poverty stems from poverty. Moreover, by making neurological structures the focus of investigation, it encourages researchers to being thinking about individual, rather than societal, interventions.

CHAPTER 5. SUMMATION

Normative Change in the Amygdala across Development

Decades of studies with animals and humans, using techniques from surgery to electrochemical stimulation, demonstrate that the amygdala operates at the nexus of affective processing (Aggleton, 2000; LeDoux & Schiller, 2009; Whalen & Phelps, 2009). Neuroscientists broadly acknowledge the amygdala's involvement in shaping the emotional lens through which we experience the world. Research links amygdala activity to our detection of emotionally-salient stimuli (Breiter, Etcoff, et al., 1996), acquisition of emotionally-conditioned behaviors (LaBar et al., 1998), and regulation of stress response during emotion-laden events (LeDoux, 2007). Developmental changes in these socioaffective systems are well-described, yet knowledge about the corresponding maturation of the amygdala is just emerging (Schore, 2015).

Specifically, there is a need to expand knowledge about the amygdala's maturation in typically developing youth. The lack of a baseline reference for "normative" amygdala development may be contributing to inconsistency across studies investigating *non*-normative variation in individuals exposed to psychosocial (Hanson et al., 2015; Tottenham et al., 2010; Weems et al., 2015, 2013). Competing empirical and theoretical lines assert that the amygdala becomes larger or smaller in the aftermath of stress (Weems, 2017). Disagreement may stem, in part, from a failure to adequately consider amygdala change in the context of broader development. The overarching process of child development is extraordinarily variable, both within and between individuals (Diehl, Hooker, & Sliwinski, 2015). Very few developmental landmarks occur within a tightly constrained time period across individuals, undermining the value of comparisons made across same-aged youth.

Nowhere is this more evident than in pubertal maturation, which exhibits considerable inter- and intraindividual variation in timing and tempo (Dorn & Biro, 2011). As the most externally visible process of human development, external signs of puberty (e.g., breast development, appearance of pubic hair) are a useful index for demarcating the progress of the complex set of physiological changes occurring as youth mature (Shirtcliff et al., 2009). While both age and puberty may be used to demarcate neural development, indexing by pubertal maturation may provide insights that are more 'true to life', in the sense that bodily and brain changes in childhood ultimately most directly stem from biological causes. Ultimately, the assumed changes in amygdala morphometry will occur regardless of the way researchers choose to index those changes. However, as different forms of 'developmental time,' age and puberty may provide complementary insights into the nature of change in the amygdala and many other structures. Ultimately, by considering growth along multiple dimensions of time, researchers might advance a more granular understanding of neurological development.

Certainly, any investigation into longitudinal developmental change requires careful consideration of the construct of "time." Strong inference about the nature of developmental change typically requires longitudinal data collection, where observations of each individual in the sample across the entire time period of interest. This may involve, for example, tracking the development of a sample of five-year-old youth through repeated assessments over the next 13 years, an approach that may be infeasible in neuroimaging investigations. An alternative, the cohort-sequential (CS; also known as accelerated longitudinal) design, provides a compromise by simultaneously tracking "cohorts" of youth at varying ages over overlapping time periods. The true nature of change across age is then closely approximated by linking the age-overlapped data segments (Cole et al., 2003; Duncan, Duncan, & Hops, 1996; Duncan, Duncan, & Strycker,

2006; Huizinga, Esbensen, & Weiher, 1994; Kofler et al., 2011; Miyazaki & Raudenbush, 2000; Stanger, Achenbach, & Verhulst, 1997). In practice, these cohorts may be as small as $n = 1$, with each individual representing the "cohort" of their own unique age relative to the rest of the sample. As an example, the cohort-sequential design of data in the current study is depicted in Figure 1, which shows longitudinal data collection for each case, rank-ordered according to age at initial assessment.

CS designs are an ideal choice for developmental neuroscience studies, where time and funds may be at a premium. Indeed, major recent investigations of age-related changes in the brain have been conducted using this approach (Albaugh et al., 2017; Goddings et al., 2014b). Still, the logistical advantages of the CS design come with a cost. Analyses of CS data require more complex analyses, and careful consideration of changes across time. Hoffman (2015) cautions researchers that proper treatment of the data requires researchers to model change in 'multiple dimensions of time', by considering how the *passage* of time may have different effects on the outcome depending on the *point* in time a participant entered the study. Current CS studies of developmental neuroscience have tended to consider the former – changes in the brain as participants age, but not the latter – the moderating influence of *when* a participant took part in the study (Albaugh et al., 2017; Goddings et al., 2014b). This ignores the fact that longitudinal growth (on the order of years) may be quite different in youth at six years of age versus age 12 or 16. In more technical terms, researchers are modeling changes in the brain as a function of within-subject effects, while ignoring between-subject differences – and in doing so violating the statistical assumption of homogeneity of variance (Hoffman, 2007). With CS data, this approach essentially assumes that the within and between-subject effects of time will converge onto a common growth trajectory, a phenomenon known as "age convergence"

(Sliwinski, Hoffman, & Hofer, 2010). Algebraically, such convergence would require that either: A.) within and between-subjects effects of age are equivalent, or B.) one or both effects are null. Were either case to be true, all youth would show the same rate of growth or change regardless of differences in age or developmental progress.

Yet, research continues to suggest that brain regions such as the amygdala show may not grow at a constant pace across development (Albaugh et al., 2017; Goddings et al., 2014b). If so, it is necessary for analyses of C data to incorporate both within and between-subject effects of development. To avoid assuming convergence, it is necessary to consider each type of developmental effect separately, to avoid 'smushing' predictors with different meanings together. Hoffman (2015) describes these terms as 'alternative metrics' of time. Briefly described, within subjects, data points vary along a metric of 'study time', or when they were collected relative to initial assessment (Time 0). This can be incorporated into predictive models by adding an effect of change in time, age, or pubertal maturation since study entry. However, this initial assessment of each participant was conducted at varying points in 'true' time (e.g., chronological age, pubertal maturation). Therefore, the observations also vary between-subjects in terms of the part of developmental trajectory depicted. This variance can be incorporated into the model by adding the point of study entry or 'cohort' as a between-subjects predictor in the form of chronological age or pubertal development.

Theoretically, parceling variance in neuroanatomical development into separate effects of time may enhance the precision and granularity of investigations into the growth of structures like the amygdala. Though previous studies have utilized CS design to investigate the amygdala, I am aware of no previous work applying this approach. The benefits of CS design for developmental neuroscience make it likely that the number of studies using this design will

continue to grow. Therefore, identification of proper methods of analyzing the resulting data is paramount. To that end, a major aim of the current study is investigation of the viability of these "alternative time" models in a large data set. Establishing the viability of this methodology is an important step forward for the field. This approach will be incorporated as part of a larger goal, identification of the normative trends in left and right amygdala growth across development. Goddings et al. (2014b) demonstrate that the way researchers choose to index developmental progress may critically impact models of neurological change in the amygdala. While analyses of CS data most commonly use chronological age, the current study will examine corresponding models that predict volumetric changes as a function of pubertal status (Tanner stage). Abiding by the analytical approach described above, separate models will predict amygdala volume from between and within-subjects effects of chronological age/time (time in study, age at first participation) as well as pubertal status (pubertal development during study, Tanner stage at first participation).

Data for the current study come from the National Institutes of Health MRI Study of Normal Brain Development, a CS design-study of typical brain development involving a population representative sample of US families. Raw MRI scan files and secondary data are available on application to the NIMH Data Archive (NDA). Previous studies have reported on this data, including Albaugh et al. (2017), who described trends in amygdala volumes across age. However, no research has applied the time by cohort approach described above, nor have lateral differences in amygdala volumes been investigated. Datasets currently available on NDA include numerical volumes for a limited number of large brain structures (e.g. cerebral lobes, thalamus) estimates using Automatic Nonlinear Image Matching and Anatomical Labelling (ANIMAL; Collins & Evans, 1997; Collins, Holmes, Peters, & Evans, 1995; Collins &

Pruessner, 2010) available as part of the Medical Imaging NetCDF (MINC) toolkit. Volumes for subcortical structures, such as the amygdala, are not provided. To that end, it will be necessary to reprocess the raw scan files to obtain these data.

An MRI scan file is comprised of several series of images or "slices" of the brain captured along the three anatomical axes of the brain. Automated extraction of numerical data from MRI scan files is a complex process wherein the scan file is routed through a multi-stage computational pipeline. Briefly described, at each stage, the images within the file undergo a collection of algorithmically driven analyses and alterations that normalize the image properties and align them to a common template. The extrinsic and intrinsic boundaries of the brain in each image are delineated to distinguish areas of brain matter (grey or white), cerebrospinal fluid, meninges, skull, and non-brain tissue. Individual structures and regions are identified by comparison with a digital atlas, and their volume is printed to a data file. Various software packages are available for performing some or all of the necessary steps. Major neuroscience research institutions will often collaborate with experts in computer science or information systems to create complex, modular pipelines for processing MRI images. Notably, per-scan processing time typically ranges from 6 to 24+ hours, depending on software and hardware choices. When available, research groups locate pipelines on high performance or supercomputing systems, where parallel operations (i.e., multiple scans processed at one time) can dramatically reduce total processing time.

However, during this study's formulation, it was discovered that no such pipeline was readily available, nor was a high performance computing environment readily accessible. Therefore, development of a valid neuroimage processing pipeline became a prerequisite for conducting the current study. Despite the widespread usage of neuroimage processing software,

the most commonly used packages continue to require extensive familiarity with computer programming, specifically, code writing in batch script and C++. Graphical user interfaces are uncommon, and most processing steps are run using complex command strings. Moreover, neuroimaging software is typically developed for Unix-like environments (e.g., Linux, macOS), which may be unfamiliar to researchers who lack a background in computer science. For the current study, an originally constructed processing pipeline was constructed over a roughly two year period. The pipeline primarily relies on MRTrix3 and FreeSurfer v6.0 for image processing, and resides on a university hosted high-performance computing cluster. After extensive pilot testing and validation, it was determined that full deconstruction of all raw MRI images provided by NIHPD would require approximately three months of processing time. Notably, the software packages used for processing in the current study vary from those originally used by NIHPD investigators (Brain Development Cooperative Group, 2012), and there is ongoing debate in the literature about the reliability and validity of commonly used neuroimage processing software. While a future investigation may utilize the analyses and results described here to contribute additional knowledge on this topic, differences in software performance were not the focus here and will not be discussed further.

Rather, the primary aim was the identification of a normative reference of left and right amygdala development. Though few in number, previous studies have attempted to identify this trend, including one exploring the same data set (Albaugh et al., 2017). However, the current study provides two major incremental contributions. First, this will be the first study to explicitly consider lateral differences in amygdala volumes, by modeling left and right amygdalae separately. Previous work has averaged amygdala volumes across hemispheres, despite cross-sectional evidence suggesting that there may be important differences in the way

the amygdalae on each side of the brain develop (Uematsu et al., 2012). Second, the current study will incorporate both within and between-subject effects of developmental time – specifically the time a participant spends in the study and their development at study entry, respectively. This approach avoids the age convergence assumption previously described, and may better capture nuanced changes in the amygdala. Building on the work of Goddings et al. (2014b), "development" will be considered in terms of both chronological age and pubertal maturation. Exploratory analyses will attempt to identify whether the inclusion of one of both indexes provides a superior representation of change in the amygdala. Hypotheses about the trajectory of the left and right amygdalae across development derive from the work of Weems (2017) as well as Uematsu et al. (2012). In both the left and right hemispheres, it is anticipated that the amygdala will show a steeper, positive rate of change earlier in development, while reaching a plateau in early to mid-adolescence, and a decline in late adolescence or young adulthood. The extreme inconsistency in results reporting larger or smaller volumes in the right or left amygdala (see Weems, 2017, Table 1), make it difficult to hypothesize about the nature of the lateral effect. Still, given past research suggesting that stress primarily produces structural effects in the right amygdala (e.g., Weems, 2017; Weems et al., 2013), it is hypothesized that the right amygdala will similarly show a larger volume generally, and an earlier peak in growth than the left.

Hypothesis #1*:* Right and left amygdala volumes will change as a function of time in study, development at study entry (age or pubertal maturation), and their interaction. It is anticipated that more dramatic growth will be evident early in development, followed by a plateau in early to mid-adolescence, and a possible decline in late adolescence or early adulthood. This trend will be evident in models that index development using chronological age,

pubertal maturation, or a combination of both. Right amygdalae will be larger on average, and reach maximum volume earlier than left amygdalae.

In addition to characterizing the trend of normative amygdala development, Weems (2017) theorizes that stressful experiences may produce a shift in this trend's inflection point and linear slope. Findings from Weems et al. (2015, 2013), as well as Tottenham et al. (2010) suggest that exposure to severe stress predicts accelerated amygdala development. In comparison to controls, these youth show a faster rate of change (steeper linear slope) in amygdala volumes, while a curvilinear trend line inflects earlier in development. Conversely, Hanson et al. (2015) examined the amygdala volumes of youth who experienced early life stress and found evidence for *delayed* amygdala development. Weems (2017) similarly posits this as a potential pathway for stress-moderated amygdala development, in that the linear slope will be attenuated, and the inflection of the curve will occur later in development.

The nature of these inconsistencies in the literature may stem, in part, from our opaque understanding of normative amygdala development. By providing a well-defined reference for typical amygdala growth, this study can make an important contribution to research on atypical growth, allowing investigators to better approximate the deviation from "normal". Enhanced modeling approaches may improve our knowledge of this structure's typical development, but also provide the precision necessary to detect subtle influences on its growth, such as stress exposure. Broadly, research examining the effects of stress on the brain has tended to presume that atypical brain development will only be evident in youth who have undergone extreme experiences, such as natural disasters, institutional deprivation, or maltreatment (De Bellis et al., 2002; Tottenham et al., 2010; Weems et al., 2013). However, normative youth do not experience an absence of stressful experiences any more than atypically developing youth experience them

in totality. There is now a need to expand research into the effects of more normative forms of stress, such as socioeconomic disadvantage. Increasingly, researchers are recognizing that even youth living within "acceptable" poverty ranges experience altered trajectories of regional brain development (S. B. Johnson et al., 2016). Therefore, as a secondary aim, the proposed study seeks to test SES as a moderator of neurodevelopmental trajectories, specifically the amygdala, which is known to play an outsized role in the response to environmental stressors.

As described above, research literature describing the effects of stress on amygdala development is inconsistent, with findings suggesting that stress exposure is linked to earlier or delayed maturation. Few studies have specifically examined the effects of socioeconomic status on amygdala growth across development, though Whittle et al. (2017) recently reported on SES as a moderator of amygdala change in adolescence. Results suggest that teens living in low SES environments may show accelerated right and left amygdala development, in that peak growth of these structures occurs at a younger age in comparison to youth in high SES environments. This is consistent with similar work from Weems et al. (2015, 2013) and Tottenham et al. (2010) who report similar variation in youth exposed to traumatic stress. Based on these findings, it is anticipated that socioeconomic status will indeed moderate amygdala development. To wit, youth who experience psychosocial stress by way of lower SES will show 'accelerated' amygdala development, in that they will reach peak volumes comparatively faster than individuals of average or high SES.

Hypothesis #2: As described in Hypothesis #1, change in left and right amygdala volumes is anticipated to occur as a function of either time in study, development at study entry, or the interaction of these terms. Socioeconomic status is further hypothesized to moderate the effect of the interaction on right, but not left, amygdala volumes. Thus, in separate models

indexing development using chronological age or pubertal maturation, a three-way interaction term between SES, time in study, and development, will reach significance. Decomposition of this term will reveal that youth living in low SES environments will show accelerated right amygdala maturation, as described by Weems (2017).

CHAPTER 6. METHODS

Participants

Recruitment

Data for the proposed study will be taken from Objective 1 of the National Institutes of Health MRI Study of Normal Brain Development (NIHPD), a longitudinal multi-method study undertaken to establish a public repository of anatomical MRI, MR spectroscopy, and DTI neurological scans of typically developing youth (as described in BDCG & Evans, 2006). Objective 1 refers to the collection of data from 1,333 youth ranging in age from 4 years, 6 months to 18 years of age at study start. Quality controlled MRI scans, as well as neuropsychological, psychiatric, and behavioral assessment data are available for 882 of these youth, and were obtained on application to the National Institute of Mental Health Data Archive (NDA). Personal identification information was not included in the data set and all scans were defaced (i.e., scan slices capturing participant faces were scrambled) prior to upload into NDA. The project was exempted from review by the Institutional Review Board due to the use of de-identified data.

As described by Brain Development Cooperative Group (BDCG) and Evans (2006), the NIHPD project investigators aimed to develop a multi-method, high-quality profile of normative brain maturation throughout childhood and adolescence. To that end, a population-based sampling method was used to recruit sought to obtain a sample representative of the millennial U.S. Census in terms of family income, race, and ethnicity (NIHPD, 2006b). Initially, the target sample size was divided into several accrual cells cross-defined according to income level (low, medium, high), and race\ethnicity (as defined in the 2000 U.S. Census; BDCG & Evans, 2006). Each cell therefore represented a unique demographic profile (e.g., medium-income, American

Indian) with an individual target sample size, referenced from the 2000 Census. Recruiting was guided by cell sizes, as well as an overarching goal of achieving a stratified sample of youth at different ages, and reflecting the national distribution of race\ethnicity, income, and gender (BDCG & Evans, 2006).

Sampling procedures are described by BDCG and Evans (2006), as well as Waber et al. (2007). Briefly summarized, recruiters used census-based geocoding to develop demographic profiles of all zip codes within a 1-hour traveling distance of each study center. These profiles were then used to engage in targeted recruiting to meet the quotas for each demographic cell. Recruitment was performed at each of six regional study centers in Boston, Cincinnati, Philadelphia, Los Angeles, Houston, and St. Louis. Enrollment targets were specified for each regional site and adhered to until 50% of the target sample was acquired. Names and addresses of 10,000 families residing in the predefined zip codes were obtained by each study center. A random number generator was used to select 200-300 families (at a time) residing in zip codes selected based on their demographic profiles. Recruited households initially received an introductory letter providing background about the study and informing families of an upcoming call from the recruitment team. A more detailed description of all sampling and recruitment procedures is provided elsewhere (BDCG & Evans, 2006; NIHPD, 2006b; Waber et al., 2007).

Given the study focus on neurological development in "normative" (i.e., typically developing) youth, multiple exclusionary criteria were specified to obtain an appropriate sample. As described in the study protocol (NIHPD, 2006b), youth were excluded if they met diagnostic criteria for any major medical illness, psychopathology, exhibited non-normative patterns of behavioral or emotional expression, or met medical criteria precluding MRI (e.g., surgical implants, dental braces). Moreover, the intensely verbal nature of some components of the

assessments precluded the inclusion of youth who did not speak English as a primary language. Relatedly, families with caregivers who were not proficient in reading English were excluded due to prospective difficulty completing parent assessments. Full exclusionary criteria for the study are provided in the appendix (Table S1).

During the initial recruiting call, caregivers were asked to confirm they had a child within the study's age range, that English was the primary language for the child and read proficiently by the caregiver, and asked to complete a brief screening interview assessing for psychiatric, learning, or neurological conditions. Assuming the family agreed to participate, and did not immediately meet exclusionary criteria, a packet was mailed out containing the Child Behavior Checklist (CBCL; Achenbach & Rescorla, 2001), and a written informed consent for a longer, more detailed telephone screening interview, to occur within the next 10 days. Upon receipt of the consent form and CBCL, recruiters contacted caregivers for the second screening interview, which consisted of a detailed medical and developmental history, and (assuming continued eligibility) administration of the Diagnostic Interview Schedule for Children Version IV (DISC-IV; Shaffer, Fisher, Lucas, Dulcan, & Schwab-Stone, 2000), the DISC Predictive Scales for youth age 11 and older (Lucas et al., 2001), and the Family History Interview for Genetic Studies (FIGS; Maxwell, 1991). Assuming continued eligibility at this point, participating families were scheduled for an appointment at the study center to complete the MRI and assessment battery.

Upon arrival at the study center, written informed consent to research procedures was completed by caregivers, and oral assent was provided by youth ages 6-17. Full physical, neurological, and neuropsychological testing as well as MRI acquisition was performed during these visits (an abbreviated description is provided below, and complete details may be found in NIHPD Protocol, 2006; see also BDCG & Evans, 2006). Assessment was generally completed in

a single day, though was extended to a second day where necessary due to family preference, child fatigue, or scanner availability. Participating families were asked to return to the center for subsequent waves of data collection twice more at two-year intervals. Follow-up assessments repeated all procedures performed during the initial visit, as well as the full phone interview. Caregivers and youth were asked to provide original consent and assent, respectively, at each wave of the study. Participating families were compensated $50-100 per day for their time and expenses (actual amount determined based on regional factors, and determined by individual study centers).

Measures

A full list of all measures and constructs assessed as part of NIHPD is provided in the appendix (Table S2). Only those constructs relevant to the current study will be reviewed below.

Socioeconomic Status

Household income levels will be used as a proxy for socioeconomic status. Participating families indicated their annual family income by selecting among a series of incremental ranges.[3] The midpoint of the selected income range was used as a raw value for subsequent refinements based on family size and geographical location. NIHPD researchers used the income-adjustment guidelines provided by the United States Department of Housing and Urban Development (U.S. Department of Housing and Urban Development, 2006; NIHPD, 2006b). The HUD formula incorporates sliding scale adjustments to income levels based on poverty level, family size, and median local and national income to compute the "Adjusted Family Income" (AFI). Specifically, this was calculated as AFI = ((A / B) / C) * D, where A = the midpoint of reported

[3] (1=$0-$5,000; 2=$5,001-$10,000; 3=$10,001-$15,000; 4=$15,001-$25,000; 5=$25,001-$35,000; 6=$35,001-$50,000; 7=$50,001-$75,000; 8=$75,001-$100,000; 9=$100,001-$150,000; 10=over $150,000)

family income range, B = HUD percentage adjustment for family size, C = median income for the local Metropolitan Statistical Area (MSA), D = national median income level (U.S. Department of Housing and Urban Development, 2006). National and MSA-specific median income levels were derived from the 2000 US Census estimates for families living in metropolitan areas (U.S. Census Bureau, 2000)

Pubertal Status

Scores from the Pubertal Development Scale (PDS; Petersen, Crockett, Richards, & Boxer, 1988) are available for participants across time points. The PDS is a 10-item interview designed to assess pubertal development through a series of questions about external physical maturation (Shirtcliff et al., 2009). Youth respond to questions about their progress on various aspects of physical development using a four-point scale including, "No" (1), "Yes (Barely)", "Yes (Definitely)", and "Development Completed" (4). The PDS was administered by an on-site neurologist, and was omitted at their discretion when participants were age 10 or under. Preliminary review of the data finds approximately 19% of cases are missing PDS data (see *Missing Data*, below). Gender-specific summed item scores do not directly correspond to the widely used Tanner scale system of assessing pubertal development (Tanner, 1962). Shirtcliff, Dahl, and Pollak (2009) provide a methodology for converting PDS scores into values corresponding to Tanner stages, along a continuous interval from one to five. The algorithm recodes PDS items based on their gender-specific indication of Tanner staged pubertal development, and computes a gender-neutral composite value reflecting of pubertal status.

MRI

Acquisition

A brief overview of scan acquisition procedures and parameters is provided below, as derived from the NIHPD MRI Manual, where a more complete description may be found

(NIHPD, 2006a). Multi-spectral magnetic resonance images were acquired at one of six different regionally-distributed sites, each equipped with 1.5 Tesla scanners. All participants were asked to provide 3D T1 and T2-weighted anatomical images, and a subset subsequently provided diffusion tensor images (DTI) and\or magnetic resonance spectroscopy (MRS). Due to the large, multi-site nature of this project, a quality control protocol was used to monitor scanner performance and variation across study centers. This process involved cross-site comparison of a "living phantom" (i.e., the same individual) as well as the American College of Radiology Phantom object. Full protocols (i.e., anatomical, DTI, MRS) from the living phantom were acquired and evaluated at the start of each wave of data collection, and in the event of scanner quench or power loss. Anatomical scans of the ACR phantom object were acquired and evaluated monthly.

Anatomical scan sessions occurred in two parts, with parameters for each provided in Table S3. The primary objective was the acquisition of a 3D T1-weighted (T1W) whole-brain image series, which provides the clearest depiction of developing neural anatomy. A secondary objective involved acquisition of proton-density/T2-weighted (PD/T2W) to be used during MRI analyses. Scan parameters used during protocols for each objective (as well as alternative fallback protocols) are provided in the appendix (Table S3). T1W images were acquired first, using an optimized 3D spoiled gradient recalled (3D SPGR) echo sequence, which provided higher signal-to-noise and contrast-to-noise ratio than alternatives.[4] Scans were acquired sagittally, generally in 1mm isotropic slices. GE scanners used in this study have a hardcoded limit of 124 sagittal slices, requiring thickness to be increased for this axis (1.0mm-1.54mm; dependent on ear-to-ear width). Acquisition of 3D T1 images typically took between 10-17

[4] e.g., magnetization prepared gradient echo sequence (MPRAGE)

minutes. However, when significant motion artifacts were observed, the scan was repeated prior to moving on to the T2-weighted sequence.

Dual contrast proton density\T2-weighted (PDW\T2W) scans were acquired next. These images provide valuable information that can augment the process of automated tissue classification and segmentation (Helms, Kallenberg, & Dechent, 2006; Viviani, Stöcker, & Stingl, 2017). Scans were acquired using an optimized 2D multi-slice dual echo fast-spin echo (FSE) sequence, at 2mm slice thickness (NIHPD, 2006b). Acquisition was performed along the axial plane parallel to the anterior commissure-posterior commissure line (BDCG, 2012). Scan time for this acquisition was approximately 7-9 min, though this sequence was repeated in cases of substantial motion artifacts. Total scanner time for the anatomical sessions was approximately 30-45 minutes, including setup, localizer scanning, scanner delays, and subject entry\removal. In cases where subjects were unable to tolerate the full 40-minute protocol (9% of scan sessions), a fallback protocol was implemented that reduced scan time though retained the integrity of anatomical images. Specifically, T1W images were acquired axially, using a 2D multi-slice spin echo sequence at 3mm slice thickness (3-5 min.). The duration of PDW/T2W acquisition was reduced by increasing the slice thickness to 3mm (3-5 min.). All MRI data were visually inspected at time of collection and scans were repeated in the event of substantial motion artifacts (NIHPD, 2006a).

Scan processing protocol

All subsequent processing and analyses were performed by the author, using an in-house neuroimage processing pipeline developed for this study. Given that lateral differences were a target of this investigation, only right handed scans

Pre-processing

Scans were received unprocessed, in compressed, NIFTI-1 format. Several preprocessing steps were performed using MRTrix3 (Tournier, Calamante, & Connelly, 2012) and included, 1) reversing the byte order for each file (little-endian to big-endian), 2) reorientation of the images to Right-Anterior-Superior format, 3) random evaluation of file integrity and completion.

Cross-sectional processing

Initially, all scans will be processed individually, without regard to non-independence of participants. Cortical reconstruction and volumetric segmentation will be performed using FreeSurfer (v6.0), a widely used and freely-distributed software package (surfer.nmr.mgh.harvard.edu) that provides automated processing and analyses of brain imaging data. The technical details underlying the multi-step technical details of these procedures are extensively described in prior publications, and a cursory review will be provided here (Dale, Fischl, & Sereno, 1999; Dale & Sereno, 1993; Fischl & Dale, 2000; Fischl, Liu, & Dale, 2001; Fischl et al., 2002; Fischl, Salat, et al., 2004; Fischl, Sereno, & Dale, 1999; Fischl, Sereno, Tootell, & Dale, 1999; Fischl, van der Kouwe, et al., 2004; Han et al., 2006; Jovicich et al., 2006; Reuter, Rosas, & Fischl, 2010; Reuter, Schmansky, Rosas, & Fischl, 2012; Segonne et al., 2004), therefore a cursory review will be provided here. Initial processing involves motion correction and averaging of intra-session scans (when available; Reuter, Rosas, & Fischl, 2010), affine transformation of the original volume to Talairach space (MNI 305), N3 intensity correction (Sled, Zijdenbos, & Evans, 1998), and the removal of non-brain tissue using a hybrid watershed\surface deformation algorithm (Segonne et al., 2004). This is followed by segmentation of subcortical white matter and deep-gray matter structures (e.g., hippocampus, amygdala; Fischl et al., 2002; Fischl, Salat, et al., 2004). Surfaces along the boundaries dividing tissue types are tessellated (Fischl et al., 2001), followed by an automated process to correct

topological improprieties (e.g., holes; (Segonne, Pacheco, & Fischl, 2007). This surface is deformed or "flexed" to follow intensity gradient maxima, indicative of the boundaries between gray/white matter (or gray matter/cerebrospinal fluid; Dale et al., 1999; Dale & Sereno, 1993; Fischl & Dale, 2000).

With the cortical surface models created, a number of deformable procedures can be performed for further data processing and analysis including surface inflation (Fischl, Sereno, & Dale, 1999), registration to a spherical atlas which is based on individual cortical folding patterns to match cortical geometry across subjects (Fischl, Sereno, Tootell, et al., 1999), parcellation of the cerebral cortex into units with respect to gyral and sulcal structure (Desikan et al., 2006; Fischl, van der Kouwe, et al., 2004), and creation of a variety of surface based data including maps of curvature and sulcal depth. The latter method uses both intensity and continuity information from the entire 3D MR volume in segmentation and deformation procedures to produce representations of cortical thickness, calculated as the closest distance from the gray/white boundary to the gray/CSF boundary at each vertex on the tessellated surface (Fischl & Dale, 2000). The maps are created using spatial intensity gradients across tissue classes and are therefore not simply reliant on absolute signal intensity. The maps produced are not restricted to the voxel resolution of the original data thus are capable of detecting submillimeter differences between groups. Procedures for the measurement of cortical thickness have been validated against histological analysis (Rosas et al., 2002) and manual measurements (Kuperberg et al., 2003; Salat et al., 2004).

Results derived from the FreeSurfer pipeline used in this study were validated by comparing volumetric estimates to ranges reported in previous studies of developing neuroanatomy. Mean values for the left and right amygdala were 1576.07 and 1632.71mm^3,

respectively, closely approximating results from similar studies reporting these estimates in typically developing youth (Goddings et al., 2014b; Østby et al., 2009; Uematsu et al., 2012; van der Plas et al., 2010), as well as Albaugh et al. (2017) who extracted the same information from the data, albeit using different processing methods. An initial validation procedure attempted to validate the FreeSurfer-derived volumetric estimates of various brain regions by comparison against original values obtained by NIHPD. Data sets accompanying the raw scan files contained ANIMAL-based estimates of several prominent regions. These included the lateral divisions of the cerebral lobes (separate estimates for grey and white matter), caudate, cerebellum, globus pallidus, putamen, and thalamus. However, subsequent investigation revealed marked discrepancies across ANIMAL and FreeSurfer in the segmentation procedures used to define these regions. For example, the original, ANIMAL-based estimates appear to incorporate portions of the insular cortex into estimates of frontal and temporal lobe volume. Similarly, whereas the original values for the thalamus' volume seem to reflect the size of the entire structure, estimates provided by FreeSurfer refer only to the thalamus proper (which does not include either the epi- or perithalamus). Ultimately, it was necessary to limit direct comparison to the left and right putamen, caudate, total intracranial volume, total grey matter, and total white matter.

Reliability of the values obtained was assessed by summarizing the similarity of measurements for these regions of interest using the intraclass correlation coefficient (ICC, two-way mixed average – consistency; (Shrout & Fleiss, 1979; Strother & Churchill, 2017)). Shou et al. (2013) developed the image intraclass correlation coefficient or I2C2, a variant on the classic ICC, extended to better capture the high-dimensional, multivariate nature of neuroimaging data. Values for the I2C2 and ICC have equivalent interpretations - both statistics are generally

bounded between 0 and 1 with higher values indicative of better reliability. Overall, both statistics suggested excellent consistency across measurements made with the ANIMAL and FreeSurfer pipelines (> 0.85; see Table 1).

Data Analysis

Accelerated Longitudinal Design

NIHPD data were collected using a cohort-sequential design, as shown in Figure 1 (Bell, 1953; Schaie, 1965; Baltes, Reese, & Nesselroade, 1977; Hoffman, 2015). Longitudinal studies of developmental change typically require researchers to make observations of each individual in the sample across the entire time period of interest. When the sample size is large or the focal period is long, it may not be feasible to collect the data. CS designs allow researchers to "accelerate" data collection by gathering overlapping repeated measurements from cohorts at varying stages (e.g., childhood, adolescence, late adulthood) of the developmental period being studied. As described by Duncan, Duncan, and Hops (1996, p. 236), "…this method consist[s] of limited repeated measurements of independent age cohorts resulting in temporally overlapping measurements of the various age groups." By linking the age-overlapped data segments, researchers can closely approximate the trend that would be obtained through a traditional longitudinal design. This approach offers a compromise between the analytical limitations inherent to cross-sectional data and the time-intensive nature of longitudinal studies. Research comparing data collected in accelerated and traditional longitudinal designs consistently finds that the former provides a close approximation of the trends identified by the latter (Cole et al., 2003; Duncan et al., 1996, 2006; Huizinga et al., 1994; Kofler et al., 2011; Miyazaki & Raudenbush, 2000; Stanger et al., 1997).

Notably, proper treatment of CS data requires researchers to model both the within and between-subjects (cohort) effects of time (Hoffman, 2015). Researchers have typically modeled

neurodevelopment in CS designs by mapping trends in regional morphometry across within-subject time in study (Albaugh et al., 2017; Goddings et al., 2014b). By design, participants in CS designs enter the study at varying ages, or stages of development. This between-subjects or "cohort" variance in age may significantly inform model predictions. Appropriately, separate variables were created for considering the effects of chronological time in the current analyses. At the within-subjects level, *Time*, was a continuous variable reflecting a participant's time since first observation (i.e., time in study) and was computed by subtracting a participant's date of birth from each scan date. A between-subjects variable, *Age@1stScan* referred to a participant's age (in years) at study entry/first MRI scan, and was captured by subtracting date of birth from date of first scan.

A second index of developmental progress was computed based on pubertal status. Similar within and between-subjects variables of "developmental time" were derived from the continuous Tanner scale scores (as described above). At the within-subjects level, the variable *TSChange* reflected the change in Tanner stage across time points. The between-subjects variable *TS@1stScan* referred to each participant's Tanner stage score at study entry (initial MRI scan).

Missing Data

Meaningful patterns of missingness in the data were evaluated using Little's test (1988), which indicated that an assumption of "Missing Completely at Random" (MCAR) was not viable, $\chi^2(42) = 211.731$, $p < .001$. A series of separate variance *t*-tests were conducted across cases with missing and non-missing values to identify meaningful variation in the incomplete data. Results indicated that younger participants were more likely to be missing data in variables derived from the Pubertal Development Scale, with a mean difference of 3.3 years across cases with and without missing values ($p < .001$). Participants providing data at second or third

assessments were also more likely to be missing data on annual family income ($p < .001$). No other meaningful patterns in missing data were detected.

Mixed Effects Modeling

Mixed effects modeling (also referred to as hierarchical or multi-level modeling), is an extension of the genera linear model to incorporate parameters that vary at more than one level of observation, and is an appropriate method of analyzing CS data (Hoffman, 2015). In the case of a two-level design (e.g., multiple observations nested within individuals), the mixed effects framework separates variance in the dependent variable attributable to the observations within individuals (within-subjects or 'Level 1' variance) or to the individuals themselves (between-subjects or 'Level 2' variance). This approach effectively accounts for the non-independence of nested data points. In longitudinal applications, mixed effects models allow researchers to simultaneously consider intra- and inter-individual change trajectories. Moreover, mixed effects models are known to be robust to uneven time spacing in collection, as well as the presence of missing data at various time points (Hoffman, 2015).

In the current analyses, mixed effects model parameters were estimated using the *lme4* package (v1.1.16; (Bates, Maechler, Bolker, & Walker, 2018) available in *R* (v3.5.x). Parameter values were derived using maximum likelihood estimation as permissible for the sample size ((Carey, 2013) and appropriate given the unbalanced nature of the data (Raudenbush, 1995). Wald tests were used to determine the significance of fixed effects, using the Kenward-Roger adjusted degrees of freedom (Halekoh & Højsgaard, 2014; Kenward & Roger, 1997). The significance of individual random effects was tested by examining the difference in fit (as -2-log-likelihood) of nested models with and without the term. The log likelihood distribution approximates the chi-square distribution; therefore, this test is akin to a chi-square difference

test. Model parameters were determined using maximum-likelihood estimation, which is appropriate for samples of this size (Hoffman, 2015). Where necessary, significant interaction were decomposed using the Johnson-Neyman technique (P. O. Johnson & Neyman, 1936), which provides the range of values along a continuous moderator (e.g., *Age@1stScan*), for which the association between the predictor and outcome is significant (Preacher, Curran, & Bauer, 2006).

Modeling Normative Amygdala Development

Effects testing was conducted using the stepped approach described by (Hoffman, 2015), who suggests a two-stage process of evaluating an incremental series of models adding fixed and random effects. In the initial stage, a series of unconditional longitudinal models (i.e., no between-subjects effects) were evaluated that tested fixed and random within-subject effects. A final unconditional model contained all fixed effects, and significant random effects. In a second stage, between-subjects predictors (e.g., *Age@1stScan*) were added to test their effect on the intercept and linear slope.

This process was repeated, separately for left and right amygdala volumes, across three types of models that incorporated different metrics of time:

1. A *Chronological Age* model that predicted change in amygdala volumes according to the years since a participant's entry into the study (*Time*), and the cohort-specific effect of chronological age at first scan (*Age@1stScan*).
2. A *Pubertal Development* model that predicted change in amygdala volumes according to the change in a participants' pubertal status since study entry (*TSChange*) and the between-subjects effect of pubertal status at study entry (*TS@1stScan*).

3. A *Combined* model that incorporated both within-subjects predictors (*Time* and *TSChange*), and both cohort effects (*Age@1stScan* and *TS@1stScan*) to predict change in amygdala volumes.

Results of secondary analyses exploring these models in subsamples of boys and girls are provided in the appendix, but are not reviewed in the text, as gender differences were not a primary aim of this study.

Testing for Moderating Effects of Socioeconomic Status

Initial socioeconomic status (adjusted family income; AFI) was subsequently added as a between-subjects predictor to *Chronological Age* and *Pubertal Development* models separately predicting left and right amygdalae[5]. Each model explains change in amygdala volumes as a function of the interaction between youths' development at the start of the study (*Age@1stScan*, *TS@1stScan*), and developmental progress across the course of their participation in the study (*Time*, *TSChange*). It was hypothesized that SES would moderate the link between amygdala volumes and the interaction term, such that youth from lower-SES environments would exhibit a steeper, more positive slope at early ages, in comparison to youth from higher SES homes. Thus, the three-way interaction (i.e., moderated moderation) between SES, initial development, and developmental progress is the focal term in these analyses. When significant, interactive effects of SES on the slopes of change in right or left amygdala volume were decomposed using the J-N technique. As necessary for interpretation, a model including this three-way term further included all nested two-way interactions, and individual predictors. These analyses also incorporated estimated total intracranial volume (*ETIV*) as a within-subjects predictor, scaled

[5] Analysis of the effect of socioeconomic status in the context of the *Combined Model* was not conducted, as the resulting four and five-way interaction terms may not be interpretable.

(10^{-5}) and grand-mean centered to aid model convergence. Past research indicates that stress may have a holistic effect on brain development (De Bellis, 2001; Herringa, 2017). In order to determine if SES had a specific influence on amygdala growth beyond its global effects on the larger brain, it was necessary to control for broader effects on intracranial volume. Though past research has focused on the effects of stress on broader brain volumes, such effects were not the focus of the current study, and are not reported here.

Comparing Theoretical Models of Amygdala Development

Finally, the proposed models of amygdala development were compared in terms of fit to the data. Despite past work suggesting the superiority of pubertal development models of amygdala growth, these analyses were largely exploratory, given the unique nature of the models considered in the current analyses (i.e., examining between and within-subject effects of time and puberty). Separate comparisons were made for left and right amygdala volumes using the Akaike Information Criterion (AIC) as appropriate for non-nested models. The AIC imposes a smaller penalty for model complexity than similar fit indices, making it more suitable for comparisons of models with different numbers of parameters (Burnham & Anderson, 2004). A difference in AIC (ΔAIC) between models of 5.9 or greater was considered indicative of superior fit (Burnham & Anderson, 2003). A related statistic, the AIC weight, provides a probabilistic indicator of the likelihood that the data were derived from each of the models tested. Notably, Vaida and Blanchard (2005), caution that the AIC may not be a valid index for selecting across models with and without random effects, and encourage authors to limit their focus to either population parameters or subject-level random effects, but not both. Given that population-level trends in amygdala development were the broader focus of this manuscript, random effects terms were not included during comparisons.

For these analyses, data were limited to those cases without missing values for pubertal development or age, ensuring an equivalent sample size across models incorporating respective predictors. Though the AIC is not sensitive to sample size per se, it was anticipated that the greater frequency of missing pubertal development data in young participants would impartially worsen the fit of the *Pubertal Development* and *Combined* models by restricting the range of the *TS@1stScan* predictor. Therefore, listwise deletion of missing values in these analyses was deemed to provide a more impartial comparison of the models.

CHAPTER 7. RESULTS

The original data package contained 1,058 MRI scans of 431 youth. Exclusion of left-handed and ambidextrous youth reduced this to 924 scans of 387 youth, while exclusion of scans that failed processing (most frequently due to motion artifacts) resulted in a final count of 637 scans of 330 youth. Participants in the final sample were majority female (54%), ranged in age from 4.88 to 18.35 years (mean = 11.37, SE = 3.75) at study entry with a mean Tanner stage of 2.62 (1.37). Mean adjusted family income for participating families was $72,000 (SE = 31,997) and followed a normal distribution across the sample.

Normative Development

Analyses began by testing the *Chronological Age* model's prediction of change in right amygdala volumes (see Table 2 for a listing of all mixed model formulas). An intraclass correlation coefficient (ICC) was calculated from a random intercept model and showed that 83% of the variance in right amygdala volumes was between persons. A fixed linear effect of time (years) in study (*Time*) and its random variance across participants were both significant ($17.30mm^3$/year, $p < .001$; $-2\Delta LL(1) = 6.92$, $p < .01$), indicating that right amygdala volumes increased on average over the course of the study, though this trend varied significantly across individuals. Age at first scan (*Age@1stScan*) was added next and exhibited a positive effect on the intercept, but a negative effect on the slope (change in amygdala volume over time since study entry). Each year of a participant's chronological age at study entry predicted a $14.12mm^3$ ($p < .001$) difference in right amygdala volumes at initial scan, while attenuating the rate of growth by $-5.81mm^3$/year ($p < .001$; see Table 3-A). Decomposition of this interaction using the J-N technique revealed that the slope of change in amygdala volumes during the study (*Time*)

remained significant (i.e., $p < .05$) from 4.9 years (the age of the youngest participant in the sample) through 14.3 years.

In the left amygdala, computation of an ICC from a random intercept model similarly indicated that 83% of variance was attributable to between-person differences. Fixed linear and random effects variances of time in study (*Time*) were both significant (8.97mm^3/year, $p < .001$; $-2\Delta LL(1) = 5.63$, $p < .05$), suggesting a positive linear increase in left amygdala volumes on average, as well as substantial variation in the trend across participants. Participant age at study entry (*Age*@1stScan) predicted the intercept of left amygdala volumes, with an increase of 6.25mm^3/year of age. The age at which participants entered the study further moderated the slope of left amygdala volume growth. Each year of chronological age at study entry predicted a -2.61mm^3/year decrease in the rate of left amygdala growth ($p < .001$; see Table 3-B). Application of the J-N technique revealed that the slope became non-significant at age 13.0 years.

Effect of Socioeconomic Status

The effects of socioeconomic status on age-driven change in amygdala volumes was tested next, by evaluating the three-way interaction between adjusted family income (AFI), *Time* and *Age@1stScan.* Estimated total intracranial volume (*ETIV*; scaled by 10^{-5} and grand-mean centered) was added to the model as a within-subjects covariate. A three-way interaction term is only interpretable when all nested two-way interactions and individual predictors are simultaneously included in the model, therefore these lower order terms were added as fixed-effects in a stepwise manner similar to previous analyses. Results from these models are presented in supplemental Tables S4-A and S4-B. The three-way interaction term denoting the moderating effect of socioeconomic status failed to reach significance in models predicting right or left amygdala volumes.

Pubertal Development Model

Normative Development

Analyses next examined growth along a pubertal development time metric, beginning with the right amygdala (see Table 2), and using the same approach. A fixed linear effect of change in pubertal status since study entry (*TSChange*; i.e., change in Tanner stages) was added to an empty means, random intercept model. The fixed effect of pubertal change was significant, with right amygdala volumes growing by 34.89mm^3 with each Tanner stage. The corresponding random effect was non-significant, suggesting that this trend was largely stable across participants. Pubertal development (Tanner stage) at study entry (*TS@1stScan*) was added to an unconditional model that included the fixed effect of pubertal change (omitting the non-significant random term). Tanner stage at study entry predicted the model intercept, in that initial right amygdalae volumes were 17.26mm^3 ($p < .05$) greater for each Tanner stage reached by study entry (Table 4-A). Pubertal development at entry did not meaningfully influence the slope of right amygdala volume growth.

Analyses next examined change in the left amygdala as a function of pubertal development. The fixed linear effect of change in pubertal status since study entry was significant, indicating that, on average, left amygdala volumes increased 16.63mm^3 ($p < .01$) with each Tanner stage. The corresponding random effect was significant ($-2\Delta LL(1) = 8.37$, $p < .01$), suggesting meaningful variation in this trend across individuals. Pubertal development at study entry (*TS@1stScan*) was added to an unconditional model that retained the fixed (but not random) effect, though did not significantly affect either the intercept or slope (Table 4-B).

Effects of Socioeconomic Status

Effects of SES on amygdala development were tested by evaluating the three-way interaction between initial pubertal development (*TS@1stScan*), pubertal change over the course

of participation in the study (*TSChange*), and adjusted family income (*AFI*). As in previous analyses, all lower-order two-way interaction terms and individual predictors were added and evaluated in incremental steps. Estimated total intracranial volume (*ETIV*) was again added as a within-subjects covariate. Results are presented in supplemental Tables S5-A, and S-5B, and show that the three-way interaction term did not reach significance in models predicting change in left or right amygdala volumes as a function of pubertal development.

Combined Model

A *Combined Model* tested the effects of chronological age and pubertal development in a single model predicting amygdala volumes (mixed model formulas provided in Table 2). Fixed effects of time in study (*Time*), change in pubertal development during the study (*TSChange*), and their interaction (*Time* x *TSChange*) were added to a random intercept model predicting right amygdala volumes. Each of these fixed effects terms (though none of the corresponding random effects) were significant in a model predicting right amygdala volumes (Table 5-A). Participants showed an increase of 10.03mm^3 ($p < .05$) for each year of participation in the study, and an increase of 50.88mm^3 ($p < .01$) for each Tanner stage reached during participation in the study, controlling for puberty and age, respectively. The significant coefficient for the interaction term (*Time* x *TSChange*) indicates that the pace of right amygdala growth slows as youth progress through puberty, in that for each Tanner stage reached, the rate of change declines by −9.74mm^3/year. A final 'unconditional' model was retained that included only the significant fixed effects.

Between-subjects predictors age at first scan (*Age@1stScan*) and pubertal status at first scan (*TS@1stScan*) were added to the unconditional model. *Age@1stScan* significantly affected the intercept, such that for each year of youths' age at initial assessment, right amygdala volumes were 24.14mm^3 larger on average ($p < .001$; Table 5-A). Pubertal development at initial

assessment (*TS@1stScan*) similarly predicted the size of right amygdalae, though the direction of the effect was reversed. For each Tanner stage reached by the time participants started the study, right amygdala volumes were −37.06mm^3 smaller on average ($p < .05$). Two-way cross-level interaction terms (*Time* x *Age@1stscan, Time* x *TS@1stScan, TSChange* x *Age@1stScan*, and *TSChange* x *TS@1stscan*) were added to the model next. Age at first scan (*Age@1stScan*) moderated the slope of growth across pubertal development (*TSChange*), in that older youth entering the study tended to show less change in right amygdala volumes as they passed through puberty. Specifically, for each year of age at study entry, the rate of change decreased by −9.42mm^3/Tanner stage ($p < .05$). No other cross-level interaction terms reached significance. Next, separate three-way cross-level interaction terms were added to the model, reflecting 'moderated moderation' of age at first scan and pubertal development at first scan on the interaction between pubertal progress and time in study (e.g., *Age@1stScan* x *TSChange* x *Time; TS@1stScan* x *TSChange* x *Time*). Neither effect was significant, as shown in Table 5-A.

Corresponding analyses were conducted to evaluate a *Combined Model* predicting left amygdala volumes. Results from these analyses are provided in Table 5-B. In an initial step, fixed effects of time in study (*Time*), change in pubertal development during the study (*TSChange*), and an interaction term (*Time* x *TSChange*) were added to a random-intercept model. None of these terms significantly predicted growth in left amygdala volumes. Adding the random effect variance of time in study (*Time*) improved the model fit (-2ΔLL(1) = 5.13, $p < .05$), as did the random effect of pubertal change since study entry (*TSChange*; -2ΔLL(1) = 8.63, $p < .01$), suggesting meaningful between-subjects differences in each trend. The random effect of the interaction term did not improve fit over a model including none, one, or both random effects for pubertal change or time since study entry (all $p > .05$), suggesting the effect of the

interaction tended not to vary across participants. A final 'unconditional' model was retained that included all fixed effects terms, as well as the two significant random effect terms (i.e., not the random effect of the interaction).

Between-subjects predictors age at first scan (*Age@1stScan*) and pubertal status at first scan (*TS@1stScan*) were added to the unconditional model. As in the right amygdala, *Age@1stScan* significantly influenced the intercept, in that for each year of a participant's age at initial assessment, left amygdala volumes were 21.95mm^3 larger on average ($p < .001$; Table 5-B). Pubertal development at study entry (*TS@1stScan*) also predicted left amygdala volumes at initial scan, though as in the right amygdala, the effect was reversed. For each Tanner stage at initial assessment, participants showed a -45.65mm^3 reduction in left amygdala volumes ($p < .01$). As in analyses of the *Combined Model* with right amygdala volumes, two-way and three-way cross-level interaction terms were added to the model in subsequent steps. However, none of the interactive effects reached significance, suggesting that neither pubertal status nor age at initial scan moderated the slope of change in left amygdala volumes by time in study, pubertal development, or the interaction between the two.

Model Comparisons

Finally, the proposed models of amygdala development were compared in terms of fit to the data, as characterized by the AIC. Separate comparisons were made for models predicting growth in right and left amygdala volumes. For these analyses, data were limited to those cases without missing values for pubertal development or age, ensuring an equivalent sample size across models incorporating respective predictors (i.e., listwise deletion). Each of the models tested included all possible fixed effects (two and three-way interactions as well as all nested predictors), though no random effect terms. Model fit to the data is presented in Table 6, which

shows the AIC, difference in AIC (ΔAIC) and AIC weight for the models, separately applied to right and left amygdala volumes.

As shown, the *Combined Model*, which included effects of chronological age as well as pubertal development (rather than either effect alone) exhibited the best fit to right amygdala volume data. The ΔAIC of 10.01 well exceeds the suggested threshold of 5.9, indicating the superiority of this model in comparison to the *Pubertal Development* or *Chronological Age* models. The AIC weight of .99, reflects the probability that the observed data were created by the *Combined Model* in comparison to the alternatives. Results comparing model fit for left amygdala volumes were less conclusive. Though the *Pubertal Development* model had the lowest AIC value, this was only slightly greater than that of the *Combined Model* (ΔAIC = 0.66). Therefore, the superiority of any one model predicting change in left amygdala volumes could not be determined.

CHAPTER 8. DISCUSSION

Though collective knowledge about the fully formed amygdala is nearly 200 years old, neuroscientists are just now beginning to examine its development. The current study builds on previous work exploring the amygdala's growth (Albaugh et al., 2017; Giedd, Vaituzis, et al., 1996; Goddings et al., 2014b), while making important empirical and methodological advances. Foremost, the findings provide a well-founded reference for amygdala growth in typically developing youth, which might be used as a baseline for assessing the severity of deviation in non-typical or disordered youth. Further, results reveal a previously unidentified difference in the growth of the left and right amygdalae, which may open avenues for future investigations. Moreover, the analyses provide a template for treating data from CS design studies of neurodevelopment, where researchers must take care to consider multiple effects of 'time'. The results demonstrate how the selection of an index of 'development', be it puberty, age, or both, can impact results. Below, I provide a more comprehensive discussion of the implications of this work, describe the strengths and limitations of the study, and explore new directions for future investigations.

As a primary aim, this study sought to map the normative course of growth in the left and right amygdalae across childhood and adolescence. Previous large-sample, CS design studies have established that the amygdala changes in size across development. Therefore, positive growth in right and left amygdala volumes was anticipated. Indeed, the findings largely affirm previous research, in that the passage of time predicted larger amygdala volumes. Notably, however, the trajectory of change appeared to differ across the left and right sides of the brain. For each year of participation in the study, right amygdala volumes increased 19.04mm^3 on

average. A similar, but more gradual increase was seen in the left amygdala, which grew at less than half the rate (9.92mm^3/year).

However, by solely modeling change as a product of within-subject effects (such as change in time), we inherently assume that any between-subjects effects are negligible. Such an assumption may be untenable in a CS design, where individuals enter the study at different stages of developmental progress (Hoffman, 2015). To account for these differences, analyses in the current study additionally modeled a between-subjects effect of age at study entry. As anticipated, the age at which children were initially scanned moderated the slope of both left and right amygdala volumes, indicating that the nature of growth varies across development. Specifically, steeper slopes were observed among youth who entered the study at an early age (i.e., < 10 yrs.). Rapid increases in volume at ages 5 and 6 become more moderate as youth enter early adolescence and may turn to declines in volume during late adolescence or early adulthood. Decomposition of the interaction between age at first scan and time in study using the JN technique found that the slope becomes non-significant at 13.1 years of age for the left amygdala, and 14.5 years for the right. Thus, the volumetric growth of the left amygdala 'peaks' earlier than the right.

However, this finding contradicts the current hypotheses, which anticipated faster development of the *right* amygdala. Weems' (2017) synthesis of the literature reveals that the right amygdala may be more susceptible to effects of stress exposure. Specifically, Weems et al (2015, 2013; also Tottenham et al., 2010) show that traumatic stress predicts accelerated development of the right, but not left amygdala. Notably, these studies targeted youth who experienced intensely traumatic events (disaster exposure, extreme neglect), whereas participants in the current sample were unlikely to have endured such extreme forms of stress. Still, even

normative youth undergo *some* stressful experiences during development; therefore, it would be reasonable to assume that the right amygdala would exhibit slightly earlier growth in a normative sample. Conversely, however, this assumes that in the pristine brain of an individual whose development was completely stress-free, we should expect the right and left amygdala to grow and change in a symmetrical fashion. On its face, this assumption seems untenable, given our extensive knowledge about functional and structural lateral differences in the brain (Ocklenburg & Güntürkün, 2018). Moreover, based on model intercept values in the results of the current study, right amygdala volumes are generally larger than left, a finding consistent with a wealth of evidence from adult studies (Guadalupe et al., 2017). Presumably, this may stem from prolonged development of the right amygdala, therefore a later 'peak' in volume as shown in the findings.

Though this study brings volumetric and developmental differences in the right and left amygdala into focus, the mechanism underlying this effect remains unclear. Theoretically, this variation might stem from differences in cellular composition. While scholars often characterize it as a unified structure, the amygdala is actually comprised of multiple sub-regions containing highly differentiated cells (Swanson & Petrovich, 1998). Recent work with functional neuroimaging reveals that these cells may show specialized responses to aspects of emotionally salient stimuli (Balderston, Schultz, Hopkins, & Helmstetter, 2015). Lateral differences in cellular composition (i.e., sub-amygdalar volumes) might account for lateral differences in responsive activation to stimuli (e.g., Phelps et al., 2001). Moreover, and relevant to the current study, such differences might also underlie the variation in size and growth seen across the left and right amygdalae. An important caveat: the small size of the amygdala places it at the boundaries of what can be reasonably investigated using 1.5T or even 3T-resolution MRI. While

there is clear need to further investigate its substructure, such research may require high-field (e.g., 7T) or multimodal approaches (Crone & Elzinga, 2015; De Martino et al., 2018)

This lateral effect on growth trends might further explain apparent differences in amygdala volumes at older ages. Weems (2017) posits a potential decline in amygdala volumes in late adolescence or early adulthood, as suggested by the cross-sectional results from Uematsu et al. (2012). Results in the current study similarly suggest a decline in both left and right amygdala volumes. Though the difference is slight, right amygdala volumes appear to decline earlier in development. Thus, in comparison to the left, the right amygdala appears to reach peak volume earlier, and begin to decline in volume earlier. While the lateral differences in the start of the decrease in size might similarly be attributable to differences in cellular composition (as in the different timing of peak volume), the amygdala's decrease in volume during early adulthood contrasts with broader age-related changes. Giorgio et al. (2010) show that total grey matter volume (which includes the amygdala) increases (slightly) throughout early adulthood, peaks in middle age, before declining in later years. This 'misalignment' of amygdala development relative to the rest of the brain aligns well with several theories positing that the temporary imbalance in cortical and subcortical systems may be core to the "storm and stress" of adolescence (Casey et al., 2010; Somerville, Jones, & Casey, 2010; Steinberg, 2008).

Theory and empirical evidence suggest that stress may moderate the interactive link between limbic and frontal areas of the brain (Herringa et al., 2016; Tottenham & Galván, 2016), and that this effect may be driven by deviated growth of the amygdala (Weems, 2017). While prior studies have focused effects of severe traumatic experiences, the current research broadened the scope to effects of socioeconomic stress, specifically the 'stress' of poverty, and it was anticipated that results would show more rapid early increases in amygdala volume among

low SES youth. Contrary to hypotheses, the findings suggest that SES-related stress may have little impact on either the age or puberty-driven changes in amygdala volumes across child development. This is surprising given the accumulating evidence linking lower childhood SES to elevated amygdala activation (Kim et al., 2013; S. E. Taylor, Eisenberger, Saxbe, Lehman, & Lieberman, 2006; S. B. Johnson et al., 2016). However, even within these studies, it may be unreasonable to assume direct effects of SES on the brain. Rather, such effects are likely mediated through the many, well-documented links between SES and factors such as family conflict, caregiver instability, or community violence, which can contribute to chronic activation of the stress response system, and consequential changes to the amygdala. While the current study used HUD-adjusted annual family income levels as a proxy for SES, future research may need to further consider factors such as housing location or parent education level, as these correlates of SES may more directly influence amygdala growth.

Though the findings reveal meaningful, dynamic change in amygdala volumes across development, it is important to consider that these results were only observed in models where development was indexed according to age in years. Specifically, analyses with the *Chronological Age* model revealed that left and right amygdala volumes changed across change in age (i.e., time in years), and that the slope of this change varied depending on the age at which participants entered the study. In contrast, corresponding analyses that predicted change in amygdala volumes according to puberty (or a combination of age and puberty), failed to show any change in the nature of amygdala growth as children developed. Initially, these results suggest that mapping amygdala volumes by chronological age provides a more nuanced, and representative account of growth. However, in a direct comparison, the *Chronological Age* model demonstrated the poorest fit to the data, by far (Table 7).

This incoherence in the results might be a product of the way this study and many others assess pubertal development. The Tanner stage system translates the appearance of several outward pubertal changes onto a graded five-level scale of development (Dorn & Biro, 2011; Tanner, 1962). Though its widespread use has led to major gains in knowledge about links between puberty, health, and development, researchers may now be asking this system to account for more than it was designed to do. A discrete, five-point scale may not provide the sensitivity necessary to index subtle changes in neuroanatomical development. Moreover, variance in Tanner stages does not appear until the start of adrenarche, which occurs at approximately 6 to 8 years of age in girls, and a year later in boys. Results in the current study show that by this point, the amygdala has already undergone dramatic change. This growth will be associated with variance in chronological age, but not pubertal development, which would remain at Tanner stage 1, prior to the onset of puberty. Similarly, declining amygdala volumes in late adolescence/early adulthood, when most youth have reached Tanner stage 5, would not be indexed by pubertal development.

Though this study provides novel insights into normative amygdala growth, the findings should be considered in light of its limitations. First, findings related to pubertal development should be interpreted with caution, given the non-random missingness in this section of the data. Specifically, younger participants were less likely to be assessed for pubertal development, potentially biasing results related to amygdala development along a pubertal index. Second, and relatedly, pubertal development was assessed using a brief self-report (Pubertal Development Scale). Though widely used, this measure falls short of the reliability achieved through the gold standard of clinician assessment. Third, quality control procedures of the post-processing estimates consisted of comparing volumes of non-focal structures (e.g., caudate) to previously

reported values computed using different neuroimage processing software. While this approach was able to confirm the *general* reliability of the processing pipeline, it provides limited support for its ability to extract appropriate values for the amygdala, specifically. Future investigations with this data set would do well to rely on any of the novel, algorithm based quality control procedures described in the literature (Backhausen et al., 2016).

The present study opens several avenues for future investigation. First, the novel finding of lateral differences in brain development encourages subsequent research investigating the sub-structural makeup of the left and right amygdala. It may be that specific regions of the amygdala drive the effect, potentially due to respective involvement in specific functions of affective processing – such as orientation to threatening stimuli. Indeed, this reflects a broader trend in human neuroscience towards investigation at the substructural, cellular, and subcellular levels. Second, despite increasing support for a decline in amygdala volumes during early adulthood (Uematsu et al., 2012), there is presently a paucity of longitudinal research examining changes in the amygdala during this period. More broadly, though there is increasing appreciation of the continuation of cortical development into the early 20's, similar research into subcortical change remains limited. Third, there is a need to consider more nuanced indexes of pubertal change, beyond visual inspection of outward bodily changes. Future research may benefit from considering neurodevelopment alongside developmental variation in hormone levels for example, which may have closer biological relevance to neurological change.

REFERENCES

Achenbach, T. M. (1991). *Manual for the Child Behavior Checklist/4-18 and 1991 profile*. Burlington, VT: University of Vermont Department of Psychiatry.

Achenbach, T. M., & Rescorla, L. A. (2001). *Manual for the ASEBA School-Age Forms & Profiles*. Burlington, VT: University of Vermont, Research Center for Children, Youth, and Families.

Aggleton, J. P. (2000). *The amygdala: A functional analysis* (2nd ed.). New York, NY: Oxford University Press.

Al Hazzouri, A. Z., Haan, M. N., Galea, S., & Aiello, A. E. (2011). Life-course exposure to early socioeconomic environment, education in relation to late-life cognitive function among older Mexicans and Mexican Americans. *Journal of Aging and Health*, *23*, 1027–1049.

Albaugh, M. D., Nguyen, T.-V., Ducharme, S., Collins, D. L., Botteron, K. N., D'Alberto, N., … Group, B. D. C. (2017). Age-related volumetric change of limbic structures and subclinical anxious/depressed symptomatology in typically developing children and adolescents. *Biological Psychology*, *124*, 133–140.

American Psychiatric Association. (2000). *Diagnostic and statistical manual of mental disorders* (4th ed., text rev.). Washington, DC: Author.

Arimitsu, T., Di Chiro, G., Brooks, R. A., & Smith, P. B. (1977). White-gray matter differentiation in computed tomography. *Journal of Computer Assisted Tomography*, *1*, 437–442.

Armony, J. L., Corbo, V., Clément, M.-H., & Brunet, A. (2005). Amygdala response in patients with acute PTSD to masked and unmasked emotional facial expressions. *American Journal of Psychiatry*, *162*, 1961–1963.

Backhausen, L. L., Herting, M. M., Buse, J., Roessner, V., Smolka, M. N., & Vetter, N. C. (2016). Quality control of structural MRI images applied using Freesurfer—a hands-on workflow to rate motion artifacts. *Frontiers in Neuroscience*, *10*.

Baird, A. A., Gruber, S. A., Fein, D. A., Mass, L. C., Steingard, R. J., Renshaw, P. F., … Yurgelun-Todd, D. A. (1999). Functional magnetic resonance imaging of facial affect recognition in children and adolescents. *Journal of the American Academy of Child & Adolescent Psychiatry*, *38*, 195–199.

Balderston, N. L., Schultz, D. H., Hopkins, L., & Helmstetter, F. J. (2015). Functionally distinct amygdala subregions identified using DTI and high-resolution fMRI. *Social Cognitive and Affective Neuroscience*, *10*, 1615–1622.

Baltes, P. B., Reese, H. W., & Nesselroade, J. R. (1977). *Life-span developmental psychology: Introduction to research methods*. Hillsdale, NJ: Lawrence Erlbaum Associates.

Banks, W. A. (2012). Brain meets body: The blood-brain barrier as an endocrine interface. *Endocrinology*, *153*, 4111–4119.

Barendse, M. E., Simmons, J. G., Byrne, M. L., Seal, M. L., Patton, G., Mundy, L., … Whittle, S. (2018). Brain structural connectivity during adrenarche: associations between hormone levels and white matter microstructure. *Psychoneuroendocrinology*, *88*, 70–77.

Barkovich, A. J., & Kjos, B. O. (1988). Normal postnatal development of the corpus callosum as demonstrated by MR imaging. *American Journal of Neuroradiology*, *9*, 487–491.

Barkovich, A. J., Kjos, B. O., Jackson Jr, D. E., & Norman, D. (1988). Normal maturation of the neonatal and infant brain: MR imaging at 1.5 T. *Radiology*, *166*, 173–180.

Bassett, D. S., & Sporns, O. (2017). Network neuroscience. *Nature Neuroscience*, *20*, 353–364.

Bates, D., Maechler, M., Bolker, B., & Walker, S. (2018). lme4: Linear Mixed-Effects Models Using "Eigen" and S4 (Version 1.1.16). Retrieved from http://cran.r-project.org/package=lme4

Bell, R. Q. (1953). Convergence: An accelerated longitudinal approach. *Child Development*, *24*, 145–152.

Belsky, J., & de Haan, M. (2011). Annual Research Review: Parenting and children's brain development: the end of the beginning. *Journal of Child Psychology and Psychiatry, and Allied Disciplines*, *52*, 409–428.

Birbaumer, N., Grodd, W., Diedrich, O., Klose, U., Erb, M., Lotze, M., … Flor, H. (1998). fMRI reveals amygdala activation to human faces in social phobics. *NeuroReport*, *9*, 1223–1226.

Blakemore, S.-J., Burnett, S., & Dahl, R. E. (2010). The role of puberty in the developing adolescent brain. *Human Brain Mapping*, *31*, 926–933.

Brain Development Cooperative Group. (2012). Total and regional brain volumes in a population-based normative sample from 4 to 18 Years: The NIH MRI Study of Normal Brain Development. *Cerebral Cortex*, *22*, 1–12.

Brain Development Cooperative Group, & Evans, A. C. (2006). The NIH MRI study of normal brain development. *NeuroImage*, *30*, 184–202.

Breiter, H. C., Etcoff, N. L., Whalen, P. J., Kennedy, W. A., Rauch, S. L., Buckner, R. L., … Rosen, B. R. (1996). Response and habituation of the human amygdala during visual processing of facial expression. *Neuron*, *17*, 875–887.

Breiter, H. C., & Rauch, S. L. (1996). Functional MRI and the study of OCD: From symptom provocation to cognitive-behavioral probes of cortico-striatal systems and the amygdala. *NeuroImage*, *4*, S127–S138.

Breiter, H. C., Rauch, S. L., Kwong, K. K., Baker, J. R., Weisskoff, R. M., Kennedy, D. N., … Rosen, B. R. (1996). Functional magnetic resonance imaging of symptom provocation in obsessive-compulsive disorder. *Archives of General Psychiatry*, *53*, 595–606.

Brooks-Gunn, J., & Markman, L. B. (2005). The contribution of parenting to ethnic and racial gaps in school readiness. *The Future of Children*, *15*, 139–168.

Brown, S., & Schäfer, E. A. (1888). An investigation into the functions of the occipital and temporal lobes of the monkey's brain. *Philosophical Transactions of the Royal Society of London: B*, *179*, 303–327.

Büchel, C., Morris, J., Dolan, R. J., & Friston, K. J. (1998). Brain systems mediating aversive conditioning: an event-related fMRI study. *Neuron*, *20*, 947–957.

Bucy, P. C. (1985). Heinrich Klüver. In P. C. Bucy (Ed.), *Neurosurgical giants: Feet of clay and iron* (pp. 349–353). New York, NY: Elsevier Science.

Bucy, P. C., & Klüver, H. (1940). Anatomic changes secondary to temporal lobectomy. *Archives of Neurology & Psychiatry*, *44*, 1142–1146.

Burdach, K. F. (1819). *Vom Baue und Leben des Gehrins* (Vol. 1). Leipzig: Dyk'schen Buchhandlung.

Burnham, K. P., & Anderson, D. R. (2003). *Model selection and multimodel inference: A practical information-theoretic approach* (2nd ed.). New York, NY: Springer-Verlag.

Burnham, K. P., & Anderson, D. R. (2004). Multimodel inference: Understanding AIC and BIC in model selection. *Sociological Methods & Research*, *33*, 261–304.

Byrne, M. L., Whittle, S., Vijayakumar, N., Dennison, M., Simmons, J. G., & Allen, N. B. (2017). A systematic review of adrenarche as a sensitive period in neurobiological development and mental health. *Developmental Cognitive Neuroscience*, *25*, 12–28.

Cahill, L., Haier, R. J., Fallon, J., Alkire, M. T., Tang, C., Keator, D., … Mcgaugh, J. L. (1996). Amygdala activity at encoding correlated with long-term, free recall of emotional information. *Proceedings of the National Academy of Sciences*, *93*, 8016–8021.

Campbell, B. C. (2011). Adrenarche and middle childhood. *Human Nature*, *22*, 327–349.

Carey, G. (2013). *Quantitative methods in neuroscience*. Boulder, CO: Author. Retrieved from http://psych.colorado.edu/~carey/qmin/QMIN_2013_03_17.pdf

Carrión, V. G., Weems, C. F., Eliez, S., Patwardhan, A., Brown, W., Ray, R. D., & Reiss, A. L. (2001). Attenuation of frontal asymmetry in pediatric posttraumatic stress disorder. *Biological Psychiatry*, *50*, 943–951.

Casey, B. J., Giedd, J. N., & Thomas, K. M. (2000). Structural and functional brain development and its relation to cognitive development. *Biological Psychology*, *54*, 241–257.

Casey, B. J., Jones, R. M., Levita, L., Libby, V., Pattwell, S. S., Ruberry, E. J., … Somerville, L. H. (2010). The storm and stress of adolescence: insights from human imaging and mouse genetics. *Developmental Psychobiology*, *52*, 225–235.

Chapman, W. P., Schroeder, H. R., Geyer, G., Brazier, M. A., Fager, C., Poppen, J. L., … Yakovlev, P. I. (1954). Physiological evidence concerning importance of the amygdaloid nuclear region in the integration of circulatory function and emotion in man. *Science*, *120*, 949–951.

Chen, B. K., Sassi, R., Axelson, D., Hatch, J. P., Sanches, M., Nicoletti, M., … Birmaher, B. (2004). Cross-sectional study of abnormal amygdala development in adolescents and young adults with bipolar disorder. *Biological Psychiatry*, *56*, 399–405.

Cicchetti, D. (1984). The emergence of developmental psychopathology. *Child Development*, *55*, 1–7.

Cole, D. A., Maxwell, S. E., Martin, J. M., Peeke, L. G., Sroczynski, S. A., Tram, J. M., … Maschman, T. (2003). The development of multiple domains of child and adolescent self□concept: A cohort sequential longitudinal design. *Child Development*, *72*, 1723–1746.

Collins, D. L., & Evans, A. C. (1997). ANIMAL: Validation and applications of nonlinear registration-based segmentation. *International Journal of Pattern Recognition and Artificial Intelligence*, *11*, 1271–1294.

Collins, D. L., Holmes, C. J., Peters, T. M., & Evans, A. C. (1995). Automatic 3□D model□ based neuroanatomical segmentation. *Human Brain Mapping*, *3*, 190–208.

Collins, D. L., & Pruessner, J. C. (2010). Towards accurate, automatic segmentation of the hippocampus and amygdala from MRI by augmenting ANIMAL with a template library and label fusion. *NeuroImage*, *52*, 1355–1366.

Crone, E. A., & Elzinga, B. M. (2015). Changing brains: how longitudinal functional magnetic resonance imaging studies can inform us about cognitive and social-affective growth trajectories. *Wiley Interdisciplinary Reviews: Cognitive Science*, *6*, 53–63.

Dale, A. M., Fischl, B., & Sereno, M. I. (1999). Cortical surface-based analysis: I. Segmentation and surface reconstruction. *NeuroImage*, *9*, 179–194.

Dale, A. M., & Sereno, M. I. (1993). Improved localization of cortical activity by combining EEG and MEG with MRI cortical surface reconstruction: A linear approach. *Journal of Cognitive Neuroscience*, *5*, 162–176.

Dalgleish, T. (2004). The emotional brain. *Nature Reviews Neuroscience*, *5*, 583–589.

Dalgleish, T., Dunn, B. D., & Mobbs, D. (2009). Affective neuroscience: Past, present, and future. *Emotion Review*, *1*, 355–368.

Darwin, C. (1964). *On the origin of species: A facsimile of the first edition* (Facsimile edition). Cambridge, MA: Harvard University Press.

Davis, M. (1992). The role of the amygdala in fear and anxiety. *Annual Review of Neuroscience*, *15*, 353–375.

De Bellis, M. D. (2001). Developmental traumatology: The psychobiological development of maltreated children and its implications for research, treatment, and policy. *Development and Psychopathology*, *13*, 539–564.

De Bellis, M. D., Casey, B. J., Dahl, R. E., Birmaher, B., Williamson, D. E., Thomas, K. M., … Ryan, N. D. (2000). A pilot study of amygdala volumes in pediatric generalized anxiety disorder. *Biological Psychiatry*, *48*, 51–57.

De Bellis, M. D., Keshavan, M. S., Clark, D. B., Casey, B. J., Giedd, J. N., Boring, A. M., … Ryan, N. D. (1999). Developmental traumatology part II: Brain development. *Biological Psychiatry*, *45*, 1271–1284.

De Bellis, M. D., Keshavan, M. S., Shifflett, H., Iyengar, S., Beers, S. R., Hall, J., & Moritz, G. (2002). Brain structures in pediatric maltreatment-related posttraumatic stress disorder: a sociodemographically matched study. *Biological Psychiatry*, *52*, 1066–1078.

De Martino, F., Yacoub, E., Kemper, V., Moerel, M., Uludağ, K., De Weerd, P., … Formisano, E. (2018). The impact of ultra-high field MRI on cognitive and computational neuroimaging. *NeuroImage*, *168*, 366–382.

Dekaban, A. S., & Sadowsky, D. (1978). Changes in brain weights during the span of human life: relation of brain weights to body heights and body weights. *Annals of Neurology*, *4*, 345–356.

Del Giudice, M., Ellis, B. J., & Shirtcliff, E. A. (2011). The adaptive calibration model of stress responsivity. *Neuroscience & Biobehavioral Reviews*, *35*, 1562–1592.

DeNavas-Walt, C., & Proctor, B. D. (2014). *Income and poverty in the United States: 2013 current population reports*. Washington, DC: US Department of Commerce, US Census Bureau.

Desikan, R. S., Ségonne, F., Fischl, B., Quinn, B. T., Dickerson, B. C., Blacker, D., … Hyman, B. T. (2006). An automated labeling system for subdividing the human cerebral cortex on MRI scans into gyral based regions of interest. *NeuroImage*, *31*, 968–980.

Di Marino, V., Etienne, Y., & Niddam, M. (2016). *The amygdaloid nuclear complex: anatomic study of the human amygdala*. New York, NY: Springer.

Di Martino, A., Fair, D. A., Kelly, C., Satterthwaite, T. D., Castellanos, F. X., Thomason, M. E., … Milham, M. P. (2014). Unraveling the miswired connectome: a developmental perspective. *Neuron*, *83*, 1335–1353.

Diehl, M., Hooker, K., & Sliwinski, M. J. (2015). A brief historical overview of intraindividual variability research across the lifespan. In M. Diehl, K. Hooker, & M. J. Sliwinski (Eds.), *Handbook of intraindividual variability across the life span* (pp. 3–15). New York, NY: Routledge.

Ding, J., Han, F., & Shi, Y. (2010). Single-prolonged stress induces apoptosis in the amygdala in a rat model of post-traumatic stress disorder. *Journal of Psychiatric Research*, *44*, 48–55.

Dorn, L. D., & Biro, F. M. (2011). Puberty and its measurement: A decade in review. *Journal of Research on Adolescence*, *21*, 180–195.

Drevets, W. C., Videen, T. O., Price, J. L., Preskorn, S. H., Carmichael, S. T., & Raichle, M. E. (1992). A functional anatomical study of unipolar depression. *Journal of Neuroscience*, *12*, 3628–3641.

Duncan, S. C., Duncan, T. E., & Hops, H. (1996). Analysis of longitudinal data within accelerated longitudinal designs. *Psychological Methods*, *1*, 236–248.

Duncan, S. C., Duncan, T. E., & Strycker, L. A. (2006). Alcohol use from ages 9 to 16: A cohort-sequential latent growth model. *Drug & Alcohol Dependence*, *81*, 71–81.

Ekman, P. (1992). An argument for basic emotions. *Cognition & Emotion*, *6*, 169–200.

Ekman, P., & Friesen, W. V. (1971). Constants across cultures in the face and emotion. *Journal of Personality and Social Psychology*, *17*, 124–129.

Evans, G. W., & Schamberg, M. A. (2009). Childhood poverty, chronic stress, and adult working memory. *Proceedings of the National Academy of Sciences*, *106*, 6545–6549.

Fanselow, M. S., & LeDoux, J. E. (1999). Why we think plasticity underlying Pavlovian fear conditioning occurs in the basolateral amygdala. *Neuron*, *23*, 229–232.

Farah, M. J. (2017). The neuroscience of socioeconomic status: correlates, causes, and consequences. *Neuron*, *96*, 56–71.

Fargo, K. N., Galbiati, M., Foecking, E. M., Poletti, A., & Jones, K. J. (2008). Androgen regulation of axon growth and neurite extension in motoneurons. *Hormones and Behavior*, *53*, 716–728.

Feindel, W., & Penfield, W. (1954). Localization of discharge in temporal lobe automatism. *AMA Archives of Neurology & Psychiatry*, *72*, 605–630.

Feinstein, J. S., Adolphs, R., Damasio, A., & Tranel, D. (2011). The human amygdala and the induction and experience of fear. *Current Biology*, *21*, 34–38.

Fischl, B., & Dale, A. M. (2000). Measuring the thickness of the human cerebral cortex from magnetic resonance images. *Proceedings of the National Academy of Sciences*, *97*, 11050–11055.

Fischl, B., Liu, A., & Dale, A. M. (2001). Automated manifold surgery: constructing geometrically accurate and topologically correct models of the human cerebral cortex. *IEEE Transactions on Medical Imaging*, *20*, 70–80.

Fischl, B., Salat, D. H., Busa, E., Albert, M. S., Dieterich, M., Haselgrove, C., … Dale, A. M. (2002). Whole brain segmentation: automated labeling of neuroanatomical structures in the human brain. *Neuron*, *33*, 341–355.

Fischl, B., Salat, D. H., van der Kouwe, A., Makris, N., Ségonne, F., Quinn, B. T., & Dale, A. M. (2004). Sequence-independent segmentation of magnetic resonance images. *NeuroImage*, *23*, S69–S84.

Fischl, B., Sereno, M. I., & Dale, A. M. (1999). Cortical surface-based analysis: II: Inflation, flattening, and a surface-based coordinate system. *NeuroImage*, *9*, 195–207.

Fischl, B., Sereno, M. I., Tootell, R. B. H., & Dale, A. M. (1999). High-resolution intersubject averaging and a coordinate system for the cortical surface. *Human Brain Mapping*, *8*, 272–284.

Fischl, B., van der Kouwe, A., Destrieux, C., Halgren, E., Ségonne, F., Salat, D. H., … Kennedy, D. N. (2004). Automatically parcellating the human cerebral cortex. *Cerebral Cortex*, *14*, 11–22.

Gentile, D. A., Swing, E. L., Anderson, C. A., Rinker, D., & Thomas, K. M. (2016). Differential neural recruitment during violent video game play in violent-and nonviolent-game players. *Psychology of Popular Media Culture*, *5*, 39–51.

Giedd, J. N. (2004). Structural magnetic resonance imaging of the adolescent brain. *Annals of the New York Academy of Sciences*, *1021*, 77–85.

Giedd, J. N. (2008). The teen brain: insights from neuroimaging. *Journal of Adolescent Health*, *42*, 335–343.

Giedd, J. N., Blumenthal, J., Jeffries, N. O., Castellanos, F. X., Liu, H., Zijdenbos, A., … Rapoport, J. L. (1999). Brain development during childhood and adolescence: a longitudinal MRI study. *Nature Neuroscience*, *2*, 861–863.

Giedd, J. N., Lenroot, R. K., Shaw, P., Lalonde, F., Celano, M. J., White, S. L., … Gogtay, N. (2008). Trajectories of anatomic brain development as a phenotype (Vol. 289, pp. 101–112). Presented at the Novartis Foundation Symposium.

Giedd, J. N., & Rapoport, J. L. (2010). Structural MRI of pediatric brain development: What have we learned and where are we going? *Neuron*, *67*, 728–734.

Giedd, J. N., Rumsey, J. M., Castellanos, F. X., Rajapakse, J. C., Kaysen, D., Vaituzis, A. C., … Rapoport, J. L. (1996). A quantitative MRI study of the corpus callosum in children and adolescents. *Developmental Brain Research*, *91*, 274–280.

Giedd, J. N., Snell, J. W., Lange, N., Rajapakse, J. C., Casey, B. J., Kozuch, P. L., … Rapoport, J. L. (1996). Quantitative magnetic resonance imaging of human brain development: Ages 4–18. *Cerebral Cortex*, *6*, 551–559.

Giedd, J. N., Vaituzis, A. C., Hamburger, S. D., Lange, N., Rajapakse, J. C., Kaysen, D., … Rapoport, J. L. (1996). Quantitative MRI of the temporal lobe, amygdala, and hippocampus in normal human development: ages 4–18 years. *Journal of Comparative Neurology*, *366*, 223–230.

Giorgio, A., Santelli, L., Tomassini, V., Bosnell, R., Smith, S., De Stefano, N., & Johansen-Berg, H. (2010). Age-related changes in grey and white matter structure throughout adulthood. *NeuroImage*, *51*, 943–951.

Glenn, C. R., Lieberman, L., & Hajcak, G. (2012). Comparing electric shock and a fearful screaming face as unconditioned stimuli for fear learning. *International Journal of Psychophysiology*, *86*, 214–219.

Goddard, G. V. (1964). Amygdaloid stimulation and learning in the rat. *Journal of Comparative and Physiological Psychology*, *58*, 23–30.

Goddings, A.-L., Mills, K., Clasen, L., Giedd, J., Viner, R., & Blakemore, S.-J. (2014a). Longitudinal MRI to assess effect of puberty on subcortical brain development: An observational study. *The Lancet*, *383*, S52.

Goddings, A.-L., Mills, K. L., Clasen, L. S., Giedd, J. N., Viner, R. M., & Blakemore, S.-J. (2014b). The influence of puberty on subcortical brain development. *NeuroImage*, *88*, 242–251.

Gogtay, N., Giedd, J. N., Lusk, L., Hayashi, K. M., Greenstein, D., Vaituzis, A. C., … others. (2004). Dynamic mapping of human cortical development during childhood through early adulthood. *Proceedings of the National Academy of Sciences of the United States of America*, *101*, 8174–8179.

Gray, J. A., & McNaughton, N. (2000). *The neuropsychology of anxiety: An enquiry into the function of the septo-hippocampal system*. New York, NY: Oxford University Press.

Guadalupe, T., Mathias, S. R., vanErp, T. G. M., Whelan, C. D., Zwiers, M. P., Abe, Y., … Francks, C. (2017). Human subcortical brain asymmetries in 15,847 people worldwide reveal effects of age and sex. *Brain Imaging and Behavior*, *11*, 1497–1514.

Gunnar, M., & Quevedo, K. (2007). The neurobiology of stress and development. *Annual Review of Psychology*, *58*, 145–173.

Guralnik, J. M., Butterworth, S., Wadsworth, M. E., & Kuh, D. (2006). Childhood socioeconomic status predicts physical functioning a half century later. *The Journals of Gerontology Series A: Biological Sciences and Medical Sciences*, *61*, 694–701.

Guyer, A. E., Monk, C. S., McClure-Tone, E. B., Nelson, E. E., Roberson-Nay, R., Adler, A. D., … Ernst, M. (2008). A developmental examination of amygdala response to facial expressions. *Journal of Cognitive Neuroscience*, *20*, 1565–1582.

Hackman, D. A., & Farah, M. J. (2009). Socioeconomic status and the developing brain. *Trends in Cognitive Sciences*, *13*, 65–73.

Hage, Z. A., Alaraj, A., & Charbel, F. T. (2016). Neuroimaging in the modern era. *Translational Research*, *175*, 1–3.

Halekoh, U., & Højsgaard, S. (2014). A Kenward-Roger approximation and parametric bootstrap methods for tests in linear mixed models–The R package pbkrtest. *Journal of Statistical Software*, *59*, 1–30.

Han, X., Jovicich, J., Salat, D. H., van der Kouwe, A., Quinn, B. T., Czanner, S., … Fischl, B. (2006). Reliability of MRI-derived measurements of human cerebral cortical thickness: The effects of field strength, scanner upgrade and manufacturer. *NeuroImage*, *32*, 180–194.

Hanson, J. L., Nacewicz, B. M., Sutterer, M. J., Cayo, A. A., Schaefer, S. M., Rudolph, K. D., … Davidson, R. J. (2015). Behavioral problems after early life stress: contributions of the hippocampus and amygdala. *Biological Psychiatry*, *77*, 314–323.

Hare, T. A., Tottenham, N., Galvan, A., Voss, H. U., Glover, G. H., & Casey, B. J. (2008). Biological substrates of emotional reactivity and regulation in adolescence during an emotional Go-NoGo task. *Biological Psychiatry*, *63*, 927–934.

Helms, G., Kallenberg, K., & Dechent, P. (2006). Contrast-driven approach to intracranial segmentation using a combination of T2- and T1-weighted 3D MRI data sets. *Journal of Magnetic Resonance Imaging*, *24*, 790–795.

Herman, J. P., & Cullinan, W. E. (1997). Neurocircuitry of stress: central control of the hypothalamo–pituitary–adrenocortical axis. *Trends in Neurosciences*, *20*, 78–84.

Herringa, R. J. (2017). Trauma, PTSD, and the developing brain. *Current Psychiatry Reports*, *19*, 69.

Herringa, R. J., Burghy, C. A., Stodola, D. E., Fox, M. E., Davidson, R. J., & Essex, M. J. (2016). Enhanced prefrontal-amygdala connectivity following childhood adversity as a protective mechanism against internalizing in adolescence. *Biological Psychiatry: Cognitive Neuroscience and Neuroimaging*, *1*, 326–334.

Herting, M. M., Gautam, P., Spielberg, J. M., Dahl, R. E., & Sowell, E. R. (2015). A longitudinal study: changes in cortical thickness and surface area during pubertal maturation. *PLoS One*, *10*, e0119774.

Hines, M., Allen, L. S., & Gorski, R. A. (1992). Sex differences in subregions of the medial nucleus of the amygdala and the bed nucleus of the stria terminalis of the rat. *Brain Research*, *579*, 321–326.

Hirase, H., & Shinohara, Y. (2014). Transformation of cortical and hippocampal neural circuit by environmental enrichment. *Neuroscience*, *280*, 282–298.

Hoffman, L. (2007). Multilevel models for examining individual differences in within-person variation and covariation over time. *Multivariate Behavioral Research*, *42*, 609–629.

Hoffman, L. (2015). *Longitudinal analysis: Modeling within-person fluctuation and change*. New York, NY: Routledge.

Holland, B. A., Haas, D. K., Norman, D., Brant-Zawadzki, M., & Newton, T. H. (1986). MRI of normal brain maturation. *American Journal of Neuroradiology*, *7*, 201–208.

Hubel, D. H., & Wiesel, T. N. (1962). Receptive fields, binocular interaction and functional architecture in the cat's visual cortex. *The Journal of Physiology*, *160*, 106–154.

Hughes, K. C., & Shin, L. M. (2011). Functional neuroimaging studies of post-traumatic stress disorder. *Expert Review of Neurotherapeutics*, *11*, 275–285.

Huizinga, D., Esbensen, F.-A., & Weiher, A. (1994). Examining developmental trajectories in delinquency using accelerated longitudinal research designs. In E. G. M. Weitekamp & H.-J. Kerner (Eds.), *Cross-national longitudinal research on human development and criminal behavior* (pp. 203–216). Dordrecth, UK: Springer.

Irwin, W., Davidson, R. J., Lowe, M. J., Mock, B. J., Sorenson, J. A., & Turski, P. A. (1996). Human amygdala activation detected with echo-planar functional magnetic resonance imaging. *NeuroReport*, *7*, 1765–1769.

Janak, P. H., & Tye, K. M. (2015). From circuits to behaviour in the amygdala. *Nature*, *517*, 284–292.

Jernigan, T. L., & Tallal, P. A. (1990). Late childhood changes in brain morphology observable with MRI. *Developmental Medicine & Child Neurology*, *32*, 379–385.

Jernigan, T. L., Trauner, D. A., Hesselink, J. R., & Tallal, P. A. (1991). Maturation of human cerebrum observed in vivo during adolescence. *Brain*, *114*, 2037–2049.

Johnson, M. A., Pennock, J. M., Bydder, G. M., Steiner, R. E., Thomas, D. J., Hayward, R., … Whitelaw, A. (1983). Clinical NMR imaging of the brain in children: Normal and neurologic disease. *American Journal of Roentgenology*, *141*, 1005–1018.

Johnson, P. O., & Neyman, J. (1936). Tests of certain linear hypotheses and their application to some educational problems. *Statistical Research Memoirs*, *1*, 57–93.

Johnson, S. B., Riis, J. L., & Noble, K. G. (2016). State of the art review: poverty and the developing brain. *Pediatrics*, *137*, 1–16.

Johnston, J. B. (1923). Further contributions to the study of the evolution of the forebrain. *The Journal of Comparative Neurology*, *35*, 337–481.

Josephs, O., Turner, R., & Friston, K. (1997). Event-related fMRI. *Human Brain Mapping*, *5*, 243–248.

Jovicich, J., Czanner, S., Greve, D. N., Haley, E., van der Kouwe, A., Gollub, R. L., … Dale, A. M. (2006). Reliability in multi-site structural MRI studies: Effects of gradient non-linearity correction on phantom and human data. *NeuroImage*, *30*, 436–443.

Karchemskiy, A., Garrett, A., Howe, M., Adleman, N., Simeonova, D. I., Alegria, D., … Chang, K. (2011). Amygdalar, hippocampal, and thalamic volumes in youth at high risk for development of bipolar disorder. *Psychiatry Research: Neuroimaging*, *194*, 319–325.

Kenward, M. G., & Roger, J. H. (1997). Small sample inference for fixed effects from restricted maximum likelihood. *Biometrics*, 983–997.

Kikusui, T., & Mori, Y. (2009). Behavioural and neurochemical consequences of early weaning in rodents. *Journal of Neuroendocrinology*, *21*, 427–431.

Killgore, W. D. S., Oki, M., & Yurgelun-Todd, D. A. (2001). Sex-specific developmental changes in amygdala responses to affective faces. *NeuroReport*, *12*, 427–433.

Killgore, W. D. S., & Yurgelun-Todd, D. A. (2004a). Activation of the amygdala and anterior cingulate during nonconscious processing of sad versus happy faces. *NeuroImage*, *21*, 1215–1223.

Killgore, W. D. S., & Yurgelun-Todd, D. A. (2004b). Sex-related developmental differences in the lateralized activation of the prefrontal cortex and amygdala during perception of facial affect. *Perceptual and Motor Skills*, *99*, 371–391.

Kim, P., Evans, G. W., Angstadt, M., Ho, S. S., Sripada, C. S., Swain, J. E., … Phan, K. L. (2013). Effects of childhood poverty and chronic stress on emotion regulatory brain function in adulthood. *Proceedings of the National Academy of Sciences*, *110*, 18442–18447.

Klauser, P., Whittle, S., Simmons, J. G., Byrne, M. L., Mundy, L. K., Patton, G. C., … Allen, N. B. (2015). Reduced frontal white matter volume in children with early onset of adrenarche. *Psychoneuroendocrinology*, *52*, 111–118.

Kleinman, P. K., Zito, J. L., Davidson, R. I., & Raptopoulos, V. (1983). The subarachnoid spaces in children: normal variations in size. *Radiology*, *147*, 455–457.

Klüver, H., & Bucy, P. C. (1937). "Psychic blindness" and other symptoms following bilateral temporal lobectomy in Rhesus monkeys. *American Journal of Physiology*, *119*, 352–353.

Klüver, H., & Bucy, P. C. (1938). An analysis of certain effects of bilateral temporal lobectomy in the rhesus monkey, with special reference to "psychic blindness." *The Journal of Psychology*, *5*, 33–54.

Klüver, H., & Bucy, P. C. (1939a). A preliminary analysis of functions of the temporal lobes in monkeys. In *Transactions of the American Neurological Society* (pp. 170–175).

Klüver, H., & Bucy, P. C. (1939b). Preliminary analysis of the functions of the temporal lobe in monkeys. *Journal of Psychology*, *5*, 33–54.

Kofler, M. J., McCart, M. R., Zajac, K., Ruggiero, K. J., Saunders, B. E., & Kilpatrick, D. G. (2011). Depression and delinquency covariation in an accelerated longitudinal sample of adolescents. *Journal of Consulting and Clinical Psychology*, *79*, 458–469.

Kolber, B. J., Roberts, M. S., Howell, M. P., Wozniak, D. F., Sands, M. S., & Muglia, L. J. (2008). Central amygdala glucocorticoid receptor action promotes fear-associated CRH activation and conditioning. *Proceedings of the National Academy of Sciences of the United States of America*, *105*, 12004–12009.

Kuperberg, G. R., Broome, M. R., McGuire, P. K., David, A. S., Eddy, M., Ozawa, F., … Fischl, B. (2003). Regionally localized thinning of the cerebral cortex in schizophrenia. *Archives of General Psychiatry*, *60*, 878–888.

LaBar, K. S., Gatenby, J. C., Gore, J. C., LeDoux, J. E., & Phelps, E. A. (1998). Human amygdala activation during conditioned fear acquisition and extinction: a mixed-trial fMRI study. *Neuron*, *20*, 937–945.

LaBar, K. S., & Warren, L. H. (2009). Methodological approaches to studying the human amygdala. In P. J. Whalen & E. A. Phelps (Eds.), *The human amygdala* (pp. 155–176). New York, NY: Guilford Press.

Lange, N., Giedd, J. N., Xavier Castellanos, F., Vaituzis, A. C., & Rapoport, J. L. (1997). Variability of human brain structure size: ages 4–20 years. *Psychiatry Research: Neuroimaging*, *74*, 1–12.

Ledoux, J. (1998). *The emotional brain: The mysterious underpinnings of emotional life*. New York, NY: Simon & Schuster.

LeDoux, J. E. (2000). Emotion circuits in the brain. *Annual Review of Neuroscience*, *23*, 155–184.

LeDoux, J. E. (2007). The amygdala. *Current Biology*, *17*, R868–R874.

LeDoux, J. E., & Schiller, D. (2009). The human amygdala: Insights from other animals. In P. J. Whalen & E. A. Phelps (Eds.), *The human amygdala* (pp. 43–60). New York, NY: Guilford Press.

Lenroot, R. K., & Giedd, J. N. (2006). Brain development in children and adolescents: insights from anatomical magnetic resonance imaging. *Neuroscience & Biobehavioral Reviews*, *30*, 718–729.

Lenroot, R. K., Gogtay, N., Greenstein, D. K., Wells, E. M., Wallace, G. L., Clasen, L. S., … Giedd, J. N. (2007). Sexual dimorphism of brain developmental trajectories during childhood and adolescence. *NeuroImage*, *36*, 1065–1073.

Levene, M. I., Whitelaw, A., Dubowitz, V., Bydder, G. M., Steiner, R. E., Randell, C. P., & Young, I. R. (1982). Nuclear magnetic resonance imaging of the brain in children. *British Medical Journal (Clinical Research Edition)*, *285*, 774–776.

Liberzon, I., Taylor, S. F., Amdur, R., Jung, T. D., Chamberlain, K. R., Minoshima, S., … Fig, L. M. (1999). Brain activation in PTSD in response to trauma-related stimuli. *Biological Psychiatry*, *45*, 817–826.

Little, R. J. (1988). A test of missing completely at random for multivariate data with missing values. *Journal of the American Statistical Association*, *83*, 1198–1202.

Loman, M. M., & Gunnar, M. R. (2010). Early experience and the development of stress reactivity and regulation in children. *Neuroscience & Biobehavioral Reviews*, *34*, 867–876.

Luby, J., Belden, A., Botteron, K., Marrus, N., Harms, M. P., Babb, C., … Barch, D. (2013). The effects of poverty on childhood brain development: the mediating effect of caregiving and stressful life events. *JAMA Pediatrics*, *167*, 1135–1142.

Lucas, C. P., Zhang, H., Fisher, P. W., Shaffer, D., Regier, D. A., Narrow, W. E., … Friman, P. (2001). The DISC Predictive Scales (DPS): Efficiently screening for diagnoses. *Journal of the American Academy of Child & Adolescent Psychiatry*, *40*, 443–449.

Makino, S., Gold, P. W., & Schulkin, J. (1994). Corticosterone effects on corticotropin-releasing hormone mRNA in the central nucleus of the amygdala and the parvocellular region of the paraventricular nucleus of the hypothalamus. *Brain Research*, *640*, 105–112.

Maninger, N., Wolkowitz, O. M., Reus, V. I., Epel, E. S., & Mellon, S. H. (2009). Neurobiological and neuropsychiatric effects of dehydroepiandrosterone (DHEA) and DHEA sulfate (DHEAS). *Frontiers in Neuroendocrinology*, *30*, 65–91.

Maxwell, M. E. (1991). Family interview for genetic studies (FIGS): Manual for FIGS. Retrieved from https://www.nimhgenetics.org/interviews/figs/FIGS%201.0.pdf

McArdle, C. B., Richardson, C. J., Nicholas, D. A., Mirfakhraee, M., Hayden, C. K., & Amparo, E. G. (1987a). Developmental features of the neonatal brain: MR imaging. Part I. Gray-white matter differentiation and myelination. *Radiology*, *162*, 223–229.

McArdle, C. B., Richardson, C. J., Nicholas, D. A., Mirfakhraee, M., Hayden, C. K., & Amparo, E. G. (1987b). Developmental features of the neonatal brain: MR imaging. Part II. Ventricular size and extracerebral space. *Radiology*, *162*, 230–234.

McEwen, B. S. (1981). Neural gonadal steroid actions. *Science*, *211*, 1303–1311.

McEwen, B. S. (1998). Stress, adaptation, and disease: Allostasis and allostatic load. *Annals of the New York Academy of Sciences*, *840*, 33–44.

McEwen, B. S. (2000a). Allostasis and allostatic load: Implications for neuropsychopharmacology. *Neuropsychopharmacology*, *22*, 108–124.

McEwen, B. S. (2000b). The neurobiology of stress: from serendipity to clinical relevance. *Brain Research*, *886*, 172–189.

McEwen, B. S., Nasca, C., & Gray, J. D. (2016). Stress effects on neuronal structure: hippocampus, amygdala, and prefrontal cortex. *Neuropsychopharmacology*, *41*, 3–23.

McGaugh, J. L. (2000). Memory--a century of consolidation. *Science*, *287*, 248–251.

McGaugh, J. L. (2002). Memory consolidation and the amygdala: a systems perspective. *Trends in Neurosciences*, *25*, 456–461.

McLaughlin, K. A. (2016). Future directions in childhood adversity and youth psychopathology. *Journal of Clinical Child & Adolescent Psychology*, *45*, 361–382.

McLaughlin, K. A., Fox, N. A., Zeanah, C. H., Sheridan, M. A., Marshall, P., & Nelson, C. A. (2010). Delayed maturation in brain electrical activity partially explains the association between early environmental deprivation and symptoms of attention-deficit/hyperactivity disorder. *Biological Psychiatry*, *68*, 329–336.

Mehta, M. A., Golembo, N. I., Nosarti, C., Colvert, E., Mota, A., Williams, S. C. R., … Sonuga-Barke, E. J. S. (2009). Amygdala, hippocampal and corpus callosum size following severe early institutional deprivation: The English and Romanian Adoptees Study Pilot. *Journal of Child Psychology and Psychiatry, and Allied Disciplines*, *50*, 943–951.

Miller, G. E., & Chen, E. (2013). The biological residue of childhood poverty. *Child Development Perspectives*, *7*, 67–73.

Miyazaki, Y., & Raudenbush, S. W. (2000). Tests for linkage of multiple cohorts in an accelerated longitudinal design. *Psychological Methods*, *5*, 44–63.

Mizukami, S., Nishizuka, M., & Arai, Y. (1983). Sexual difference in nuclear volume and its ontogeny in the rat amygdala. *Experimental Neurology*, *79*, 569–575.

Monk, C. S., McClure, E. B., Nelson, E. E., Zarahn, E., Bilder, R. M., Leibenluft, E., … Pine, D. S. (2003). Adolescent immaturity in attention-related brain engagement to emotional facial expressions. *NeuroImage*, *20*, 420–428.

Morris, J. S., Frith, C. D., Perrett, D. I., Rowland, D., Young, A. W., Calder, A. J., & Dolan, R. J. (1996). A differential neural response in the human amygdala to fearful and happy facial expressions. *Nature*, *383*, 812–815.

Morris, John S., Öhman, A., & Dolan, R. J. (1998). Conscious and unconscious emotional learning in the human amygdala. *Nature*, *393*, 467–470.

Murphy, D. G., DeCarli, C., Daly, E., Haxby, J. V., Allen, G., White, B. J., … Rapoport, S. I. (1993). X-chromosome effects on female brain: a magnetic resonance imaging study of Turner's syndrome. *Lancet*, *342*, 1197–1200.

Nakamura, T., Tomida, M., Yamamoto, T., Ando, H., Takamata, T., Kondo, E., … Asanuma, N. (2013). The endogenous opioids related with antinociceptive effects induced by electrical stimulation into the amygdala. *The Open Dentistry Journal*, *7*, 27–35.

National Center for Health Statistics. (2002). 2000 CDC growth charts for the United States: Methods and development. *Vital Health Statistics*, *11*, 1–190.

Nellhaus, G. (1968). Head circumference from birth to eighteen years. *Pediatrics*, *41*, 106–114.

Neufang, S., Specht, K., Hausmann, M., Güntürkün, O., Herpertz-Dahlmann, B., Fink, G. R., & Konrad, K. (2009). Sex differences and the impact of steroid hormones on the developing human brain. *Cerebral Cortex*, *19*, 464–473.

Nguyen, T.-V., McCracken, J. T., Ducharme, S., Cropp, B. F., Botteron, K. N., Evans, A. C., & Karama, S. (2013). Interactive effects of dehydroepiandrosterone and testosterone on cortical thickness during early brain development. *Journal of Neuroscience*, *33*, 10840–10848.

NIHPD. (2006a, November). The MRI Study of Normal Brain Development: MRI procedure manual. Retrieved from https://pediatricmri.nih.gov/nihpd/info/Documents/Protocol_Nov06.pdf

NIHPD. (2006b, November). The MRI Study of Normal Brain Development Protocol: November 2006. Retrieved from https://pediatricmri.nih.gov/nihpd/info/Documents/Protocol_Nov06.pdf

Noble, K. G., Houston, S. M., Kan, E., & Sowell, E. R. (2012). Neural correlates of socioeconomic status in the developing human brain. *Developmental Science*, *15*, 516–527.

Noble, K. G., McCandliss, B. D., & Farah, M. J. (2007). Socioeconomic gradients predict individual differences in neurocognitive abilities. *Developmental Science*, *10*, 464–480.

Ocklenburg, S., & Güntürkün, O. (2018). *The lateralized brain: the neuroscience and evolution of hemispheric asymmetries*. London: Academic Press.

Østby, Y., Tamnes, C. K., Fjell, A. M., Westlye, L. T., Due-Tønnessen, P., & Walhovd, K. B. (2009). Heterogeneity in subcortical brain development: a structural magnetic resonance imaging study of brain maturation from 8 to 30 years. *Journal of Neuroscience*, *29*, 11772–11782.

Parent, A.-S., Teilmann, G., Juul, A., Skakkebaek, N. E., Toppari, J., & Bourguignon, J.-P. (2003). The timing of normal puberty and the age limits of sexual precocity: Variations around the world, secular trends, and changes after migration. *Endocrine Reviews*, *24*, 668–693.

Payne, C., Machado, C. J., Bliwise, N. G., & Bachevalier, J. (2010). Maturation of the hippocampal formation and amygdala in Macaca mulatta: a volumetric magnetic resonance imaging study. *Hippocampus*, *20*, 922–935.

Penfield, W. (1958). Some mechanisms of consciousness discovered during electrical stimulation of the brain. *Proceedings of the National Academy of Sciences*, *44*, 51–66.

Petersen, A. C., Crockett, L., Richards, M., & Boxer, A. (1988). A self-report measure of pubertal status: Reliability, validity, and initial norms. *Journal of Youth and Adolescence*, *17*, 117–133.

Pfefferbaum, A., Mathalon, D. H., Sullivan, E. V., Rawles, J. M., Zipursky, R. B., & Lim, K. O. (1994). A quantitative magnetic resonance imaging study of changes in brain morphology from infancy to late adulthood. *Archives of Neurology*, *51*, 874–887.

Phelps, E. A., & LeDoux, J. E. (2005). Contributions of the amygdala to emotion processing: From animal models to human behavior. *Neuron*, *48*, 175–187.

Phelps, E. A., O'Connor, K. J., Gatenby, J. C., Gore, J. C., Grillon, C., & Davis, M. (2001). Activation of the left amygdala to a cognitive representation of fear. *Nature Neuroscience*, *4*, 437–441.

Phoenix, C. H., Goy, R. W., Gerall, A. A., & Young, W. C. (1959). Organizing action of prenatally administered testosterone propionate on the tissues mediating mating behavior in the female guinea pig. *Endocrinology*, *65*, 369–382.

Preacher, K. J., Curran, P. J., & Bauer, D. J. (2006). Computational tools for probing interactions in multiple linear regression, multilevel modeling, and latent curve analysis. *Journal of Educational and Behavioral Statistics*, *31*, 437–448.

Raichle, M. E. (1998). Behind the scenes of functional brain imaging: a historical and physiological perspective. *Proceedings of the National Academy of Sciences*, *95*, 765–772.

Randall, V. A., Hibberts, N. A., Thornton, M. J., Hamada, K., Merrick, A. E., Kato, S., … Messenger, A. G. (2000). The hair follicle: A paradoxical androgen target organ. *Hormone Research in Paediatrics*, *54*, 243–250.

Rauch, S. L., van der Kolk, B. A., Fisler, R. E., Alpert, N. M., Orr, S. P., Savage, C. R., … Pitman, R. K. (1996). A symptom provocation study of posttraumatic stress disorder using positron emission tomography and script-driven imagery. *Archives of General Psychiatry*, *53*, 380–387.

Rauch, S. L., Whalen, P. J., Shin, L. M., McInerney, S. C., Macklin, M. L., Lasko, N. B., … Pitman, R. K. (2000). Exaggerated amygdala response to masked facial stimuli in posttraumatic stress disorder: a functional MRI study. *Biological Psychiatry*, *47*, 769–776.

Raudenbush, S. W. (1995). Maximum likelihood estimation for unbalanced multilevel covariance structure models via the EM algorithm. *British Journal of Mathematical and Statistical Psychology*, *48*, 359–370.

Reiman, E. M., Lane, R. D., Ahern, G. L., Schwartz, G. E., Davidson, R. J., Friston, K. J., … Chen, K. (1997). Neuroanatomical correlates of externally and internally generated human emotion. *American Journal of Psychiatry*, *154*, 918–925.

Reiss, A. L., Abrams, M. T., Singer, H. S., Ross, J. L., & Denckla, M. B. (1996). Brain development, gender and IQ in children: A volumetric imaging study. *Brain*, *119*, 1763–1774.

Reiss, A. L., Lee, J., & Freund, L. (1994). Neuroanatomy of fragile X syndrome: The temporal lobe. *Neurology*, *44*, 1317–1317.

Reuter, M., Rosas, H. D., & Fischl, B. (2010). Highly accurate inverse consistent registration: A robust approach. *NeuroImage*, *53*, 1181–1196.

Reuter, M., Schmansky, N. J., Rosas, H. D., & Fischl, B. (2012). Within-subject template estimation for unbiased longitudinal image analysis. *NeuroImage*, *61*, 1402–1418.

Roozendaal, B., Brunson, K. L., Holloway, B. L., McGaugh, J. L., & Baram, T. Z. (2002). Involvement of stress-released corticotropin-releasing hormone in the basolateral amygdala in regulating memory consolidation. *Proceedings of the National Academy of Sciences of the United States of America*, *99*, 13908–13913.

Rosas, H. D., Liu, A. K., Hersch, S. M., Glessner, M., Ferrante, R. J., Salat, D. H., … Fischl, B. (2002). Regional and progressive thinning of the cortical ribbon in Huntington's disease. *Neurology*, *58*, 695–701.

Salat, D., Buckner, R. L., Snyder, A. Z., Greve, D. N., Desikan, R. S., Busa, E., … Fischl, B. (2004). Thinning of the cerebral cortex in aging. *Cerebral Cortex*, *14*, 721–730.

Sapolsky, R. M. (2004). *Why zebras don't get ulcers* (3rd ed.). New York, NY: Holt.

Saygin, Z. M., Kliemann, D., Iglesias, J. E., van der Kouwe, A. J. W., Boyd, E., Reuter, M., … Augustinack, J. C. (2017). High-resolution magnetic resonance imaging reveals nuclei of

the human amygdala: manual segmentation to automatic atlas. *NeuroImage*, *155*, 370–382.

Saygin, Z. M., Osher, D. E., Koldewyn, K., Martin, R. E., Finn, A., Saxe, R., … Sheridan, M. (2015). Structural connectivity of the developing human amygdala. *PLOS ONE*, *10*, e0125170.

Schaie, K. W. (1965). A general model for the study of developmental problems. *Psychological Bulletin*, *64*, 92–107.

Schore, A. N. (2015). *Affect Regulation and the Origin of the Self: The Neurobiology of Emotional Development*. Routledge.

Schulz, K. M., Molenda-Figueira, H. A., & Sisk, C. L. (2009). Back to the future: the organizational–activational hypothesis adapted to puberty and adolescence. *Hormones and Behavior*, *55*, 597–604.

Schumann, C. M., Hamstra, J., Goodlin-Jones, B. L., Lotspeich, L. J., Kwon, H., Buonocore, M. H., … Amaral, D. G. (2004). The amygdala is enlarged in children but not adolescents with autism; the hippocampus is enlarged at all ages. *Journal of Neuroscience*, *24*, 6392–6401.

Segonne, F., Dale, A. M., Busa, E., Glessner, M., Salat, D. H., Hahn, H. K., & Fischl, B. (2004). A hybrid approach to the skull stripping problem in MRI. *NeuroImage*, *22*, 1060–1075.

Segonne, F., Pacheco, J., & Fischl, B. (2007). Geometrically accurate topology-correction of cortical surfaces using nonseparating loops. *IEEE Transactions on Medical Imaging*, *26*, 518–529.

Shaffer, D., Fisher, P., Lucas, C. P., Dulcan, M. K., & Schwab-Stone, M. E. (2000). NIMH Diagnostic Interview Schedule for Children Version IV (NIMH DISC-IV): Description, differences from previous versions, and reliability of some common diagnoses. *Journal of the American Academy of Child & Adolescent Psychiatry*, *39*, 28–38.

Sheridan, M. A., Fox, N. A., Zeanah, C. H., McLaughlin, K. A., & Nelson, C. A. (2012). Variation in neural development as a result of exposure to institutionalization early in childhood. *Proceedings of the National Academy of Sciences*, *109*, 12927–12932.

Shin, L. M., McNally, R. J., Kosslyn, S. M., Thompson, W. L., Rauch, S. L., Alpert, N. M., … Pitman, R. K. (1997). A positron emission tomographic study of symptom provocation in PTSD. *Annals of the New York Academy of Sciences*, *821*, 521–523.

Shirtcliff, E. A., Dahl, R. E., & Pollak, S. D. (2009). Pubertal development: Correspondence between hormonal and physical development. *Child Development*, *80*, 327–337.

Shou, H., Eloyan, A., Lee, S., Zipunnikov, V., Crainiceanu, A. N., Nebel, M. B., … Crainiceanu, C. M. (2013). Quantifying the reliability of image replication studies: the image intra-

class correlation coefficient (I2C2). *Cognitive, Affective & Behavioral Neuroscience*, *13*, 714–724.

Shrout, P. E., & Fleiss, J. L. (1979). Intraclass correlations: Uses in assessing rater reliability. *Psychological Bulletin*, *86*, 420–428.

Sled, J. G., Zijdenbos, A. P., & Evans, A. C. (1998). A nonparametric method for automatic correction of intensity nonuniformity in MRI data. *Medical Imaging, IEEE Transactions On*, *17*, 87–97.

Sliwinski, M., Hoffman, L., & Hofer, S. M. (2010). Evaluating convergence of within-person change and between-person age differences in age-heterogeneous longitudinal studies. *Research in Human Development*, *7*, 45–60.

Somerville, L. H., Jones, R. M., & Casey, B. (2010). A time of change: Behavioral and neural correlates of adolescent sensitivity to appetitive and aversive environmental cues. *Brain and Cognition*, *72*, 124.

Sprengelmeyer, R., Young, A. W., Schroeder, U., Grossenbacher, P. G., Federlein, J., Buttner, T., & Przuntek, H. (1999). Knowing no fear. *Proceedings of the Royal Society of London B: Biological Sciences*, *266*, 2451–2456.

Stanger, C., Achenbach, T. M., & Verhulst, F. C. (1997). Accelerated longitudinal comparisons of aggressive versus delinquent syndromes. *Development and Psychopathology*, *9*, 43–58.

Steinberg, L. (2008). A social neuroscience perspective on adolescent risk-taking. *Developmental Review*, *28*, 78–106.

Stiles, J., & Jernigan, T. L. (2010). The basics of human development. *Neuropsychology Review*, *20*, 327–348.

Strother, S. C., & Churchill, N. (2017). Neuroimage preprocessing. In H. Ombao, M. Lindquist, W. Thompson, & J. Aston (Eds.), *Handbook of neuroimaging data analysis* (pp. 264–308). Boca Raton, FL: Taylor & Francis.

Styne, D. M., & Grumbach, M. M. (2016). Physiology and disorders of puberty. In S. Melmed, K. S. Polonsky, P. R. Larsen, & H. M. Kronenberg (Eds.), *Williams textbook of endocrinology* (13th ed., pp. 1074–1218). Philadelphia, PA: Elsevier.

Swanson, L. W., & Petrovich, G. D. (1998). What is the amygdala? *Trends in Neurosciences*, *21*, 323–331.

Sybert, V. P., & McCauley, E. (2004). Turner's Syndrome. *New England Journal of Medicine*, *351*, 1227–1238.

Tanner, J. M. (1962). *Growth at adolescence*. Springfield, IL: Thomas.

Taylor, S. E., Eisenberger, N. I., Saxbe, D., Lehman, B. J., & Lieberman, M. D. (2006). Neural responses to emotional stimuli are associated with childhood family stress. *Biological Psychiatry*, *60*, 296–301.

Taylor, S. J., Whincup, P. H., Hindmarsh, P. C., Lampe, F., Odoki, K., & Cook, D. G. (2001). Performance of a new pubertal self-assessment questionnaire: a preliminary study. *Paediatric and Perinatal Epidemiology*, *15*, 88–94.

Teicher, M. H., & Samson, J. A. (2016). Annual research review: enduring neurobiological effects of childhood abuse and neglect. *Journal of Child Psychology and Psychiatry*, *57*, 241–266.

Thomas, K. M., Drevets, W. C., Whalen, P. J., Eccard, C. H., Dahl, R. E., Ryan, N. D., & Casey, B. J. (2001). Amygdala response to facial expressions in children and adults. *Biological Psychiatry*, *49*, 309–316.

Tottenham, N., & Galván, A. (2016). Stress and the adolescent brain: Amygdala-prefrontal cortex circuitry and ventral striatum as developmental targets. *Neuroscience & Biobehavioral Reviews*, *70*, 217–227.

Tottenham, N., Hare, T. A., Quinn, B. T., McCarry, T. W., Nurse, M., Gilhooly, T., … Eigsti, I.-M. (2010). Prolonged institutional rearing is associated with atypically large amygdala volume and difficulties in emotion regulation. *Developmental Science*, *13*, 46–61.

Tottenham, N., & Sheridan, M. A. (2009). A review of adversity, the amygdala and the hippocampus: a consideration of developmental timing. *Frontiers in Human Neuroscience*, *3*.

Tournier, J.-D., Calamante, F., & Connelly, A. (2012). MRtrix: Diffusion tractography in crossing fiber regions. *International Journal of Imaging Systems and Technology*, *22*, 53–66.

Uematsu, A., Matsui, M., Tanaka, C., Takahashi, T., Noguchi, K., Suzuki, M., & Nishijo, H. (2012). Developmental trajectories of amygdala and hippocampus from infancy to early adulthood in healthy individuals. *PloS One*, *7*, e46970.

Ulrich-Lai, Y. M., & Herman, J. P. (2009). Neural regulation of endocrine and autonomic stress responses. *Nature Reviews. Neuroscience*, *10*, 397–409.

U.S. Census Bureau. (2000). *Income and Poverty in 1999: 2000 - United States -- Urban/Rural and Inside/Outside Metropolitan Area, Census 2000 Sumary File 4 (SF 4) - Sample Data*. Retrieved from https://factfinder.census.gov/bkmk/table/1.0/en/DEC/00_SF4/GCTP14.US93/0100000US

U.S. Department of Housing and Urban Development. (2006). *Transmittal of Fiscal Year 2006 Income Limits for the Section 221(d)(3)BMIR, Section 235, and Section 236 Programs* (No. PDS-2006-03). Retrieved from https://www.huduser.gov/datasets/il/il06/sec236Notice_2006.pdf

Vaida, F., & Blanchard, S. (2005). Conditional Akaike information for mixed-effects models. *Biometrika*, *92*, 351–370.

van Bodegom, M., Homberg, J. R., & Henckens, M. J. A. G. (2017). Modulation of the hypothalamic-pituitary-adrenal axis by early life stress exposure. *Frontiers in Cellular Neuroscience*, *11*.

van der Plas, E. A., Boes, A. D., Wemmie, J. A., Tranel, D., & Nopoulos, P. (2010). Amygdala volume correlates positively with fearfulness in normal healthy girls. *Social Cognitive and Affective Neuroscience*, *5*, 424–431.

Viviani, R., Stöcker, T., & Stingl, J. C. (2017). Multimodal FLAIR/MPRAGE segmentation of cerebral cortex and cortical myelin. *NeuroImage*, *152*, 130–141.

Vyas, A., Mitra, R., Rao, B. S., & Chattarji, S. (2002). Chronic stress induces contrasting patterns of dendritic remodeling in hippocampal and amygdaloid neurons. *Journal of Neuroscience*, *22*, 6810–6818.

Waber, D. P., De Moor, C., Forbes, P. W., Almli, C. R., Botteron, K. N., Leonard, G., … Brain Development Cooperative Group. (2007). The NIH MRI study of normal brain development: Performance of a population based sample of healthy children aged 6 to 18 years on a neuropsychological battery. *Journal of the International Neuropsychological Society: JINS*, *13*, 729–746.

Wechsler, D. (1999). *Wechsler Abbreviated Scale of Intelligence*. San Antonio, TX: Psychological Corporation.

Weems, C. F. (2017). Severe stress and the development of the amygdala in youth: A theory and its statistical implications. *Developmental Review*, *46*, 44–53.

Weems, C. F., Klabunde, M., Russell, J. D., Reiss, A. L., & Carrión, V. G. (2015). Post-traumatic stress and age variation in amygdala volumes among youth exposed to trauma. *Social Cognitive and Affective Neuroscience*, *10*, 1661–1667.

Weems, C. F., Scott, B. G., Russell, J. D., Reiss, A. L., & Carrión, V. G. (2013). Developmental variation in amygdala volumes among children with posttraumatic stress. *Developmental Neuropsychology*, *38*, 481–495.

Weiskrantz, L. (1956). Behavioral changes associated with ablation of the amygdaloid complex in monkeys. *Journal of Comparative and Physiological Psychology*, *49*, 381–391.

Whalen, P. J., & Phelps, E. A. (2009). *The human amygdala*. New York, NY: Guilford Press.

Whalen, P. J., Rauch, S. L., Etcoff, N. L., McInerney, S. C., Lee, M. B., & Jenike, M. A. (1998). Masked presentations of emotional facial expressions modulate amygdala activity without explicit knowledge. *Journal of Neuroscience*, *18*, 411–418.

Whittle, S., Vijayakumar, N., Simmons, J. G., Dennison, M., Schwartz, O., Pantelis, C., … Allen, N. B. (2017). Role of positive parenting in the association between neighborhood social disadvantage and brain development across adolescence. *JAMA Psychiatry*, *74*, 824–832.

Wierenga, L., Langen, M., Ambrosino, S., van Dijk, S., Oranje, B., & Durston, S. (2014). Typical development of basal ganglia, hippocampus, amygdala and cerebellum from age 7 to 24. *NeuroImage*, *96*, 67–72.

Witchel, S. F., & Plant, T. M. (2014). Puberty: gonadarche and adrenarche. In J. F. Strauss & R. L. Barbieri (Eds.), *Yen & Jaffe's reproductive endocrinology: Physiology, pathophysiology, and clinical management* (7th ed., pp. 377–421). Philadelphia, PA: Elsevier Saunders.

Woodcock, R. W., McGrew, K. S., & Mather, N. (2001). *Woodcock-Johnson III Test*. Itasca, IL: Riverside Publishing Company.

Yurgelun-Todd, D. A., & Killgore, W. D. S. (2006). Fear-related activity in the prefrontal cortex increases with age during adolescence: A preliminary fMRI study. *Neuroscience Letters*, *406*, 194–199.

Zajonc, R. B. (1980). Feeling and thinking: Preferences need no inferences. *American Psychologist*, *35*, 151–175.

Table 1

Consistency of volumetric estimates derived from NIHPD ANIMAL and FreeSurfer pipelines

	ICC[a]	I2C2
Caudate		
Right	.92	.94
Left	.90	.94
Putamen		
Right	.91	.91
Left	.92	.91
Intracranial Volume	.97	.96
Intracranial Grey Matter	.94	.92
Cerebral White Matter	.93	.95

[a] $df_{1,2}$ = 633, 633

Note. ICC = Intraclass Correlation Coefficient (two-way mixed average measure, consistency). I2C2 = Image Intraclass Correlation Coefficient.

Table 2

Formulas of Mixed Models Predicting Amygdala Volumes

Without ETIV Covariate	
Chronological Age	$Right/Left\ Amygdala_{ti} = \pi_{0i} + \pi_{1i}*(Time_{ti}) + e_{ti}$
	$\pi_{0i} = \beta_{00} + \beta_{01}*(Age@1stScan_i) + r_{0i}$
	$\pi_{1i} = \beta_{10} + \beta_{11}*(Age@1stScan_i)$
Pubertal Development	$Right/Left\ Amygdala_{ti} = \pi_{0i} + \pi_{1i}*(TSChange_{ti}) + e_{ti}$
	$\pi_{0i} = \beta_{00} + \beta_{01}*(TS@1stScan_i) + r_{0i}$
	$\pi_{1i} = \beta_{10} + \beta_{11}*(TS@1stScan_i)$
Combined	$Right/Left\ Amygdala_{ti} = \pi_{0i} + \pi_{1i}*(Time_{ti}) + \pi_{2i}*(TSChange_{ti}) + \pi_{3i}*(TSChange_{ti}*Time_{ti}) + e_{ti}$
	$\pi_{0i} = \beta_{00} + \beta_{01}*(Age@1stScan_i) + \beta_{02}*(TS@1stScan_i) + r_{0i}$
	$\pi_{1i} = \beta_{10} + \beta_{11}*(Age@1stScan_i) + \beta_{12}*(TS@1stScan_i)$
	$\pi_{2i} = \beta_{20} + \beta_{21}*(Age@1stScan_i) + \beta_{22}*(TS@1stScan_i)$
	$\pi_{3i} = \beta_{30} + \beta_{31}*(Age@1stScan_i) + \beta_{32}*(TS@1stScan_i)$
With ETIV Covariate	
Chronological Age	$Right/Left\ Amygdala_{ti} = \pi_{0i} + \pi_{1i}*(Time_{ti}) + \pi_{2i}*(ETIV_{ti}) + e_{ti}$
	$\pi_{0i} = \beta_{00} + \beta_{01}*(Age@1stScan_i) + r_{0i}$
	$\pi_{1i} = \beta_{10} + \beta_{11}*(Age@1stScan_i)$
	$\pi_{2i} = \beta_{20}$
Pubertal Development	$Right/Left\ Amygdala_{ti} = \pi_{0i} + \pi_{1i}*(TSChange_{ti}) + \pi_{2i}*(ETIV_{ti}) + e_{ti}$
	$\pi_{0i} = \beta_{00} + \beta_{01}*(TS@1stScan_i) + r_{0i}$
	$\pi_{1i} = \beta_{10} + \beta_{11}*(TS@1stScan_i)$
	$\pi_{2i} = \beta_{20}$
Combined	$Right/Left\ Amygdala_{ti} = \pi_{0i} + \pi_{1i}*(Time_{ti}) + \pi_{2i}*(TSChange_{ti}) + \pi_{3i}*(TSChange_{ti}*Time_{ti}) + \pi_{4i}*(ETIV_{ti}) + e_{ti}$
	$\pi_{0i} = \beta_{00} + \beta_{01}*(Age@1stScan_i) + \beta_{02}*(TS@1stScan_i) + r_{0i}$
	$\pi_{1i} = \beta_{10} + \beta_{11}*(Age@1stScan_i) + \beta_{12}*(TS@1stScan_i)$
	$\pi_{2i} = \beta_{20} + \beta_{21}*(Age@1stScan_i) + \beta_{22}*(TS@1stScan_i)$
	$\pi_{3i} = \beta_{30} + \beta_{31}*(Age@1stScan_i) + \beta_{32}*(TS@1stScan_i)$
	$\pi_{4i} = \beta_{40}$

Table 3-A

Change in Right Amygdala Volumes as a Function of Time and Age at Initial Scan

	Right Amygdala Volume (mm^3)							
	B	*SE*	*B*	*SE*	*B*	*SE*	*B*	*SE*
Fixed Effects Parameters								
Intercept	1635.98***	10.69	1619.09***	11.03	1457.41***	34.37	1430.47***	34.96
Time			17.30***	2.54	19.31***	2.91	65.64***	8.52
Age@1stscan					14.12***	2.87	16.50***	2.92
Time x Age@1stScan							-4.13***	0.71
Random Effects Parameters								
σ^2	7862.962		6763.200		4727.013		5052.716	
τ_{00}	32926.234		33988.404		32218.316		32341.531	
n	330		330		330		330	
Scans	637		637		637		637	
Deviance	8226.705		8183.853		8154.062		8124.501	

Note. Time = Age at current scan – Age at first scan. *Age@1stScan* = chronological age at initial assessment/study entry.
$^{*}p < .05$. $^{**}p < .01$. $^{***}p < .001$

Table 3-B

Change in Left Amygdala Volumes as a Function of Time and Age at Initial Scan

	Left Amygdala Volume (mm^3)							
	B	*SE*	*B*	*SE*	*B*	*SE*	*B*	*SE*
Fixed Effects Parameters								
Intercept	1580.11***	9.81	1571.33***	10.12	1499.86***	32.06	1478.63***	32.60
Time			8.96***	2.38	9.76***	2.63	39.43***	8.34
Age@1stscan					6.25*	2.68	8.10**	2.73
Time x Age@1stScan							-2.61***	0.70
Random Effects Parameters								
σ^2	6302.988		5985.237		4888.177		4821.210	
τ_{00}	27944.557		28347.536		27642.634		27725.735	
n	330		330		330		330	
Scans	637		637		637		637	
Deviance	8102.344		8088.627		8077.645		8064.034	

Note. Time = Age at current scan – Age at first scan. *Age@1stScan* = chronological age at initial assessment/study entry.
*$p < .05$. **$p < .01$. ***$p < .001$

Table 4-A

Johnson-Neyman Significance Regions for the Conditional Effect of Age at First Scan on Change in Right Amygdala Volumes across Time in Study

Age at 1st Scan	Slope	SE	LCI	UCI	*t*	*p*
20.00	-17.55	6.44	-30.17	-4.93	-2.73	.007
19.00	-13.41	5.81	-24.79	-2.02	-2.31	.022
18.00	-9.26	5.19	-19.45	0.92	-1.78	.075
17.00	-5.12	4.60	-14.14	3.90	-1.11	.267
16.00	-0.98	4.04	-8.90	6.94	-0.24	.809
15.00	3.16	3.53	-3.75	10.08	0.90	.370
14.00	7.31	3.08	1.26	13.35	2.37	.018
13.00	11.45	2.74	6.08	16.83	4.17	< .001
12.00	15.59	2.55	10.60	20.59	6.12	< .001
11.00	19.74	2.53	14.78	24.70	7.80	< .001
10.00	23.88	2.70	18.59	29.17	8.85	< .001
9.00	28.02	3.02	22.11	33.94	9.29	< .001
8.00	32.17	3.45	25.41	38.92	9.33	< .001
7.00	36.31	3.95	28.56	44.05	9.19	< .001
6.00	40.45	4.51	31.62	49.28	8.98	< .001
5.00	44.60	5.09	34.61	54.58	8.76	< .001

Note. LCI = 95% lower confidence interval. UCI = 95% upper confidence interval.

Table 4-B

Johnson-Neyman Significance Regions for the Conditional Effect of Age at First Scan on Change in Left Amygdala Volumes across Time in Study

Age at 1st Scan	Slope	SE	LCI	UCI	*t*	*p*
20.00	-12.92	6.28	-25.24	-0.60	-2.06	.041
19.00	-10.33	5.67	-21.44	0.79	-1.82	.069
18.00	-7.74	5.07	-17.68	2.20	-1.53	.128
17.00	-5.15	4.49	-13.95	3.66	-1.15	.253
16.00	-2.55	3.95	-10.29	5.18	-0.65	.518
15.00	0.04	3.44	-6.72	6.79	0.01	.992
14.00	2.63	3.01	-3.27	8.53	0.87	.383
13.00	5.22	2.68	-0.03	10.47	1.95	.052
12.00	7.81	2.49	2.93	12.68	3.14	.002
11.00	10.40	2.47	5.56	15.24	4.21	< .001
10.00	12.99	2.63	7.83	18.15	4.93	< .001
9.00	15.58	2.95	9.81	21.36	5.29	< .001
8.00	18.17	3.37	11.58	24.77	5.40	< .001
7.00	20.76	3.86	13.20	28.33	5.38	< .001
6.00	23.35	4.40	14.73	31.98	5.31	< .001
5.00	25.95	4.97	16.20	35.69	5.22	< .001

Note. LCI = 95% lower confidence interval. UCI = 95% upper confidence interval.

Table 5-A

Change in Right Amygdala Volumes as a Function of Pubertal Development and Tanner Stage at Initial Scan

	Right Amygdala Volume (mm^3)							
	B	*SE*	*B*	*SE*	*B*	*SE*	*B*	*SE*
Fixed Effects Parameters								
Intercept	1635.98***	10.69	1636.84***	11.95	1592.97***	25.18	1591.72***	25.27
TSChange			34.89***	6.25	35.72***	6.26	43.50**	14.27
TS@1stScan					17.26	8.74	17.93*	8.81
TSChange x TS@1stScan							-4.63	7.64
Random Effects Parameters								
σ^2	7862.962		6997.066		6996.983		6970.463	
τ_{00}	32926.234		33702.795		33171.360		33184.714	
n	330		274		274		274	
Scans	637		513		513		513	
Deviance	8226.705		6608.093		6604.245		6603.312	

Note. TSChange = Tanner stage at current scan – Tanner stage at first scan. *TS@1stScan* = pubertal development (Tanner Stage) at initial assessment/study entry.
*$p < .05$. **$p < .01$. ***$p < .001$

Table 5-B

Change in Left Amygdala Volumes as a Function of Pubertal Development and Tanner Stage at Initial Scan

	Left Amygdala Volume (mm^3)							
	B	*SE*	*B*	*SE*	*B*	*SE*	*B*	*SE*
Fixed Effects Parameters								
Intercept	1580.11***	9.81	1579.65***	11.13	1573.30***	23.40	1572.80***	23.47
TSChange			16.63**	5.78	19.96**	7.24	24.28	16.32
TS@1stScan					2.37	8.14	2.64	8.19
TSChange x TS@1stScan							-2.35	7.94
Random Effects Parameters								
σ^2	6302.988		5956.590		5042.971		5042.055	
τ_{00}	27944.557		29257.289		29280.836		29293.357	
n	330		274		274		274	
Scans	637		513		513		513	
Deviance	8102.344		6530.239		6521.780		6521.692	

Note. TSChange = Tanner stage at current scan – Tanner stage at first scan. *TS@1stScan* = pubertal development (Tanner stage) at initial assessment/study entry.
*$p < .05$. **$p < .01$. ***$p < .001$

Table 6-A

Change in Right Amygdala Volumes as a Function of Chronological Time and Pubertal Maturation

	Right Amygdale Volume (mm^3)									
	B	*SE*	*B*	*SE*	*B*	*SE*	*B*	*SE*	*B*	*SE*
Fixed Effects Parameters										
Intercept	1635.98***	10.69	1631.55***	12.16	1435.06***	48.45	1389.41***	49.40	1390.70***	49.52
Time			10.03*	4.24	10.47*	4.26	36.56*	15.44	35.52*	16.27
TSChange			50.88**	16.30	48.96**	16.31	131.25**	45.53	91.77	84.37
Time x TSChange			-9.74*	4.82	-9.71*	4.82	-10.97*	5.07	1.97	25.00
Age@1stScan					24.14***	6.43	29.11***	6.53	29.08***	6.55
TS@1stScan					-37.06*	16.52	-42.66*	16.69	-43.16*	16.73
Time x Age@1stScan							-1.72	2.27	-1.67	2.48
Time x TS@1stScan							-1.83	6.32	-1.46	6.82
TSChange x Age@1stScan							-9.42*	4.75	-8.39	8.59
TSChange x TS@1stScan							15.52	13.02	30.97	24.45
Time x TSChange x Age1stScan									-0.33	2.65
Time x TSChange x TS@1stScan									-5.28	7.47
Random Effects Parameters										
σ^2	7862.962		6704.878		6696.349		6129.389		6104.549	
τ_{00}	32926.234		34093.613		31834.560		32054.573		32055.209	
n	330		274		274		274		274	
Scans	637		513		513		513		513	
Deviance	8226.705		6599.369		6582.388		6560.180		6559.093	

Note. Time = Age at current scan – Age at first scan; *TSChange* = Tanner stage at current scan – Tanner stage at first scan; *Age@1stScan* = chronological age at initial assessment/study entry; *TS@1stScan* = pubertal development (Tanner stage) at initial assessment/study entry.
$^{*}p < .05$. $^{**}p < .01$. $^{***}p < .001$

Table 6-B

Change in Left Amygdala Volumes as a Function of Chronological and Developmental Time

	Left Amygdala Volume (mm^3)									
	B	*SE*	*B*	*SE*	*B*	*SE*	*B*	*SE*	*B*	*SE*
Fixed Effects Parameters										
Intercept	1580.11***	9.81	1579.21***	11.30	1430.70***	44.99	1412.56***	45.60	1411.38***	45.71
Time			1.15	3.99	1.42	3.97	11.66	14.85	14.18	15.62
TSChange			12.76	15.34	7.67	15.46	74.96	47.97	83.88	79.81
Time x TSChange			0.64	4.54	2.88	4.45	3.48	4.82	-0.28	23.57
Age@1stScan					21.95***	5.97	24.26***	6.03	24.56***	6.05
TS@1stScan					-45.65**	15.29	-49.40**	15.41	-50.49**	15.44
Time x Age@1stScan							-1.43	2.21	-2.06	2.42
Time x TS@1stScan							1.91	6.16	3.96	6.63
TSChange x Age@1stScan							-8.39	5.17	-12.43	8.22
TSChange x TS@1stScan							17.07	14.24	39.72	23.50
Time x TSChange x Age1stScan									1.57	2.50
Time x TSChange x TS@1stScan									-8.43	7.03
Random Effects Parameters										
σ^2	6302.988		5943.494		4693.055		4663.495		4650.129	
τ_{00}	27944.557		29340.910		27860.193		27851.561		27877.427	
n	330		274		274		274		274	
Scans	637		513		513		513		513	
Deviance	8102.344		6530.337		6508.588		6500.777		6499.371	

Note. Time = Age at current scan – Age at first scan. *TSChange* = Tanner stage at current scan – Tanner stage at first scan. *Age@1stScan* = chronological age at initial assessment/study entry. *TS@1stScan* = pubertal development (Tanner stage) at initial assessment/study entry.
$^{*}p < .05$. $^{**}p < .01$. $^{***}p < .001$

Table 7

Comparative Fit of Models Predicting Change in Right and Left Amygdala Volumes

	k	AIC	ΔAIC	AIC Weight
Right Amygdala				
1. Combined	14	5432.24	—	0.99
2. Pubertal Development	6	5442.25	10.01	0.01
3. Chronological Age	6	6647.69	1215.45	0.00
Left Amygdala				
1. Pubertal Development	6	5376.83	—	0.58
2. Combined	14	5377.49	0.66	0.42
3. Chronological Age	6	6591.40	1214.57	0.00

Note. k = # of model parameters. AIC = Akaike Information Criterion.

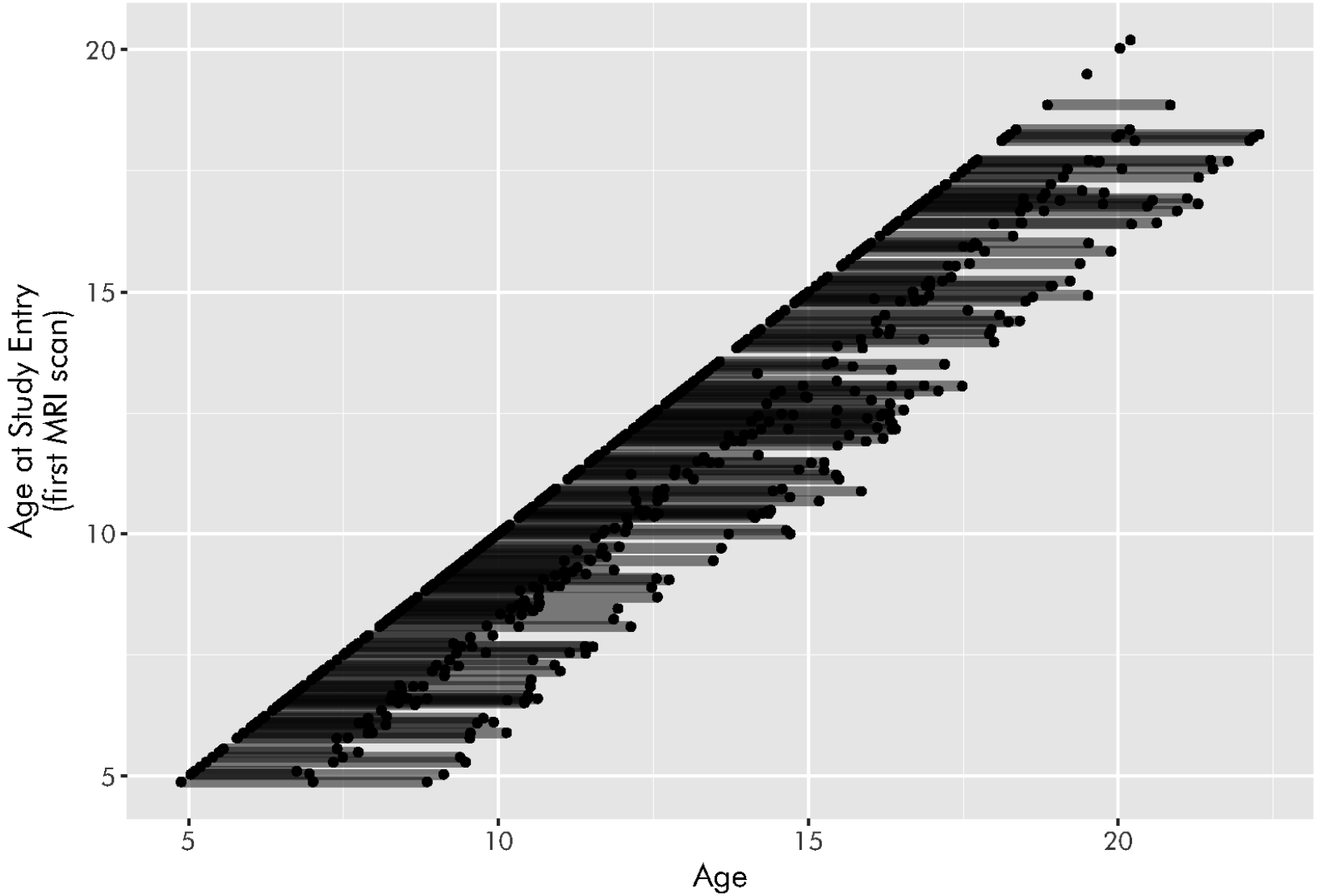

Figure 1. Accelerated longitudinal design of data collection in NIHPD. Points denote times of data collection while contiguous lines represent individual cases.

APPENDIX – SUPPLEMENTAL TABLES

Table S1. *Exclusionary Criteria for the NIH MRI Study of Normal Brain Development*

Exclusionary Criteria	**Description**
Demographic	Family history unavailable (e.g., some adopted children). Non-fluent English speaker (youth) or reader (caregiver).
Pregnancy and Birth	Prenatal: Fetal exposure to teratogenic substances, including nicotine (>1/2 pack/day), alcohol (>2 drinks/ week), certain prescription medications, illicit drugs. Pre-eclampsia, pre-natal anesthesia, gestational diabetes. Perinatal: Multiple births, fetal distress, malpresentation, high forceps/vacuum extraction, C-section due to maternal\fetal distress, general anesthesia, gestational age (< 37 weeks or > 42 weeks). Neonatal: Resuscitation by chest compression, respiratory distress, 5 min. Apgar < 8, seizure, infection, hyperbilirubinemia (> 2 days) requiring transfusion or phototherapy, phenylketonuria, limb or craniofacial abnormalities.
Developmental	Stunted growth: height, weight, or head circumference < 3rd percentile [a]
Familial	History of inherited neurological disorder. First-degree relative with intellectual disability not caused by traumatic brain injury. First-degree relative with lifetime history of DSM-IV-TR Axis I disorder.
Medical	Lifetime history of any major medical disorder with neurological implications (e.g., epilepsy). History of closed head injury producing loss of consciousness > 30 min.
Psychiatric	Lifetime history of any DSM-IV-TR Axis I disorder,[b] or language disorder. Any CBCL subscale score ≥ 70. WASI IQ < 70. Any WJ-III subtest score < 70.
Neurological	Any abnormality on neurological examination (e.g., hypertonia, reflex asymmetry).

Notes. DSM-IV-TR = Diagnostic and Statistical Manual of Mental Disorders, Fourth edition, Text revision (American Psychiatric Association, 2000). CBCL = Child Behavior Checklist (Achenbach, 1991). WASI = Wechsler Abbreviated Intelligence Scale (Wechsler, 1999). WJ-III = Woodcock-Johnson III (Woodcock, McGrew, & Mather, 2001)

a. Height, weight referenced to (National Center for Health Statistics, 2002). Head circumference referenced to (Nellhaus, 1968).

b. With exceptions for simple and social phobias, adjustment disorder, oppositional defiant disorder, enuresis, encopresis, nicotine dependency.

Table S2. *Clinical, Behavioral, and Neuropsychological Instruments*

TEST	REPORTER	AGES
Behavior Rating Inventory of Executive Control (BRIEF)	Parent	All
California Verbal Learning Test	Child	
Children's Version (CVLT-C)		4:6 - 15:11
Adult Version (CVLT-II)		16+
CANTAB (Cambridge Neuro Test Automated Battery)	Child	All
Motor Screening Task		
Spatial Span Task		
Spatial Working Memory Task		
Big Little Circle		
Set-Shifting Task		
Child Behavior Checklist		
CBCL for Ages 1:5 – 5	Parent	1:5 - 5
CBCL for Ages 6 – 18	Parent	6 - 18
CBCL Young Adult Self-Report	Child	18+
Diagnostic Interview Schedule for Children	Parent	All
Computerized Diagnostic Interview (C-DISC-4)		
Predictive Scales (DPS-4)		
Differential Abilities Scale	Child	4:6 - 5:11
FAS Verbal Fluency Test	Child	12+
Family History Interview for Genetic Studies (FIGS)	Parent	4:6 - 18
Junior Temperament Character Inventory		
Parent Report	Parent	
Child Self-Report	Child	
Adult Self-Report	Child	
NEPSY-I – Verbal Fluency Test	Child	All
Parenting Stress Index	Parent	4:6 - 18
Preschool Language Scale-3 (PLS-3)	Child	4:6 - 6:11
Purdue Pegboard Test	Child	
Half Board		4:6 - 5:11
Full Board		6+
Wechsler Abbreviated Scale of Intelligence	Child	6+
Vocabulary		
Similarities		
Block Design		
Matrix Reasoning		
Wechsler Intelligence Scale for Children (WISC-III)	Child	12+
Digit Span		
Coding		
Wechsler Adult Scale of Intelligence, Revised (WAIS-R)	Child	17+
Digit Span		
Digit Symbol		

Table S3. *MRI Protocols and Parameters*

	Primary Protocol		**Fallback Protocol**	
	T1-Weighted	*PD/T2-Weighted*	*T1-Weighted*	*PD/T2-Weighted*
Sequence	3D SPGR	2D FSE	2D SE	2D dual-echo FSE
TR	25 (22)[a] ms	3500 ms	500 ms	3500 ms
TE	11 (10)[a] ms	—	10 (12)[a] ms	—
TE 1 (effective)	—	17 ms	—	17 ms
TE 2 (effective)	—	119 ms	—	119 ms
Flip Angle	30°	90°	90°	90°
FoV	256 x 160-180 mm	250 x 220 mm	250 x 190 mm	250 x 190 mm
Matrix	256 x 256	256 x 224	256 x 192	256 x 192
Orientation	Sagittal	Oblique axial[b]	Oblique axial[b]	Oblique axial[b]
No. of Slices	Ear to Ear	Apex to below cerebellum	Apex to below cerebellum	Apex to below cerebellum
Slice Thickness	1.0-1.5 mm[c]	2 mm	3 mm	3 mm

a. GE scanners
b. Parallel to the anterior commissure-posterior commissure plane.
c. Larger slice thicknesses were used in some GE systems with 124 slice limits.

Table S4-A.

Effects of Annual Family Income on Change in Right Amygdala Volumes across Chronological Age

	Right Amygdala Volume (mm^3)											
	B	*SE*	*B*	*SE*	*B*	*SE*	*B*	*SE*	*B*	*SE*	*B*	*SE*
Fixed Effects Parameters												
Intercept	1635.98***	10.69	1635.79***	7.79	1629.27***	8.18	1583.27***	30.99	1569.88***	32.80	1575.48***	57.95
ETIV †			9.27***	0.48	8.98***	0.50	8.96***	0.52	8.65***	0.53	8.64***	0.53
Time					6.51**	2.44	5.84*	2.60	18.05	11.63	27.26	23.09
Age@1stscan							5.61*	2.23	7.70**	2.35	7.12	4.90
AFI							-0.00	0.00	-0.00	0.00	-0.00	0.00
Time x Age@1stScan									-1.95**	0.73	-2.75	1.86
Time x AFI									0.00	0.00	0.00	0.00
AFI x Age@1stScan											0.00	0.00
Time x Age@1stScan x AFI											0.00	0.00
Random Effects Parameters												
σ^2	7862.962		6253.536		6083.659		5817.829		5520.721		5517.748	
τ_{00}	32926.234		16237.791		16429.595		15743.839		16064.185		16053.153	
n	330		330		330		314		314		314	
Scans	637		637		637		578		578		578	
Deviance	8226.705		7947.714		7940.732		7192.737		7181.026		7180.676	

Note. ETIV = Estimated Total Intracranial Volume; *Time* = Age at current scan – Age at first scan; *Age@1stScan* = chronological age at initial assessment/study entry. *AFI* = Adjusted Family Income.

†Scaled by 10^{-5} and grand-mean centered

*$p < .05$. **$p < .01$. ***$p < .001$

Table S4-B.

Effects of Annual Family Income on Change in Left Amygdala Volumes across Chronological Age

	Left Amygdala Volume (mm^3)											
	B	*SE*	*B*	*SE*	*B*	*SE*	*B*	*SE*	*B*	*SE*	*B*	*SE*
Fixed Effects Parameters												
Intercept	1580.11***	9.81	1579.89***	7.59	1579.85***	7.95	1586.92***	30.50	1585.55***	32.37	1586.67***	57.70
ETIV †			7.43***	0.47	7.42***	0.48	7.53***	0.51	7.50***	0.52	7.49***	0.52
Time					0.04	2.37	-0.87	2.57	0.32	11.77	6.67	23.38
Age@1stscan							-0.36	2.19	-0.15	2.31	-0.30	4.87
AFI							-0.00	0.00	-0.00	0.00	-0.00	0.00
Time x Age@1stScan									-0.20	0.74	-0.75	1.89
Time x AFI									0.00	0.00	-0.00	0.00
AFI x Age@1stScan											0.00	0.00
Time x Age@1stScan x AFI											0.00	0.00
Random Effects Parameters												
σ^2	6302.988		5737.018		5736.691		5703.595		5696.809		5697.395	
τ_{00}	27944.557		15538.948		15540.133		15175.498		15191.373		15181.326	
n	330		330		330		314		314		314	
Scans	637		637		637		578		578		578	
Deviance	8102.344		7904.153		7904.152		7176.972		7176.851		7176.717	

Note. ETIV = Estimated Total Intracranial Volume; *Time* = Age at current scan – Age at first scan; *Age@1stScan* = chronological age at initial assessment/study entry; *AFI* = Adjusted Family Income.

†Scaled by 10^{-5} and grand-mean centered

*$p < .05$. **$p < .01$. ***$p < .001$

Table S5-A.

Effects of Annual Family Income on Change in Right Amygdala Volumes across Pubertal Development

	Right Amygdala Volume (mm^3)											
	B	*SE*	*B*	*SE*	*B*	*SE*	*B*	*SE*	*B*	*SE*	*B*	*SE*
Fixed Parts												
Intercept	1635.98***	10.69	1635.79***	7.79	1639.45***	8.93	1636.70***	25.69	1642.35***	26.33	1654.31***	42.50
ETIV †			9.27***	0.48	8.95***	0.57	9.08***	0.59	9.04***	0.60	9.04***	0.60
TSChange					10.78	6.05	11.24	6.26	-2.99	22.33	3.79	37.34
TS@1stScan							5.97	6.73	6.35	6.83	1.56	14.92
AFI							-0.00	0.00	-0.00	0.00	-0.00	0.00
TSChange x TS@1stScan									-1.46	7.47	-5.90	18.05
TSChange x AFI									0.00	0.00	0.00	0.00
TS@1stScan x AFI											0.00	0.00
TSChange x TS@1stScan x AFI											0.00	0.00
Random Parts												
σ^2	7862.962		6253.536		6409.940		5987.143		5928.535		5928.334	
τ_{00}	32926.234		16237.791		16819.857		16572.229		16664.663		16643.474	
n	330		330		274		260		260		260	
Scans	637		637		513		470		470		470	
Deviance	8226.705		7947.714		6421.981		5870.269		5868.893		5868.616	

Note. ETIV = Estimated Total Intracranial Volume; *TSChange* = Tanner stage at current scan – Tanner stage at first scan; *TS@1stScan* = pubertal development at first scan (Tanner stage); *AFI* = Adjusted Family Income.

†Scaled by 10^{-5} and grand-mean centered

*$p < .05$. **$p < .01$. ***$p < .001$

Table S5-B.

Effects of Annual Family Income on Change in Left Amygdala Volumes across Pubertal Development

	Left Amygdala Volume (mm^3)											
	B	*SE*	*B*	*SE*	*B*	*SE*	*B*	*SE*	*B*	*SE*	*B*	*SE*
Fixed Parts												
Intercept	1580.11***	9.81	1579.89***	7.59	1581.88***	8.61	1610.86***	24.94	1603.80***	25.37	1617.07***	41.51
ETIV †			7.43***	0.47	7.67***	0.55	7.89***	0.57	7.86***	0.58	7.86***	0.58
TSChange					-3.43	5.81	-3.40	6.29	11.71	24.91	-5.02	41.80
TS@1stScan							-9.66	6.47	-9.62	6.51	-14.86	14.48
AFI							-0.00	0.00	0.00	0.00	-0.00	0.00
TSChange x TS@1stScan									0.07	8.04	8.53	19.58
TSChange x AFI									-0.00	0.00	0.00	0.00
TS@1stScan x AFI											0.00	0.00
TSChange x TS@1stScan x AFI											-0.00	0.00
Random Parts												
σ^2	6302.988		5737.018		5891.846		6129.718		5746.152		5707.223	
τ_{00}	27944.557		15538.948		15719.198		14932.233		14850.920		14880.926	
n	330		330		274		260		260		260	
Scans	637		637		513		470		470		470	
Deviance	8102.344		7904.153		6382.425		5854.755		5851.929		5851.631	

Note. ETIV = Estimated Total Intracranial Volume; *TSChange* = Tanner stage at current scan – Tanner stage at first scan; *TS@1stScan* = pubertal development at first scan (Tanner stage); *AFI* = Adjusted Family Income.

†Scaled by 10^{-5} and grand-mean centered

*$p < .05$. **$p < .01$. ***$p < .001$

Table S6-A

Change in Right Amygdala Volumes as a Function of Time and Age at Initial Scan among Boys

	Right Amygdala Volume (mm^3)							
	B	*SE*	*B*	*SE*	*B*	*SE*	*B*	*SE*
Fixed Effects Parameters								
Intercept	1741.49***	13.94	1726.71***	14.51	1542.42***	45.30	1513.61***	46.10
Time			16.91***	4.03	18.12***	4.52	70.13***	12.99
Age@1stscan					15.94***	3.74	18.40***	3.81
Time x Age@1stScan							-4.54***	1.07
Random Effects Parameters								
σ^2	7815.889		6686.744		4735.929		5198.186	
τ_{00}	23328.475		24567.899		22543.395		22265.877	
n	146		146		146		146	
Scans	266		266		266		266	
Deviance	3401.317		3385.191		3364.323		3350.306	

Note. Time = Age at current scan – Age at first scan. *Age@1stScan* = chronological age at initial assessment/study entry.
*$p < .05$. **$p < .01$. ***$p < .001$

Table S6-B

Johnson-Neyman Significance Regions for the Conditional Effect of Age at First Scan on Change in Right Amygdala Volumes across Time in Study in Boys

Age at 1st Scan	Slope	SE	LCI	UCI	*t*	*p*
20.00	-21.08	9.87	-40.41	-1.74	-2.14	.034
19.00	-16.51	8.89	-33.94	0.92	-1.86	.065
18.00	-11.95	7.95	-27.52	3.63	-1.50	.135
17.00	-7.39	7.04	-21.18	6.40	-1.05	.296
16.00	-2.82	6.18	-14.93	9.29	-0.46	.648
15.00	1.74	5.40	-8.83	12.32	0.32	.747
14.00	6.31	4.73	-2.96	15.57	1.33	.184
13.00	10.87	4.23	2.57	19.17	2.57	.011
12.00	15.43	3.97	7.65	23.22	3.89	< .001
11.00	20.00	3.99	12.18	27.82	5.01	< .001
10.00	24.56	4.28	16.16	32.96	5.73	< .001
9.00	29.12	4.81	19.70	38.54	6.06	< .001
8.00	33.69	5.49	22.93	44.45	6.14	< .001
7.00	38.25	6.28	25.94	50.57	6.09	< .001
6.00	42.82	7.15	28.80	56.83	5.99	< .001
5.00	47.38	8.07	31.57	63.19	5.87	< .001

Note. LCI = 95% lower confidence interval. UCI = 95% upper confidence interval.

Table S7-A

Change in Right Amygdala Volumes as a Function of Time and Age at Initial Scan among Girls

	Right Amygdala Volume (mm^3)							
	B	*SE*	*B*	*SE*	*B*	*SE*	*B*	*SE*
Fixed Effects Parameters								
Intercept	1553.60***	12.68	1533.87***	13.09	1403.00***	39.44	1381.02***	40.29
Time			18.21***	3.23	21.44***	3.97	65.70***	11.84
Age@1stscan					11.46***	3.32	13.45***	3.40
Time x Age@1stScan							-3.98***	1.00
Random Effects Parameters								
σ^2	7864.698		6784.542		4143.717		4368.976	
τ_{00}	25062.644		25380.051		24061.928		24396.493	
n	184		184		184		184	
Scans	371		371		371		371	
Deviance	4738.711		4709.187		4694.625		4679.824	

Note. Time = Age at current scan – Age at first scan. *Age@1stScan* = chronological age at initial assessment/study entry.
*$p < .05$. **$p < .01$. ***$p < .001$

Table S7-B

Johnson-Neyman Significance Regions for the Conditional Effect of Age at First Scan on Change in Right Amygdala Volumes across Time in Study in Girls

Age at 1st Scan	Slope	SE	LCI	UCI	*t*	*p*
20.00	-13.74	8.17	-29.76	2.27	-1.68	.094
19.00	-10.02	7.38	-24.48	4.43	-1.36	.176
18.00	-6.30	6.60	-19.24	6.63	-0.95	.341
17.00	-2.58	5.85	-14.05	8.89	-0.44	.660
16.00	1.14	5.14	-8.93	11.21	0.22	.825
15.00	4.86	4.48	-3.92	13.65	1.08	.279
14.00	8.58	3.91	0.92	16.25	2.20	.029
13.00	12.30	3.46	5.52	19.09	3.55	< .001
12.00	16.03	3.20	9.76	22.29	5.01	< .001
11.00	19.75	3.15	13.56	25.93	6.26	< .001
10.00	23.47	3.35	16.91	30.03	7.01	< .001
9.00	27.19	3.74	19.87	34.51	7.28	< .001
8.00	30.91	4.27	22.54	39.28	7.24	< .001
7.00	34.63	4.90	25.03	44.23	7.07	< .001
6.00	38.35	5.59	27.39	49.32	6.86	< .001
5.00	42.07	6.33	29.67	54.48	6.65	< .001

Note. LCI = 95% lower confidence interval. UCI = 95% upper confidence interval.

Table S8-A

Change in Left Amygdala Volumes as a Function of Time and Age at Initial Scan among Boys

	Right Amygdala Volume (mm^3)							
	B	*SE*	*B*	*SE*	*B*	*SE*	*B*	*SE*
Fixed Effects Parameters								
Intercept	1664.49***	13.89	1654.31***	14.33	1555.04***	45.59	1541.66***	46.14
Time			11.70**	3.71	12.79**	4.28	38.84**	13.56
Age@1stscan					8.57*	3.77	9.71*	3.82
Time x Age@1stScan							-2.28	1.13
Random Effects Parameters								
σ^2	6163.180		5625.818		3797.357		3868.289	
τ_{00}	24153.246		24793.151		23520.456		23506.584	
n	146		146		146		146	
Scans	266		266		266		266	
Deviance	3371.547		3362.099		3346.928		3343.062	

Note. Time = Age at current scan – Age at first scan. *Age@1stScan* = chronological age at initial assessment/study entry.
*$p < .05$. **$p < .01$. ***$p < .001$

Table S8-B

Johnson-Neyman Significance Regions for the Conditional Effect of Age at First Scan on Change in Left Amygdala Volumes across Time in Study in Boys

Age at 1st Scan	Slope	SE	LCI	UCI	*t*	*p*
20.00	-8.05	10.30	-28.24	12.14	-0.78	.436
19.00	-5.66	9.29	-23.87	12.55	-0.61	.544
18.00	-3.27	8.31	-19.55	13.02	-0.39	.695
17.00	-0.88	7.36	-15.30	13.55	-0.12	.905
16.00	1.51	6.46	-11.16	14.18	0.23	.815
15.00	3.90	5.65	-7.17	14.97	0.69	.491
14.00	6.29	4.94	-3.40	15.98	1.27	.205
13.00	8.68	4.41	0.03	17.33	1.97	.051
12.00	11.07	4.12	3.00	19.14	2.69	.008
11.00	13.46	4.11	5.40	21.52	3.27	.001
10.00	15.85	4.40	7.23	24.47	3.60	< .001
9.00	18.24	4.93	8.59	27.89	3.70	< .001
8.00	20.63	5.62	9.61	31.65	3.67	< .001
7.00	23.02	6.44	10.40	35.64	3.57	< .001
6.00	25.41	7.33	11.04	39.78	3.47	< .001
5.00	27.80	8.28	11.57	44.03	3.36	.001

Note. LCI = 95% lower confidence interval. UCI = 95% upper confidence interval.

Table S9-A

Change in Left Amygdala Volumes as a Function of Time and Age at Initial Scan among Girls

	Right Amygdala Volume (mm^3)							
	B	*SE*	*B*	*SE*	*B*	*SE*	*B*	*SE*
Fixed Effects Parameters								
Intercept	1514.17***	11.60	1505.63***	12.07	1472.88***	37.63	1444.31***	38.93
Time			7.89*	3.08	7.95*	3.11	35.67***	10.03
Age@1stscan					2.90	3.16	5.43	3.28
Time x Age@1stScan							-2.45**	0.84
Random Effects Parameters								
σ^2	6371.956		6161.550		6057.982		5749.073	
τ_{00}	21114.662		21209.119		21081.373		21324.370	
n	184		184		184		184	
Scans	371		371		371		371	
Deviance	4666.733		4660.258		4659.428		4651.250	

Note. Time = Age at current scan – Age at first scan. *Age@1stScan* = chronological age at initial assessment/study entry.
*$p < .05$. **$p < .01$. ***$p < .001$

Table S9-B

Johnson-Neyman Significance Regions for the Conditional Effect of Age at First Scan on Change in Left Amygdala Volumes across Time in Study in Girls

Age at 1st Scan	Slope	SE	LCI	UCI	*t*	*p*
20.00	-13.02	7.83	-28.36	2.32	-1.66	.098
19.00	-10.61	7.06	-24.45	3.24	-1.50	.135
18.00	-8.20	6.32	-20.59	4.19	-1.30	.196
17.00	-5.79	5.60	-16.77	5.19	-1.03	.303
16.00	-3.38	4.92	-13.02	6.26	-0.69	.493
15.00	-0.97	4.29	-9.38	7.44	-0.23	.822
14.00	1.44	3.74	-5.90	8.78	0.38	.701
13.00	3.85	3.32	-2.65	10.35	1.16	.247
12.00	6.26	3.06	0.26	12.26	2.05	.042
11.00	8.67	3.02	2.75	14.59	2.87	.005
10.00	11.08	3.20	4.80	17.36	3.46	.001
9.00	13.49	3.58	6.48	20.50	3.77	< .001
8.00	15.90	4.09	7.89	23.91	3.89	< .001
7.00	18.31	4.69	9.11	27.51	3.90	< .001
6.00	20.72	5.36	10.22	31.22	3.87	< .001
5.00	23.13	6.07	11.24	35.02	3.81	< .001

Note. LCI = 95% lower confidence interval. UCI = 95% upper confidence interval.

Table 10-A

Change in Right Amygdala Volumes as a Function of Pubertal Development and Tanner Stage at Initial Scan in Boys

	Right Amygdala Volume (mm^3)							
	B	*SE*	*B*	*SE*	*B*	*SE*	*B*	*SE*
Fixed Effects Parameters								
Intercept	1741.49***	13.94	1743.06***	15.91	1655.02***	30.69	1657.95***	30.92
TSChange			33.84***	8.16	35.21***	8.13	18.15	18.07
TS@1stScan					35.76**	10.82	34.15**	10.97
TSChange x TS@1stScan							10.48	9.91
Random Effects Parameters								
σ^2	7815.889		5914.187		5908.070		5774.728	
τ_{00}	23328.475		25261.374		22816.602		23100.023	
n	146		119		119		119	
Scans	266		204		204		204	
Deviance	3401.317		2594.028		2583.564		2582.470	

Note. TSChange = Tanner stage at current scan – Tanner stage at first scan. *TS@1stScan* = pubertal development (Tanner Stage) at initial assessment/study entry.
*$p < .05$. **$p < .01$. ***$p < .001$

Table 10-B

Change in Right Amygdala Volumes as a Function of Pubertal Development and Tanner Stage at Initial Scan in Girls

	Right Amygdala Volume (mm^3)							
	B	*SE*	*B*	*SE*	*B*	*SE*	*B*	*SE*
Fixed Effects Parameters								
Intercept	1553.60***	12.68	1556.58***	14.23	1535.29***	31.43	1530.27***	31.68
TSChange			36.33***	9.02	36.99***	9.06	69.18**	20.72
TS@1stScan					8.15	10.73	10.75	10.89
TSChange x TS@1stScan							-18.71	10.83
Random Effects Parameters								
σ^2	7864.698		7489.697		7495.301		7290.921	
τ_{00}	25062.644		25669.875		25533.029		25913.427	
n	184		155		155		155	
Scans	371		309		309		309	
Deviance	4738.711		3942.342		3941.767		3938.850	

Note. TSChange = Tanner stage at current scan – Tanner stage at first scan. *TS@1stScan* = pubertal development (Tanner Stage) at initial assessment/study entry.
$^{*}p < .05$. $^{**}p < .01$. $^{***}p < .001$

Table 11-A

Change in Left Amygdala Volumes as a Function of Pubertal Development and Tanner Stage at Initial Scan in Boys

	Right Amygdala Volume (mm^3)							
	B	*SE*	*B*	*SE*	*B*	*SE*	*B*	*SE*
Fixed Effects Parameters								
Intercept	1664.49***	13.89	1664.98***	16.28	1637.06***	32.40	1638.04***	32.50
TSChange			19.69*	8.17	25.91*	11.17	16.42	24.66
TS@1stScan					11.14	11.47	10.59	11.54
TSChange x TS@1stScan							5.18	11.66
Random Effects Parameters								
σ^2	6163.180		5911.114		4383.390		4320.865	
τ_{00}	24153.246		26705.686		27059.893		27149.292	
n	146		119		119		119	
Scans	266		204		204		204	
Deviance	3371.547		2599.696		2592.273		2592.086	

Note. TSChange = Tanner stage at current scan – Tanner stage at first scan. *TS@1stScan* = pubertal development (Tanner Stage) at initial assessment/study entry.
*$p < .05$. **$p < .01$. ***$p < .001$

Table 11-B

Change in Left Amygdala Volumes as a Function of Pubertal Development and Tanner Stage at Initial Scan in Girls

	Right Amygdala Volume (mm^3)							
	B	*SE*	*B*	*SE*	*B*	*SE*	*B*	*SE*
Fixed Effects Parameters								
Intercept	1514.17***	11.60	1515.40***	13.00	1514.61***	28.43	1513.20***	28.57
TSChange			14.40	8.03	18.28	9.53	29.55	22.02
TS@1stScan					0.05	9.73	0.75	9.82
TSChange x TS@1stScan							-6.06	10.76
Random Effects Parameters								
σ^2	6371.956		5912.222		5309.455		5256.545	
τ_{00}	21114.662		21683.511		21450.353		21548.189	
n	184		155		155		155	
Scans	371		309		309		309	
Deviance	4666.733		3878.266		3875.318		3875.010	

Note. TSChange = Tanner stage at current scan – Tanner stage at first scan. *TS@1stScan* = pubertal development (Tanner Stage) at initial assessment/study entry.
*$p < .05$. **$p < .01$. ***$p < .001$

Table 12-A

Change in Right Amygdala Volumes as a Function of Chronological Time and Pubertal Maturation in Boys

	Right Amygdale Volume (mm^3)									
	B	*SE*	*B*	*SE*	*B*	*SE*	*B*	*SE*	*B*	*SE*
Fixed Effects Parameters										
Intercept	1741.49***	13.94	1741.53***	16.15	1587.09***	69.52	1551.05***	70.57	1558.84***	70.34
Time			2.96	6.78	1.75	6.81	13.18	29.69	-4.06	31.17
TSChange			45.24*	20.61	46.79*	20.65	177.19*	76.41	-41.24	132.99
Time x TSChange			-4.76	6.13	-4.63	6.12	-3.56	6.28	76.64	41.28
Age@1stScan					9.40	8.75	13.91	8.85	13.10	8.83
TS@1stScan					16.23	21.17	8.43	21.37	9.17	21.31
Time x Age@1stScan							-0.72	4.17	2.07	4.50
Time x TS@1stScan							-3.81	9.84	-9.38	10.57
TSChange x Age@1stScan							-17.20*	7.70	0.10	12.63
TSChange x TS@1stScan							49.87**	17.36	54.07	30.63
Time x TSChange x Age1stScan									-6.81	4.02
Time x TSChange x TS@1stScan									0.34	9.10
Random Effects Parameters										
σ^2	7815.889		5849.899		5850.789		4911.845		4740.756	
τ_{00}	23328.475		25376.219		22658.876		23209.086		23066.451	
n	146		119		119		119		119	
Scans	266		204		204		204		204	
Deviance	3401.317		2593.385		2581.860		2566.562		2562.377	

Note. Time = Age at current scan – Age at first scan; *TSChange* = Tanner stage at current scan – Tanner stage at first scan; *Age@1stScan* = chronological age at initial assessment/study entry; *TS@1stScan* = pubertal development (Tanner stage) at initial assessment/study entry.
$^{*}p < .05$. $^{**}p < .01$. $^{***}p < .001$

Table 12-B

Change in Right Amygdala Volumes as a Function of Chronological Time and Pubertal Maturation in Girls

	Right Amygdale Volume (mm^3)									
	B	*SE*	*B*	*SE*	*B*	*SE*	*B*	*SE*	*B*	*SE*
Fixed Effects Parameters										
Intercept	1553.60***	12.68	1547.10***	14.51	1413.98***	54.67	1357.85***	56.47	1359.01***	56.66
Time			16.32**	5.40	16.92**	5.43	45.18*	17.56	44.88*	18.65
TSChange			58.46*	24.53	56.02*	24.55	176.59**	57.80	148.03	101.32
Time x TSChange			-15.64*	7.27	-15.67*	7.27	-24.17**	7.54	-15.10	30.06
Age@1stScan					20.48**	7.71	25.93**	7.92	25.94**	7.95
TS@1stScan					-42.45*	20.79	-45.91*	21.16	-46.51*	21.22
Time x Age@1stScan							0.35	2.79	0.21	3.17
Time x TS@1stScan							-9.44	8.51	-8.56	9.52
TSChange x Age@1stScan							-11.70	6.80	-12.39	11.68
TSChange x TS@1stScan							5.55	20.56	24.81	37.89
Time x TSChange x Age1stScan									0.30	3.71
Time x TSChange x TS@1stScan									-6.75	11.92
Random Effects Parameters										
σ^2	7864.698		6994.688		6985.479		6006.507		5985.740	
τ_{00}	25062.644		25966.162		24657.478		25368.308		25368.717	
n	184		155		155		155		155	
Scans	371		309		309		309		309	
Deviance	4738.711		3931.837		3924.711		3902.175		3901.578	

Note. Time = Age at current scan – Age at first scan; *TSChange* = Tanner stage at current scan – Tanner stage at first scan; *Age@1stScan* = chronological age at initial assessment/study entry; *TS@1stScan* = pubertal development (Tanner stage) at initial assessment/study entry.
$^{*}p < .05$. $^{**}p < .01$. $^{***}p < .001$

Table 13-A

Change in Left Amygdala Volumes as a Function of Chronological Time and Pubertal Maturation in Boys

	Right Amygdale Volume (mm^3)									
	B	*SE*	*B*	*SE*	*B*	*SE*	*B*	*SE*	*B*	*SE*
Fixed Effects Parameters										
Intercept	1664.49***	13.89	1663.31***	16.51	1510.18***	72.07	1493.20***	72.63	1491.02***	73.01
Time			4.38	6.81	4.54	6.92	39.14	31.68	43.78	31.27
TSChange			16.64	20.68	12.67	19.90	46.76	88.54	4.03	135.73
Time x TSChange			-0.85	6.14	1.75	5.73	5.03	6.23	19.65	41.94
Age@1stScan					17.65	9.06	19.84*	9.11	20.44*	9.16
TS@1stScan					-25.60	21.88	-29.57	22.00	-32.08	22.13
Time x Age@1stScan							-5.02	4.50	-6.00	4.58
Time x TS@1stScan							8.14	10.60	11.75	10.76
TSChange x Age@1stScan							-5.28	9.01	-8.70	13.15
TSChange x TS@1stScan							19.65	20.75	72.52*	30.95
Time x TSChange x Age1stScan									1.40	4.08
Time x TSChange x TS@1stScan									-19.66*	8.86
Random Effects Parameters										
σ^2	6163.180		5874.788		3816.389		3621.445		3545.318	
τ_{00}	24153.246		26758.551		25895.853		26052.961		26361.082	
n	146		119		119		119		119	
Scans	266		204		204		204		204	
Deviance	3371.547		2599.279		2586.656		2581.305		2575.373	

Note. Time = Age at current scan – Age at first scan; *TSChange* = Tanner stage at current scan – Tanner stage at first scan; *Age@1stScan* = chronological age at initial assessment/study entry; *TS@1stScan* = pubertal development (Tanner stage) at initial assessment/study entry.
*$p < .05$. **$p < .01$. ***$p < .001$

Table 13-B

Change in Left Amygdala Volumes as a Function of Chronological Time and Pubertal Maturation in Girls

	Right Amygdale Volume (mm^3)									
	B	*SE*	*B*	*SE*	*B*	*SE*	*B*	*SE*	*B*	*SE*
Fixed Effects Parameters										
Intercept	1514.17***	11.60	1514.70***	13.29	1434.67***	50.16	1413.87***	51.72	1413.71***	51.94
Time			1.68	4.96	0.90	4.85	1.30	16.59	0.79	17.70
TSChange			6.86	22.52	4.37	22.92	108.89	58.57	116.82	97.79
Time x TSChange			1.39	6.68	3.64	6.72	1.24	7.30	-1.03	28.75
Age@1stScan					13.64	7.07	16.32*	7.26	16.25*	7.29
TS@1stScan					-31.58	19.02	-35.84	19.38	-35.36	19.46
Time x Age@1stScan							0.87	2.64	1.12	3.02
Time x TS@1stScan							-4.18	8.09	-5.17	9.10
TSChange x Age@1stScan							-14.69	6.96	-13.25	11.29
TSChange x TS@1stScan							32.94	20.87	19.96	36.89
Time x TSChange x Age1stScan									-0.59	3.55
Time x TSChange x TS@1stScan									4.75	11.52
Random Effects Parameters										
σ^2	6371.956		5895.303		5202.258		5247.934		5251.515	
τ_{00}	21114.662		21729.970		20941.317		21080.319		21108.822	
N	184		155		155		155		155	
Scans	371		309		309		309		309	
Deviance	4666.733		3878.049		3871.317		3864.423		3864.207	

Note. Time = Age at current scan – Age at first scan; *TSChange* = Tanner stage at current scan – Tanner stage at first scan; *Age@1stScan* = chronological age at initial assessment/study entry; *TS@1stScan* = pubertal development (Tanner stage) at initial assessment/study entry.
*$p < .05$. **$p < .01$. ***$p < .001$